Evaluation of Stormwater Control Measures from the Micro and Macro Perspectives: Low Cost Monitoring of Nutrients in Non-Vegetated Systems and Watershed-Scale Effects of Rain Gardens

A Thesis

Presented to

The Faculty of the Department of Civil and Environmental Engineering

Villanova University

In Partial Fulfillment

Of the Requirements for the Degree of

Master of Civil Engineering

By

Erin Lawrence Dovel

May 2013

Under the Direction of

Dr. Andrea Welker

Evaluation of Stormwater Control Measures from the Micro and Macro Perspectives: Low Cost Monitoring of Nutrients in Non-Vegetated Systems and Watershed-Scale Effects of Rain Gardens

By

Erin Lawrence Dovel

May 2013

Andrea Welker, Ph.D., P.E. Associate Professor	Date
Bridget M. Wadzuk, Ph.D. Associate Professor	Date
Ronald A. Chadderton, Ph.D., P.E. Chairman, Dept. of Civil and Environmental Engineering	Date
Gary A. Gabriel, Ph.D. Dean, College of Engineering	Date

Statement by Author

This dissertation has been submitted in partial fulfillment of requirements for an advanced degree at the Villanova University and is deposited in the Falvey Memorial Library to be made available to borrowers under rules of the Library.

Brief quotations from this dissertation are allowable without special permission, provided that accurate acknowledgement of source is made. Requests for permission for extended quotation from or reproduction of this manuscript in whole or in part may be granted by the head of the major department or the Associate Dean for Graduate Studies and Research of the College of Engineering when in his or her judgment the proposed use of the material is in the interests of scholarship. In all other instances, however, permission must be obtained from the author.

Acknowledgements

I would like to thank the faculty and staff in the Villanova University Civil and Environmental Engineering Department for all their assistance throughout my graduate career. My graduate advisor, Dr. Andrea Welker has served as my mentor and teacher throughout my journey at Villanova. I would also like to specifically thank Dr. John Komlos, Dr. Robert Traver, Dr. Bridget Wadzuk, Dr. Francis Hampton, Dr. Stanley Kemp, and George Pappas for offering expertise during the many phases of my research work. Furthermore, I would like to thank the William Penn Foundation for making this research possible.

I would also like to thank my fellow graduate students, Mike Rinker, Amanda Hess, Kaitlin Vacca, Cara Lyons, and Laura Lord for all of their assistance and camaraderie in and out of the classroom. I would like to thank my family and my fiancé, Erik Herbert, whose guidance over the years has been invaluable.

Table of Contents

List of Tables

List of Figures

Abstract

Stormwater Control Measures (SCMs) have become one of the standard methods to handle the peak flows and increased pollution in stormwater runoff due to anthropogenic activities. This thesis presents a two-part study focused on the holistic evaluation of SCMs at the individual and watershed scales. The first phase of research focused on post-construction water quality monitoring of non-vegetated control measures. A laboratory experiment was created to simulate a pervious concrete system and a sand infiltration bed. After calibrating the experiment to typical summer conditions, temperature reduction of the inflow was used as a proxy for nutrient removal through the control measure. This procedure can be coupled with existing low-level monitoring techniques to gain an understanding of how an SCM is functioning post construction.

The second phase of the research assessed the effects that rain gardens may have on water quantity at a watershed scale. EPA's SWMM 5.0 software was used as it is a widely accepted program within the industry, and contains a robust method of modeling low impact development (LID) practices. The Mill Creek watershed, located in Montgomery County, PA, was used as a basis for the development of a "typical urban watershed." In total, 45 models were created which varied the percent impervious area of the watershed, and ratio of rain gardens implemented per structure. Effects of these control measures were assessed by looking at total volume, peak outflow, velocity, and depth of a typical summer storm. Generally, low reductions to the water quantity parameters were witnessed with the addition of rain gardens on a watershed scale.

Furthermore, nesting criteria of the River Chub species were used as an indicator to judge ecological stream health within the 45 SWMM models. It was found that the addition of rain gardens decreased the probability of nest destruction during a typical summer storm event for watershed impervious areas of 9-25%. An impervious area of 60% or greater would not produce habitable conditions for the River Chub, even with the maximum number of rain gardens implemented.

Part I

The Use of Temperature as a Proxy for Nutrient Reduction: a Low Cost Inspection Tool for Stormwater Control Measures

Chapter 1

Introduction

Urbanization caused by an increase in population continues to place stressors on natural hydrologic systems and environments. Due to the implementation of more and more impervious areas in urban locations, the hydraulics of a watershed are often times disrupted leading to a decline in the health of the surrounding ecosystem. In the United States, the conversion of agricultural land to urban and suburban areas is proceeding at an unprecedented rate, with the majority of the country now living in these developed areas (NRC 2008).

The disruption to the natural ecosystem via urbanization can be classified into two main categories: interruption of the hydrologic cycle and introduction of pollutants into natural waterways at elevated concentrations. High surface runoff flows and velocities are experienced during storm events over urbanized locations. Minimal water can infiltrate the ground, and the high runoff makes its way to water bodies much faster than in natural systems. Hydologic alterations tend to inhibit groundwater recharge, increase erosion, and physically block natural waterways within the drainage area. Furthermore, increased runoff leads to the transport of non-point source pollutants associated with urban

activities which will increase the contaminant loadings in rivers and streams. Due to the urbanization of watersheds, an estimated 41,500 water bodies are currently impaired in the United States (USEPA 2013).

Stormwater Control Measures (SCMs) offer a way to decrease the effect of urbanization on the surrounding watershed through physical and chemical mechanisms. A variety of SCMs have been developed to serve specific or several stormwater control functions. Table 1.1 details common types of SCMs coupled with their associated functionalities. By using these tools as an effective means for stormwater control management, one can protect water quality, enhance water availability, and reduce flooding potential (PADEP 2006).

Table 1.1: Types of SCMs and Their Functions

	Stormwater Control Goals				
Type of SCM	Volume of Runoff	Peak Flow Rate	Pollutant Control	Promote Evapo-transpiration	Establish Wetland Function
Infiltration Trench/ Pervious Pavement	Yes	Yes	Yes	No	No
Rain Garden (Bioinfiltration)	Yes	Yes	Yes	Yes	No
Green Roof	Yes	Yes	Yes	Yes	No
Constructed Wetland	Yes	Yes	Yes	Yes	Yes
Wet Pond (Retention Basin)	Yes	Yes	Yes	Yes	Yes

(Welker, et al. in press)

To ensure the effectiveness of these SCMs, post construction maintenance and inspection must be conducted. These tasks often times become the responsibility of the property owner in which the control measures reside, and may prove to be onerous and expensive. Low level monitoring plans have been developed in the form of user friendly visual

inspection checklists. Higher level monitoring systems involve soil analysis such as infiltration testing with a greater investment in time and money (Greising 2011). Overall, these monitoring systems are able to identify problems in the functionality of SCMs by evaluating their capacity to remove storm runoff volumes.

In terms of cost and time, determining the pollutant removal efficiency of a SCM can be considered a high-level monitoring method. Typically, this level of monitoring is not feasible when considering a control measure on private or commercial property. In an attempt to reduce these burdens, phase I of this research investigated the use of temperature reduction through a SCM as a proxy to estimate nutrient removal in the forms of nitrogen and phosphorus. Using Villanova's pervious concrete parking lot as a basis for design, two polyvinyl chloride columns were constructed in order to obtain a correlation between temperature reduction and removal during a typical summer storm event.

Chapter 2

Literature Review

2.1 Overview of Stream Impairment

During the first 18 years of the Clean Water Act, regulatory efforts were primarily focused on point source pollution, such as waste water discharges and industrial effluent. After the implementation of widespread water quality monitoring programs set forth by the government, the focus shifted towards non point source pollutants (Burton and Pitt 2002). Non point source pollution typically results from precipitation, atmospheric deposition, land runoff, infiltration, drainage, seepage, or hydrologic modification. As runoff from rainfall (or snowmelt) traverses the landscape, it picks up and carries natural pollutants and pollutants due to human activity, ultimately transporting them into rivers, lakes, wetlands, coastal waters, and groundwater (EPA 2005).

Under section 303(d) of the Clean Water Act, states and territories in the United States are required to develop lists of impaired waters. These waters are defined as being too polluted to meet the water quality standards set by the state or territory. In 1995, the EPA reported that 57% of rivers and streams fully support their ecological uses; with pathogens being the leading cause of impairment. The second and third causes of impairment are caused by the concentration of metals and nutrients respectively (EPA 2013).

Sources of water body impairment are typically due to human activity. Agricultural processes lead to a spike in nitrogen and phosphorus runoff after crop fertilization. Interruption in the hydrologic cycle, such as an increase in impervious area can lead to high and fast storm runoff flows having the ability to carry a large pollutant load. Disruption of the natural hydrologic cycle such as dams can rob the watershed of its ability to properly recharge groundwater and mitigate stormwater flows. Figure 2.1 displays the effect that urbanization has on water body impairment, with ocean shorelines being the most affected by urban runoff, and rivers being the least.

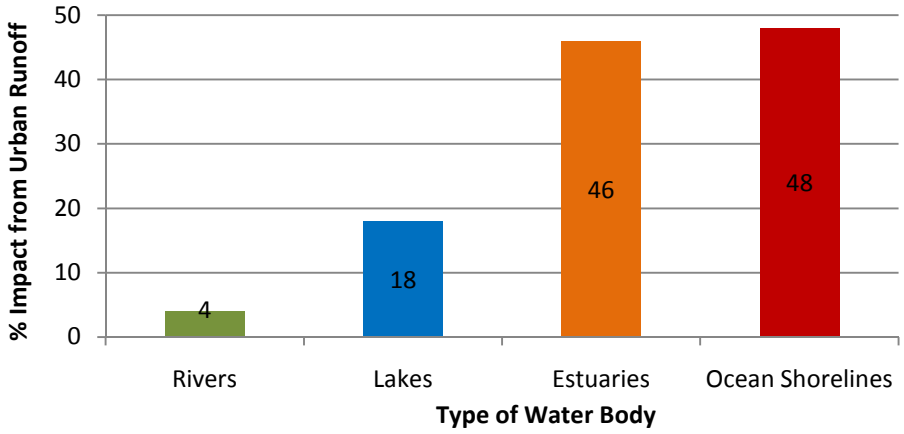

Figure 2.1: Contribution to Impairment Due to Urban Runoff (Burton and Pitt 2002)

In an effort to combat or reverse the negative impacts to water quality of U.S. water bodies, regulators are focusing on the implementation of stormwater control measures (SCMs). The system selected is based on the impairing pollutant, with removal processes being physical, chemical, or biological. Table 2.1 displays the main types of pollution control mechanisms in SCMs.

Table 2.1: SCM Pollutant Removal Mechanisms		
Type	**Description**	**Process**
Sedimentation	Infiltrating stormwater deposits suspended solids due to slowing flow velocity	Physical
Filtration	Infiltrating stormwater deposits solids while flowing through media with small voids	Physical
Adsorption	Dissolved solutes are removed from solution and partitioned or surface-complexed to an adsorbant such as soil particles	Chemical
Precipitation	Removal of ionic species from solution in the form of insoluble chemicals	Chemical
Nutrient Conversion	Microbes utilize nutrients for metabolic processes	Biological
Degradation of oil and grease	Microbes degrade hydrophobic substances for metabolism	Biological

(Field and Sullivan 2003)

For this study, pervious pavement systems will be specifically investigated. The main pollutant removal mechanisms associated these control measures are sedimentation and filtration of total suspended solids, adsorption of nutrients such as phosphate, and possible long term nitrogen removal through biological processes.

2.2 Pervious Pavement Systems

Pervious/ porous pavement systems consist of a permeable surface course underlain by uniformly graded stone bed which can provide for temporary storage. Once stormwater has travelled into the aggregate bed, infiltration then occurs into the underlying native soil if no barrier layer is present (PADEP 2006). Evaporation can theoretically occur if the water level within the aggregate bed is close enough to the surface (Nemirovsky, et al. 2013). Figure 2.2 displays a general schematic of the pervious pavement system.

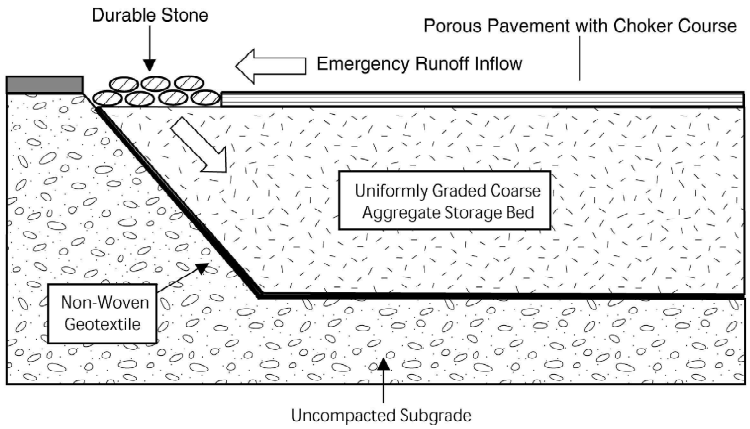

Figure 2.2: Typical Pervious Pavement System (NJDEP 2004)

The pervious pavement layer can consist of pervious concrete, porous asphalt, or pavers spaced to allow for infiltration. Pervious concrete and porous asphalt consist of the same material as their impervious counterparts, except that all of the fine material has been removed. In the absence of fines, these pervious pavements typically have void ratios of 15-20% and can reach infiltration rates of approximately 480 inch/hr (Tennis, et al. 2007). Typically, a 12-36" aggregate bed consisting of AASHTO #57 stone is directly beneath the pervious pavement surface layer. This bed should have a void ratio of approximately 40% (PADEP 2006). Some designs allow for overflow into the existing stormwater system if the aggregate bed reaches volume capacity during a storm event.

Pervious pavement systems can function well in highly urbanized areas as they do not require vegetation. They can be retrofitted into parking lots, sidewalks, and parks. These systems have limited applications on major roads with high frequency loads due to inadequate strength. In general, their primary function is to reduce inflow stormwater volumes. Pollutant removal capacitates of these systems are not well known, and seem to vary with design, location, and pollutant concentration (Clary, et al. 2011). In a side-by-

side study performed on Villanova's campus, it was found that no differences in pollutant removal magnitudes were evident for pervious concrete and porous asphalt (Welker, et al. 2012a).

2.2.1 Nitrogen Removal

The fate of nitrogen within pervious pavement SCMs is not currently well defined. As illustrated in Table 2.2, field and laboratory studies have shown that nitrogen removal can be quite variable. Typically, non-vegetated infiltration systems, such as porous pavements do not show short term nitrogen removal capabilities. Furthermore, when outflow is produced from these systems, forms of nitrogen and total nitrogen (TN) are predicted to export from the gravel bed (Chang 2010).

Table 2.2: Pervious Pavement Systems and Nitrogen Fate

Location	Type of System	Removal	Reference
Prince William, VA	Porous Pavement	80% TN by mass	Tennis, et al. 2007
Rockvill, MD	Porous Pavement	85% TN by mass	Tennis, et al. 2007
NH	Porous Asphalt	Nitrate Export	Roseen, et al. 2012
Goldsboro, NC	Concrete Grid Pavers	27% TN	Collins, et al. 2010
Melborne, Australia	Gravel Filter Media	27-45% TN	Hatt, et al. 2007

Short term nitrogen mass retention is a physical process, and should be expected in a functioning pervious pavement system due to storm volume reduction (VADCR 2011). The length and magnitude of this initial retention period is dependent on the storage capacity of the control measure (Bernot and Dodds 2005). Long term biological removal can be expected in systems connected to the native subgrade where infiltration can allow for denitrification and plant uptake (Abustan, et al. 2012).

Nitrification processes via microbial action have been observed within the aggregate beds of mature porous pavement systems. One study observed the natural development of aerobic bacterial communities that thrived off of oil trapped within the geotextile layer of the system (Newman, et al. 2006). Once established, these colonies can perform nitrification in which ammonium (NH_4^+) is converted into nitrate (NO_3^-). This conversion to nitrate would increase the available nitrogen for denitrification processes in the subsoil in which nitrate is ultimately converted to nitrogen gas (N_2) by anaerobic bacteria (Kadlec and Wallace 2009). Through the cultivation of a microbial habitat within the pervious pavement itself, the long term nitrogen removal efficiency within the subsoils can be increased.

2.2.2 Phosphorus Removal

Phosphorus in stormwater is found in either a dissolved form or a particulate bound form. Ratios of these two types of phosphorus have been observed to vary based on land use. Generally, dissolved and particulate bound phosphorus associated with urban areas are present at a 1:1 concentration ratio (Perry, et al. 2009). Phosphorus removal is achieved two ways in pervious pavement systems: capture of sediments in the void space of the pavement, and sorption onto the aggregate bed and subsoils beneath the system (Welker, et al. 2012b). Intuitively, the particulate bound phosphorus will settle out via sedimentation or filtration, and the dissolved phosphorus forms will readily adsorb to the soil and aggregate surfaces during infiltration.

Particulate phosphorus transport occurs when the stormwater flow reaches a large enough velocity to carry the sediment bound chemical. Sedimentation of the suspended solids involves the velocity decrease of the stormwater as it infiltrates the top layers of pervious concrete systems (USDI 2006). This theory is justified as sediment typically clogs only the upper portion of the control measures (Balades, et al. 1995). Dissolved phosphorus preferentially adsorbs to solid surfaces rather than remaining in the liquid phase. Physical adsorption of the phosphorus compound is caused by Van der Waals and electrostatic forces. The magnitude of these forces are dictated by the surface area and polarity of the adsorbent (Slejko 1985).

As compared to total nitrogen removal behavior in pervious pavement systems, total phosphorus (TP) removal seems to be more consistent. Table 2.3 displays various total phosphorus removal rates found from laboratory and field scale studies.

Table 2.3: Pervious Pavement Systems and Phosphorus Fate

Location	Type of System	Removal	Reference
Prince William, VA	Porous Pavement	65% TP by mass	Tennis, et al. 2007
Rockvill, MD	Porous Pavement	65% TP by mass	Tennis, et al. 2007
NH	Porous Asphalt	42% TP	Roseen, et al. 2012
Melborne, Australia	Gravel Filter Media	53-83% TP	Hatt, et al. 2007

From the studies investigated, it seems that 50-80% of total phosphorus is typically removed from pervious pavement systems. The capacity of the material to adsorb phosphorus depends on the total surface area of contact, and thus varies for different grain sizes. Typically, finer grained soils, such as silt, have a higher adsorption capacity compared to gravel (Wang 2009). Non-vegetated systems can effectively capture

phosphorus for many years, as the adsorption capacity is usually far greater than the inflow concentration of phosphorus.

2.3 Villanova's Pervious Concrete Parking Lot

Built in 2007 as a comparison site, Villanova's pervious concrete parking lot was constructed in conjunction with an adjacent porous asphalt site. The control measure consists of an infiltration bed overlain by a 50' x 30' pervious concrete surface and an equally sized porous asphalt surface. Figure 2.3 displays the design of the pervious concrete side of the system.

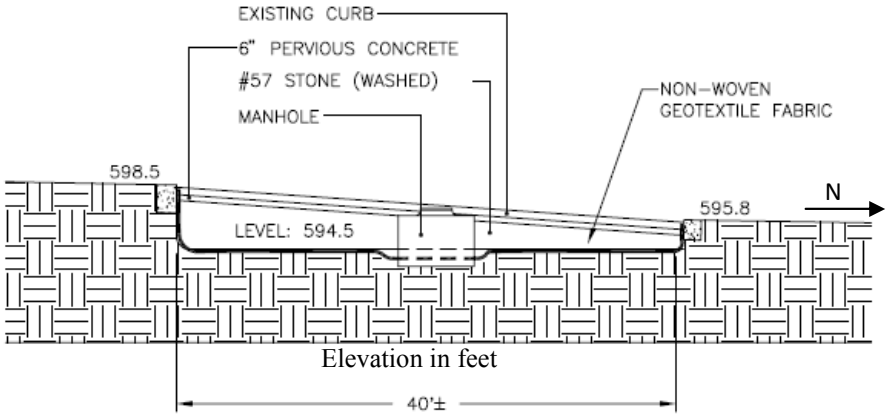

Figure 2.3: Design of Villanova's Pervious Concrete System

This stormwater control measure was constructed as a retrofit, and was required to conform to the existing pavement. Therefore, the average surface slope was designed to be 6.8% to the North, and 2% towards the East. Furthermore, the infiltration bed depth ranged from 1.3 to 4 feet throughout the system. The bed is comprised of washed stone with an approximate 40% void ratio. Initially, the infiltration beds underneath each section of pervious pavement were separated by a jersey barrier but reconstruction in 2009 prompted their hydrologic connection.

The pervious concrete/ porous asphalt site was instrumented at time of construction to allow for water quality and quantity data collection. Currently, a pressure transducer measures temperature and water depth within the aggregate infiltration bed on the pervious concrete side. Since the infiltration beds were connected in 2009, this pressure transducer offers a depth measurement representative of the entire aggregate bed. A rain gage was implemented on a nearby building to monitor precipitation over the site. Porewater samplers were implemented at depths beneath the infiltration bed to allow for collection of infiltrated runoff. Water quality testing was discontinued in the spring of 2011, but water quantity data is presently monitored.

2.3.1 Storm Volume Reduction

The infiltration bed underneath the pervious concrete/ porous pavement site was built to effectively handle storm magnitudes of 6 inches or less. A volume performance study was conducted in the summer of 2011 to check for post-construction site functionality. When constructed in 2007, the capacity of the infiltration bed was approximately 4150 ft^3 with an associated impervious drainage area of 7,800 ft^2. Table 2.4 displays a compilation of storms studied along with runoff volume, and any overflow.

Table 2.4: Volume Reduction Capacity of Villanova's Pervious Pavement Site

Storm Date	Storm intensity (inch)	Runoff Volume (ft^3)	Outflow Volume (ft^3)	% Volume Retained
7/8/2011	0.64	416	-	100
7/25/2011	0.97	631	-	100
8/14/2011	3.15	2048	-	100
8/27/2011	6.73	4375	229	94.8
9/6/2011	6.21	4037	-	100

The storm intensity was measured via a nearby rain gage while the outflow volume was monitored with a pressure transducer behind a v-notch weir. Interestingly, the only storm that produced outflow from the control measure was hurricane Irene on August 27th, 2011. Based on the volume reduction data, it can be concluded that the control measure is still properly functioning.

2.3.2 Fate of Nutrients

The fate of nutrients in a pervious pavement system has been seen to be variable when observing published laboratory and field studies (Sections 2.2.1 and 2.2.2). Total phosphorus and total nitrogen removal at Villanova's pervious concrete/ porous asphalt site was observed during 2007 and 2008. It was found that there was no statistical difference in nutrient removal between the pervious concrete and the porous asphalt sections. This is most likely due to the fact that the infiltration bed is the main mechanism for storm volume reduction and nutrient removal/retention.

For the 19 rain events tested, it was found that the total nitrogen concentration within the underlying soils were consistently higher than the influent stormwater runoff. Furthermore, since the site can handle volume up to the 6 inch storm, it can be assumed that all of the total nitrogen is retained in the infiltration bed (and eventually dissipated into the subsoil) during typical storm events. When looking at total phosphorus, the inflow concentration from the storms tested were typically greater than the concentrations found within the underlying soil (Barbis 2009). As stated before, total removal of phosphorus from the stormwater is inherent in the complete volume reduction of 6 inch

or less storm events. Removal of orthophosphate from the stormwater is expected to occur within the infiltration bed due to adsorption.

2.4 Post-Construction Monitoring Practices

To ensure longevity and efficiency of stormwater control measures, post-construction monitoring and maintenance is required. Unfortunately, only general guidelines exist on how to properly care for these systems, with the detail of monitoring required often up for interpretation. The USEPA has developed general maintenance and repair guidelines for the main types of control measures. Table 2.5 displays maintenance activities, their expected cost as a function of construction cost, and an implementation schedule.

Table 2.5: Recommended Maintenance Schedule

Management Practice	Annual Cost (% of Construction cost)	Maintenance Activity	Schedule
Detention Ponds/ wetlands	1-6%	Debris removal after major storm events (>2" rainfall), harvesting vegetation, erosion repair	Annual or as needed
		Accumulated sediment removal from forebays	5 year cycle
		Accumulated sediment removal from ponds	20 year cycle
Infiltration trench/ basin	1-20%	Debris removal after major storm events (>2" rainfall), mowing and maintaining vegetated areas	Annual or as needed
		Accumulated sediment removal in forebays or storage areas	3-5 year cycle
Filtration practices (including bioretention)	5-13%	Removal of trash from control openings, replace the top few inches of material once clogged	Annual or as needed
		Maintaining vegetation, removing invasive species, repair erosion areas	Annual or as needed
		Accumulated sediment removal to restore original infiltration rates	3-5 year cycle

(EPA 2012)

These general guidelines attempt to address a wide range of stormwater control measures and therefore are inherently non-specific. Visual inspection checklists with greater detail

have been set forth on a state level in an attempt to address more specific problems associated with aging stormwater control measures (NCDENR 2007; SEMCOG 2008; SCVURPPP 2012; Welker, et al. in press).

The monitoring techniques discussed thus far can be categorized as low level monitoring systems, where visual inspections are employed to assure that the control measure is functioning as designed. Medium level monitoring provides more detailed information to better define pollutant removal levels. Lastly, high level monitoring includes detailed water quality data collection and more sophisticated ecological monitoring (Welker, et al. in press). Low level monitoring practices are widely used in practice due to the inherent increase in costs of the higher level monitoring programs whereas high level monitoring methods are usually found in a research environment.

Chapter 3

Methods

In this section, the methods in which experimental parameters were developed are described for both the proof-of-concept and final design. Furthermore, testing procedures used to determine chemical concentrations are presented along with the testing protocol for the proof-of-concept and final design experiments. The proof-of-concept experiments involves pervious concrete systems within a 14 inch and 42 inch polyvinyl chloride column. The final design experiment involves a 24 inch pervious concrete system and sand infiltration bed within polyvinyl chloride columns.

3.1 Water Quality Testing

3.1.1 Total Phosphorus and Total Nitrogen

The DR/4000 HACH Spectrophotometer was used to measure the total phosphorus and total nitrogen concentrations for both the proof-of-concept and final design experiments. The HACH spectrophotometer is designed to measure the concentration of a chemical or compound in an aqueous medium. This is accomplished by measuring the amount of light absorbed through the medium at a specific wavelength, and relating this to various chemical parameters.

The total phosphorus testing method is dictated by HACH program 3036. Five mL of raw sample are prepared in HACH test tubes and digested for 30 minutes in the HACH Chemical Oxygen Demand (COD) Reactor (model 45600) at 150°C. After cooling, two mL of 1.54 N sodium hydroxide is added to each test tube, along with PhosVer 3 reagent

which will change the sample to a blue hue if phosphorus is present. A deep hue of blue indicates a large presence of phosphorus. This test method is valid for a phosphorus concentration range of 0.06 to 3.50 mg/L as PO_4^{3-} or 0.019 to 1.085 mg/L as P (Dukart 2008a).

The total nitrogen testing method is dictated by HACH program 2558. Similar to the total phosphorus test, two mL of raw sample are prepared in HACH test tubes. A 30 minute digestion occurs at 105°C in the COD Reactor. Once cooled, three sets of reagents are added to the test tubes and sufficient reaction times are allowed to convert all of the available nitrogen into the nitrate species. The samples are then transferred into another batch of HACH test tubes to react with a strong acid. This reaction will turn the contents of the tube bright yellow if there is a presence of nitrogen. This test method is valid for a nitrogen concentration range of 1.7 to 25.0 mg/L as N (Dukart 2008a).

Test results for both total nitrogen and total phosphorus are validated using the same procedures. For each test, a blank is prepared with filtered deionized water and tested in the HACH to establish a zero point. Then, samples prepared with a known standard are tested on the HACH machine, and are deemed acceptable if the measured concentration is within 10% of the standard. Lastly, a spike and duplicate sample are prepared and their concentrations are calculated by hand. The actual concentrations of the spike are measured on the HACH machine and checked against calculations for accuracy. A possible interference to the total nitrogen test during the final design experiments was the presence of chloride as a tracer. It was found that chloride in excess of 1000 mg/L could

positively skew data. This was not deemed a concern, as the concentration of chloride used for tracer did not exceed 700 mg/L.

3.1.2 Chlorides

Chlorides were used as a tracer for the final design experiment as a way to determine the fate of phosphorus and nitrogen in a system mass balance. A Systea EasyChem Spectrophotometer was used to test chloride concentration of samples. Raw samples are prepared in two mL EasyChem cups and placed directly into the machine. A calibration curve for chlorides is developed prior to each test using freshly prepared chloride reagent along with seven standards of known chloride concentrations. The chloride reagent consists of mercuric thiocyanate solution mixed with ferric nitrate solution (Dukart 2008b). Upon mixing of these two chemicals, an amber colored ferric complex is formed. The reagent is mixed with raw sample in the EasyChem machine, and the color intensity is measured and correlated to a chloride concentration based off of the calibration curve.

Quality assurance for testing chlorides on the EasyChem includes running several samples of filtered deionized water through the machine prior to testing until they read close to zero chloride concentration. During chloride testing, a sample of known concentration and a blank are tested after every 10^{th} sample to ensure accuracy of the machine. It is important to monitor the blank concentrations and ensure they produce concentrations lower than that of the lowest concentration on the chloride calibration curve.

3.2 Temperature Data Loggers

This section is an overview of the methods used to record surface and bed temperature of the experimental columns. Maxim Thermochron I-buttons were used to record temperature during the proof-of-concept phase, while Omega E Thermocouples were used to record and monitor real time temperature for the final design experiments.

3.2.1 I-buttons and Data Logger Software

Maxim DS1921G Thermochron I-buttons were used to measure and record surface and bed temperatures during proof-of-concept experiments. Figure 3.1 shows the dimensions (in mm) and outer appearance of a typical I-button.

Figure 3.1: Outer Shell (left) and Dimensions (right) of Typical I-button (EDS 2012)

The DS1921G model is able to remotely store 2048 temperature recordings at a user defined time interval. It records temperature in 0.5°C increments and has an accuracy of ±1°C within a temperature range of -30°C to 70°C. The internal clock has an average error of ±2 minutes per month of data recording. Temperature data can be extracted from the device by using a DS9490B "1 Wire" USB adaptor (Figure 3.2). The "1 Wire" I-button software allows the user to define recording intervals, calibrate the internal clock

of the I-button, set up a new data collection session, view previous data collections, and save temperature data sets to the computer.

Figure 3.2: "1 Wire" I-button USB Adaptor (EDS 2012)

The Thermochron I-button is typically placed within a Maxim DS9107 I-button capsule to protect the instrument during data sampling. This case serves to protect the I-button from moisture, solvents, and pressure. Constructed from polyphenylene sulfide, it remains stable during both long and short-term exposure to high temperatures, has inherent flame resistance, and high chemical resistance to strong bases, fuels, and acids. It is also UV resistant, and is not expected to degrade when exposed to long term sun light. Figure 3.3 shows the general appearance and dimensions (in millimeters) of the I-button case.

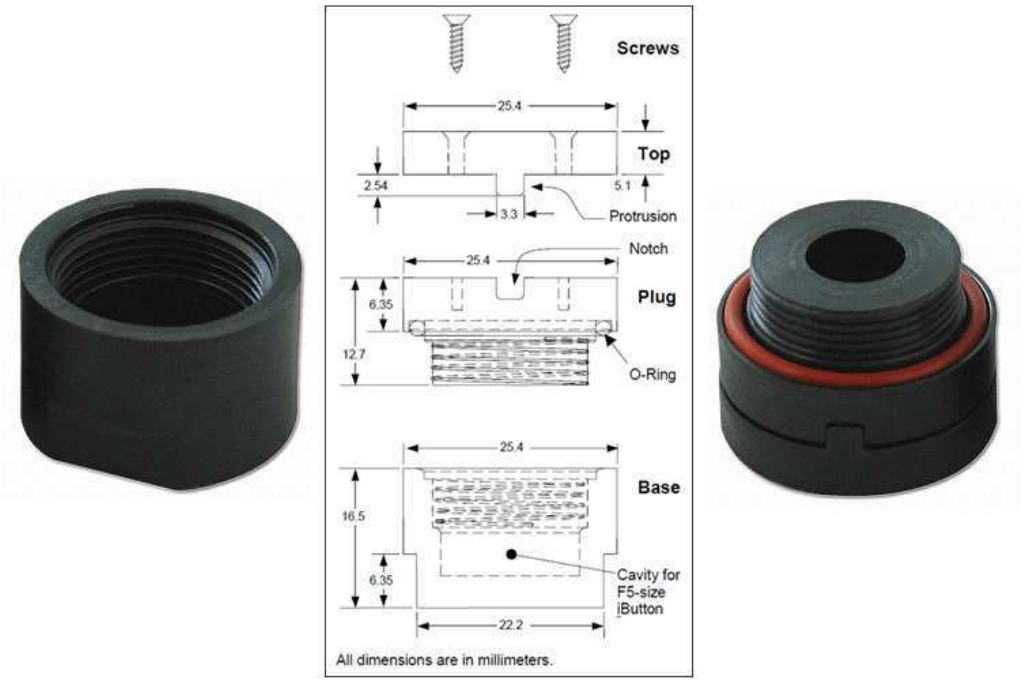

Figure 3.3: I-button Case (left and right) and Dimensions in mm (center) (EDS 2012)

3.2.2 Thermocouples and Data Logger Software

Omega E type thermocouples were used to record surface and bed temperature during the finalized design experiments. Generally, a thermocouple consists of two conductors comprised of different metal alloys. A voltage is produced from these conductors which is dependent on the difference in temperature between them. Specific alloys have a predictable and repeatable relationship between temperature difference and measured voltage (Williams 1988).

Specifically, Omega type E thermocouples contain one nickel-chromium conductor and one copper-nickel conductor. According to Omega, the type E thermocouple contains a 0.5% temperature error when reading from 0 to 200°C. Figure 3.4 shows the probe, wiring, and coupler assembly of a type E thermocouple.

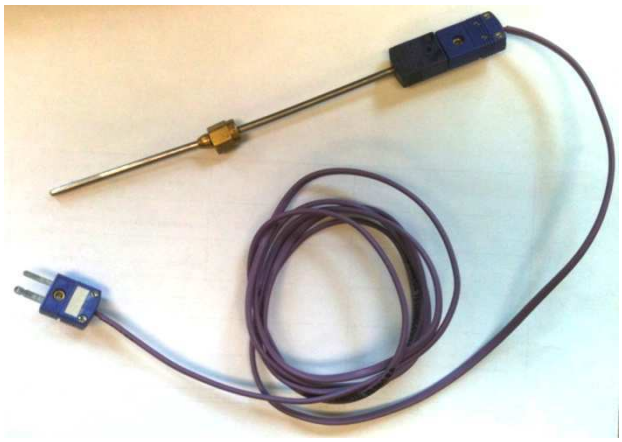

Figure 3.4: Type E Thermocouple Assembly

To view, record, and modify collection parameters the thermocouple assembly is connected to a PICO TC-08 Thermocouple Data Logger (Figure 3.5). This data logger can record up to eight channels simultaneously, and has an accurate temperature range of -270 to 1820°C with a ±0.5°C margin of error. The data logger connects to a computer via USB cable, and data can be accessed through "PicoLog" software. Within the PicoLog interface, the user can input sampling interval, total sampling time, and can also view real time temperature readings from the thermocouples.

Figure 3.5: TC-08 Thermocouple Data Logger (PICO 2012)

3.3 Proof-of-concept Experimental Parameters

To validate the temperature reduction and nutrient removal throughout a pervious concrete system, an experimental proof-of-concept was developed consisting of a 14 inch and 42 inch long columns contained in polyvinyl chloride. To simulate typical storm conditions at Villanova University, parameters such as storm intensity, temperature, and nutrient loading were determined.

3.3.1 Experimental Prototypes

Two previously constructed PVC columns were retrofitted and utilized for proof-of-concept testing. Villanova's pervious concrete parking lot served as a basis for design in terms of material composition and layer thickness. Table 3.1 presents the relevant dimensions and features of both columns, as well as a comparison to the Villanova pervious concrete parking lot.

Table 3.1: Proof-of-concept Column Dimensions and Relevant Features

	Column 1[a]	Column 2[a]	VU PC site
Top Layer			
Material	Pervious concrete	Pervious concrete	Pervious concrete
Thickness	3 inches	6 inches	6 inches
Porosity	0.20	0.20	0.15-0.20[b]
Hydraulic conductivity	24.8 m/hr	24.8 m/hr	7.2-43.2 m/hr[b]
Aggregate Layer			
Material	AASHTO#57 stone	AASHTO #57 stone	AASHTO #57 stone[c]
Thickness	11 inches	36 inches	48-16 inch range[c]
Porosity	≅0.40	≅0.40	0.40[c]

[a](Nemirovsky 2011)
[b](Tennis, et al. 2007)
[c](Jeffers 2009)

By using two columns of different lengths, unique temperature responses are expected, and non-uniform nutrient removal efficiencies may be observed.

3.3.2 Storm Simulation Development

To determine the inflow volume into columns 1 and 2 (14 inch and 42 inch long respectively) caused by a typical storm event, a storm simulation needed to be developed that accounted for the geographic location and drainage area of Villanova's pervious concrete site. This pervious concrete parking lot measures 50 x 30 feet, and has a 100% impervious drainage area of 3900 ft^2. Hence, the directly connected impervious area (DCIA) ratio to the system is 2.6 to 1. However, the PADEP recommends a 5 to 1 impervious drainage area to infiltration area for most stormwater control measures (PADEP 2006). Therefore, a DCIA of 5 to1 was chosen for the development of the storm simulation which would produce a theoretical drainage area of 0.44 ft^2 for a 4 inch diameter column. This parameter is needed in determining the experimental inflow volume into the column, which will be discussed shortly.

Storm magnitudes of 1,5, 25, and 100 years were chosen to display temperature and nutrient responses of typical and extreme storm events as they are simulated though the columns. Table 3.2 displays the corresponding storm magnitude of each chosen return period for Montgomery County (USDC 1963).

Table 3.2: Storm Simulation Magnitudes

Return Period (yr)	1	5	25	100
Magnitude (inches)	1.15	1.75	2.55	3.38

A storm duration of one hour was chosen based on physical time constraints of the experiment. The Soil Conservation Service (SCS) type II storm distribution was applied to reflect the incremental rainfall of the three chosen storms over a one hour storm duration. The cumulative rainfall distributions over a one hour period can be seen in Figure 3.6.

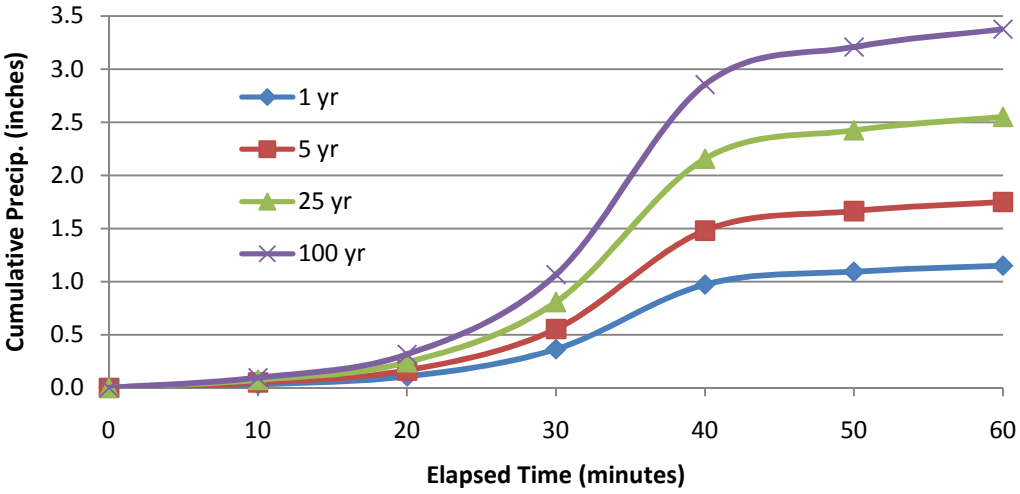

Figure 3.6: SCS Type II Distributions for One Hour Design Storms

The Simple Method was employed to determine the runoff from the theoretical drainage area of each column given a known rainfall. Developed by Schueler (1987), this method utilizes the relationship between percent imperviousness and the fraction of rainfall that is converted to runoff. This relationship is defined as:

$$R_{V=}0.05 + 0.9I_A$$

Where R_V is the runoff coefficient (unitless) and I_A is the impervious fraction of the drainage area. Once R_V was determined, the volume of runoff due to a design storm can be calculated as:

$$V = 3630R_D R_V A$$

Where V is the calculated runoff in cubic feet, R_D is the storm rainfall depth in inches, and A is the watershed area in acres. By applying this method to the one hour incremental rainfall distribution, the incremental runoff volume for the 1, 25, and 100 year 1 hour storms were determined, and are displayed in Table 3.3. These runoff volumes will be utilized as inflow volumes as each storm is simulated through column 1 and 2.

Table 3.3: Cumulative Inflow Volume for Chosen Storms

Elaped time (min)	1 yr 1 hour (mL)	5 yr 1 hour (mL)	25 yr 1 hour (mL)	100 yr 1 hour (mL)
0	0	0	0	0
10	31	47	68	90
20	100	153	222	294
30	338	516	750	993
40	906	1380	2010	2660
50	1018	1550	2258	2989
60	1072	1631	2376	3145

3.3.3 Spiked Inflow Development

This section details the methodology behind nutrient loading concentrations that were chosen to simulate urban runoff due to a typical summer storm event. Phosphorus and nitrogen concentrations at Villanova's pervious concrete parking lot were investigated, as well as stream water quality standards implemented by the PADEP and the EPA.

3.3.3.1 Nitrogen

In an effort to closely mimic site conditions, inflow total nitrogen concentration data at Villanova's pervious concrete site was investigated. In a 2007-2008 water quality study, an average total nitrogen concentration of 2.87 mg/L was found to enter the pervious concrete system based off of data from 19 storm events (Barbis 2009). This value is reasonably low, and implies a relatively clean urban runoff in terms of total nitrogen

concentration. To clearly reflect possible nitrogen removal through the test columns, a higher concentration of incoming nitrogen was used in the experiment.

Villanova's pervious concrete parking lot infiltrates stormwater runoff and conveys flow to Mill Creek in the form of groundwater and through the conventional storm sewer system given a large enough storm event. To determine a reasonable total nitrogen inflow, parameters of Mill Creek were investigated such as level and type of stream impairment, and allowable point and non point discharges. Upon investigating a stream report published by the Lower Merion Conservancy (2009), it was found that Mill Creek is an impaired watershed for suspended solids, and also reaches temperatures of about 75°F during the summer months; which is high enough to stress or eliminate trout populations. Temperature and suspended solids impairment is most likely due to urban storm water runoff.

Currently, Mill Creek is not impaired with high nitrogen levels, and therefore nitrogen influent to Mill Creek is governed by PA code § 93.7: Specific Water Quality Criteria. This clause dictates that the concentration of nitrate and nitrite species should not exceed 10 mg/L at any time. Furthermore, the Environmental Protection Agency lists that most fish can tolerate ammonia/ammonium concentrations of up to 40 mg/L N (EPA 2012). Upon considering State and Federal water quality standards, and the detection limits of laboratory equipment, an inflow concentration of 25 mg/l as nitrogen was chosen for storm simulations.

3.3.3.2 Phosphorus

In the 2007-2008 water quality study of Villanova's pervious concrete site, the average total phosphorus inflow was found to be 0.77 mg/L for the 19 storms sampled (Barbis 2009). From the 2009 Mill Creek report (LMC), phosphorus has not been deemed an impairing nutrient. Based on the PADEP Implementation Guidance for Code 95.9, there is no need for phosphorus control if no nutrient impairment is evident (1997). However, this document stipulates that if a Stream Enrichment Risk Analysis (SERA) indicates future phosphorus impairment, then a cap of 0.62 mg/l phosphorus discharge should be implemented on point sources. Based on these factors, a phosphorus concentration of 0.81 mg/L was chosen as inflow concentration for storm simulations in the form of orthophosphate (PO_4^{3-}).

3.3.4 Temperature Parameters

Ambient temperature parameters were determined for the proof-of-concept experiments by analyzing summer temperature data at Villanova's pervious concrete parking lot. Initial aggregate bed temperature was determined from a pressure transducer located adjacent to the sites rock bed. This pressure transducer records depth of water in the aggregate bed, as well as ambient temperature at ten minute intervals. The average rock bed temperature was found to consistently range from 68 to 75°F, with an average temperature of 74°F during June-September of 2011. Since the ambient temperature of the Soils Laboratory on Villanova's campus fluctuated within the same range, this location was chosen for experimental testing.

The surface temperature of the column and storm simulation inflow temperature was found by averaging storm temperature responses at the pervious concrete parking lot. Table 3.4 shows the surface and first flush inflow temperatures for eight storms on record. These temperatures were recorded using Thermochron I-buttons which were set to remotely store temperature data every 20 seconds.

Table 3.4: Storm Temperature Data

Storm Date	PC runoff Temp (F)	PC Surface Temp (F)
8/10/2008	79.3	82.4
9/5/2008	85.6	101.9
7/3/2009	81.5	91.4
8/2/2009	83.3	72.5
8/8/2009	88.3	98.6
8/12/2009	82.0	80.0
8/3/2011	84.7	93.8
8/9/2011	91.9	100.9
AVG	**84.6**	**90.2**

Upon review of this data, an average surface temperature of 90°F and an average inflow temperature of 85°F were used for the proof-of-concept experiments.

3.4 Proof-of-concept Experimental Procedure

Proof-of-concept experimentation was carried out on the 14 inch and 42 inch long pervious concrete columns, which had been constructed by Evgeny Nemirovsky (2011). A simple visual representation of the experimental process can be seen in Figure 3.7. As a storm is simulated through the test column, it is expected that a temperature reduction of storm runoff will occur as water trickles through the aggregate bed of the pervious concrete system. Furthermore, nutrient reductions are expected to occur based on observed behavior of Stormwater Control Measures. The proof-of-concept testing was set

forth to verify the temperature and nutrient response of a pervious concrete system. For simplicity, the temperature and nutrient responses were evaluated separately for the proof-of-concept testing. The 1, 25, and 100 year, one hour storms were simulated through both columns to observe temperature responses. For these tests, deionized water was used without a nutrient spike. The 5 year one hour storm was simulated through the 42 inch long column to observe nutrient responses using the previously mentioned phosphorus and nitrogen concentrations.

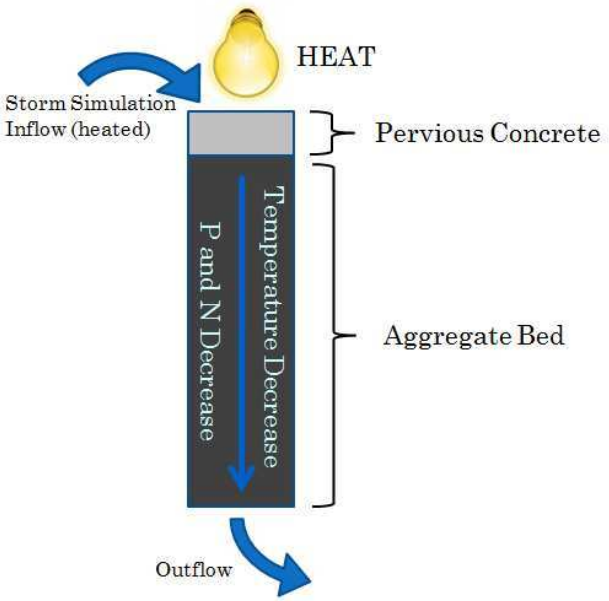

Figure 3.7: Visual Representation of Experimental Processes

Initially, the surface of the pervious concrete column was heated to 90°F via a Workforce portable lamp with a halogen bulb. To achieve a consistent temperature, the distance of the lamp from the surface was varied, and the power output of the lamp was occasionally switched between 125 and 250 Watts. The lamp remained on during the duration of the storm simulation (which was later revised for the final experimental procedure). The surface temperature of the test column was monitored with an ASTM 5F thermometer, as no real time monitoring can be achieved using a Thermochron I-button.

Prior to simulating the storm through the test columns, the inflow was heated to 85°F through the use of a Rival electric griddle (Figure 3.8). The storm inflow was contained in various sizes of glass Erlenmeyer flasks. The griddle temperature was controlled by a temperature knob, and temperature was observed with an ASTM 5F thermometer. Two Thermochron I-buttons were used to record temperature of the column. One I-button was placed at the surface of the pervious concrete, while the other was placed inside the base of the column to record bed temperature. For proof-of-concept testing, the I-buttons were set to record temperature readings every 20 seconds.

Figure 3.8: Heating of Storm Simulation Inflow

Once the surface of the column and the inflow was sufficiently heated, a one hour storm was simulated though the test column. The 1, 25, and 100 year one hour storms were simulated though the 14 and the 42 inch long columns, resulting in six experimental runs. The inflow magnitude at each time increment can be viewed in Table 3.3. The complete experimental set up is shown in Figure 3.9, located in Villanova's Soil Laboratory. To

replicate heat transfer behavior in the field, both columns were insulated with R-13 fiberglass insulation to combat horizontal heat transfer.

Figure 3.9: Proof-of-concept Experimental Setup, 14" Column (left) and 42" Column (right)

As mentioned previously, the 42 inch column was used to verify nutrient removal through the system during a 5 year 1 hour storm. The storm simulation inflow was spiked 0.81 mg/L P and 25 mg/L N. During the incremental addition of inflow to the test column, three outflow samples were collected and stored to be used for total nitrogen and total phosphorus testing. The temperature and nutrient responses of the proof-of-concept experiments are provided in Chapter 4.1.

3.5 Final Design Experimental Parameters

3.5.1 I-buttons Versus Thermocouples

The proof-of-concept testing revealed that the Thermochron Ibuttons were inadequate for this laboratory experiment. The Maxim DS1921G I-button recorded temperature in 0.5°C

increments and therefore was limited in resolution. Furthermore, real time temperature cannot be read from an I-button, which left room for error when heating the surface of the test column up to the target temperature. Based on these drawbacks, Omega type E thermocouples were chosen to record temperature in the final column experiments.

3.5.2 Pervious Concrete Column Construction

Two test columns were constructed for the purpose of the final experimental apparatus. Similar to the proof-of-concept, one column was designed based on Villanova's pervious concrete faculty parking lot. A cross section of the pervious concrete SCM is shown in Figure 3.10.

Figure 3.10: Villanova's Pervious Concrete Parking Lot

The pervious concrete layer remains a constant 6 inches thick throughout the lot. The aggregate bed depth ranges between 15.6 and 48 inches. The PADEP BMP manual recommends an aggregate bed depth between 12 and 36 inches (2006). Based on these

considerations, 6 inches was chosen for the thickness of the pervious concrete layer, and 18 inches was chosen of the thickness of the underlying aggregate bed.

Construction of the pervious concrete column began with the creation of the 6 inch pervious concrete layer encased in 4 inch diameter PVC pipe. The concrete was comprised of 1 part cement, 0.4 parts water, and 4.67 parts coarse aggregate by weight, based off of Dr. Francis Hampton's mix design. Villanova's Structural Laboratory was utilized to create three pervious concrete samples which were left to cure for 4 weeks between December 2011 and January 2012 (Figure 3.11). These sections will be referred to "PC1", "PC2" and "PC3" throughout the text.

Figure 3.11: Pervious Concrete Construction for Final Design

Once cured, the pervious concrete sections were tested for hydraulic conductivity, and porosity. "ASTM C1701: Standard Test Method for Infiltration Rate of in Place Pervious Concrete" was used as a basis for hydraulic conductivity testing. By maintaining a constant water head and timing the amount of water infiltrated, the hydraulic conductivity was found using the equation:

$$I = \frac{KM}{(D^2 t)}$$

Where I is the infiltration rate in inches per hour, K is the conversion ratio (126,870 for imperial units), M is the weight of infiltrated water in pounds, D is the inside diameter of the sample being tested in inches, and t is the time required for measured amount of water to infiltrate the specimen in seconds. Three tests were performed on each PC section and results were averaged. Table 3.5 displays the results of hydraulic conductivity testing as compared to the conditions at Villanova's parking lot.

Table 3.5: Hydraulic Conductivity of Pervious Concrete Sections

Sample	Hydraulic Conductivity (inch/hr)	Average
PC1	649	637
	628	
	635	
PC2	271	253
	250	
	239	
PC3	599	586
	581	
	578	
Villanova's PC lot	-	*505-1542

*(Jeffers 2009)

The infiltration rates of PC1 and PC3 remained within acceptable design limits when compared to Villanova's pervious concrete lot. PC1 infiltrated water at the fastest rate, indicating minimal clogging of pore spaces. PC2 and PC3 showed visible "sealing" which led to a decrease in hydraulic conductivity. Sealing occurs when the water content in the concrete mix is too high upon pouring, resulting in the cement sealing off portions of the pores within the concrete itself. PC 2 showed the highest amount of visible sealing which was verified by its poor infiltration results.

Volume displacement (VD), mass balance (MB), and volume capture (VC) porosity tests were performed on the cured PC sections. The volume displacement method involves immersing the pervious concrete sections into a known volume of water. The amount of displaced water indicates the volume of solids, and ultimately the volume of voids within the concrete. In this method, one must subtract the volume of the PVC shell from the total volume to obtain an accurate porosity. The mass balance method involved measuring the change in mass as water was infiltrated into the PC sections. This method involved capping one end of the concrete so that no water could escape. Similarly, the volume capture porosity test involved measuring the volume of water that the sections could hold with one end capped (Hagar 2009). Table 3.6 shows the porosity test results as compared to Villanova's pervious concrete lot.

Table 3.6: Porosity of Pervious Concrete Sections

Sample	Porosity	Average
PC1	VD- 0.12	0.13
	MB- 0.13	
	VC- 0.15	
PC2	VD- 0.09	0.09
	MB- 0.08	
	VC- 0.11	
PC3	VD- 0.07	0.10
	MB- 0.11	
	VC- 013	
Typical Pervious Concrete	-	*0.15-0.20

*(Tennis, Lemming, and Akers 2007)

In general, PC1 was found to have the highest porosity as compared to the other sections. PC2 performed relatively poorly, possibly as a result of the noticeable sealing that could block off internal pore spaces. Overall, PC1 reflected a hydraulic conductivity and porosity the closest to field conditions, and was therefore used in the final column design.

An 18 inch section of 4 inch diameter PVC pipe was obtained, and filled with AASHTO #57 stone. In accordance with ASTM D448-12 "Standard Classification for Sizes of Aggregate for Road and Bridge Construction," #57 stone should have the following grain size distribution listed in Table 3.7.

Table 3.7: AASHTO #57 Stone Grain Size Distribution

Sieve Size Opening	% Passing
1 ½" (37.5 mm)	100
1" (25.0mm)	95-100
½" (12.5 mm)	25-60
No. 4 (4.75 mm)	0-10
No. 8 (2.36 mm)	0-5

To hold the aggregate bed in place, a drainage cap was constructed using a PVC female adaptor, PVC threaded cap, and Fernco rubber coupling. The Fernco coupling is flexible and becomes water tight once affixed to PVC piping via stainless steel clamps. To ensure sufficient drainage of the column during experiments, seventeen 3/8" holes were drilled into the PVC threaded cap which was then affixed to the PVC female adaptor. This assembly was attached to the 18 inch PVC column by the Fernco coupling. An exploded view of the drainage system is shown in Figure 3.12.

Figure 3.12: Drainage Assembly for Final Design

A false drain was constructed using the same components as the aforementioned drainage system to secure the thermocouple at the base of the apparatus (to record bed temperature). In this way, the thermocouple can be easily placed and retrieved by loosening and tightening the Fernco coupling. Having a false drain also ensures that no aggregate will be disturbed while adjusting the thermocouple.

The last stages of column assembly included attaching PC1 to the top of the aggregate layer by another Fernco coupling, and wrapping the exterior of the column with R-13 fiber glass insulation to inhibit horizontal heat fluctuations. Figure 3.13 shows a slice perspective of the completed pervious concrete column. By using Fernco couplings and avoiding adhesives, the column can be assembled (and unassembled) modularly, thus holding a high recycle value for future projects.

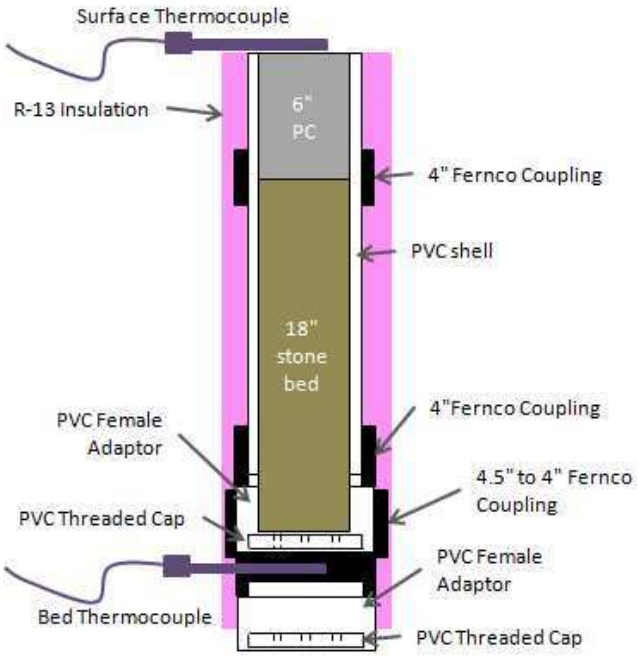

Figure 3.13: Final Design: Pervious Concrete Column

3.5.3 Sand Column Construction

In an effort to increase pollutant removal efficiencies, recent research has investigated the implementation of sand filters to serve as the bed layer in various Stormwater Control Measures and some wastewater treatment applications (Collins, et al. 2010, IDEM 2007, Healy, et al. 2007). The second test column was constructed to contain a 24 inch sand bed in order to identify nutrient removal differences as a function of grain size.

A 24 inch section of 4 inch diameter PVC piping was cut to create the shell of the sand bed. Sand was obtained from Villanova's Soils Laboratory. A grain size analysis test was performed based on ASTM C136-06 "Standard Test Method for Sieve Analysis of Fine and Coarse Aggregates". Figure 3.14 shows the grain size distribution curve for approximately 2200 grams of soil mixture.

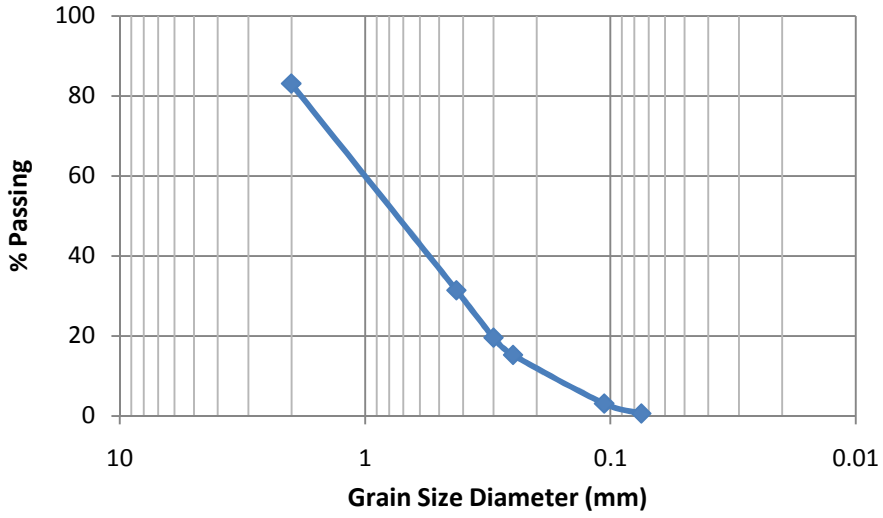

Figure 3.14: Grain Size Distribution Curve for Sand Column

According to the AASHTO Soil Classification System, the soil sample is A-1-b or coarse sand. Based on the United Soil Classification System (USCS) the soil is SP, or poorly graded sand. This soil type was deemed acceptable and was used as the sand bed layer in

the second column design. To retain the sand in the column, a geocomposite was affixed to the base of the 24 inch PVC column with Loctite Heavy Duty Epoxy. The geocomposite consists of a geonet sandwiched between two non-woven geotextiles. A bulk density test was performed on the sand following "ASTM D7263-09: Standard Test Methods for Laboratory Determination of Density (Unit Weight) of Soil Specimens." Approximately 63.6 inch^3 of coarse sand was used producing a bulk density value of 99.3 pcf. An infiltration test was performed on the sand column and displayed in Figure 3.15. The column was initially saturated in an attempt to parallel experimental conditions.

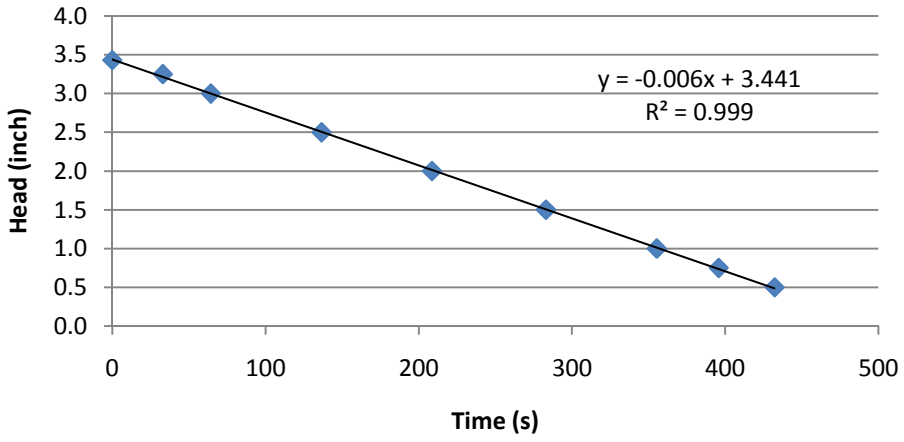

Figure 3.15: Saturated Infiltration Rate of the Sand Column

A linear trend line revealed the infiltration rate to be 0.006 inches/second, or 21.6 inches per hour. This saturated infiltration rate is within the expected range for sand (Massman and Butchart 2001).

A drain and false drain were constructed for the sand column which paralleled the drains constructed for the pervious concrete column. The sand column was also wrapped in R-13 insulation to inhibit horizontal heat transfer. A cutaway drawing of the completed sand

bed column is displayed in Figure 3.16. As mentioned previously, the false drain allows for easy adjustment of the bed thermocouple.

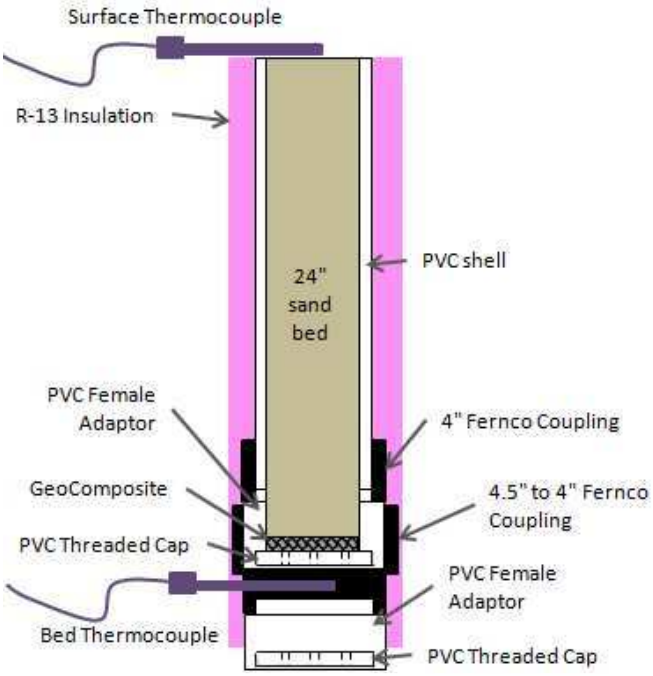

Figure 3.16: Final Design: Sand Column

3.5.4 Column Base Construction and Sample Collection

To support the columns during experimental testing, a wooden base was constructed. It was needed to elevate a test column a sufficient height off the ground to allow for sample collection. A 30 x 10.5 x 1.5 inch piece of wood was used as the top of the base in which a 4 inch diameter hole was cut out of the center using a battery powered reciprocating saw. Two 30 x 10.5 x 1.5 inch pieces of wood were used as the legs of the base. The legs were affixed to the top via 3 inch long stainless steel flat-head screws. A 27 x 1 x 1 inch length of wood was used to brace the two legs on one side. The other side was left open to allow for water sample collection. Figure 3.17 shows the completed wooden base.

Figure 3.17: Wooden Base for Final Design Experiments

To ensure the stability of the column, the entire apparatus needed to be level. A hand level was used to verify that the floor of the Soils Laboratory had zero pitch. During construction of the base, the top was intermittently tested and adjusted so that the column would remain in a vertical position. Finally, the 4 inch diameter hole in the base was tapered with sand paper to ensure a good fit with the false drain of the test columns.

3.5.5 The First Flush Phenomenon

The storm simulations from the proof-of-concept testing were revised to only include the first flush volume. The California Department of Transportation (2005) defines the first flush as a phenomenon associated with the occurrence that the first portion of stormwater runoff in a storm event is the most contaminated. Figure 3.18 shows a visual representation of this concept. As the storm progresses, the most polluted water samples occur when runoff just begins, and the samples become incrementally less polluted as the storm progresses through time (as seen visually with the suspended solids content). In theory, the first flush should also be warmed from traversing hot pavement during summer months. In this way, the first flush should contain the highest amount of

pollutants, and should show the greatest temperature response as it travels through a Stormwater Control Measure.

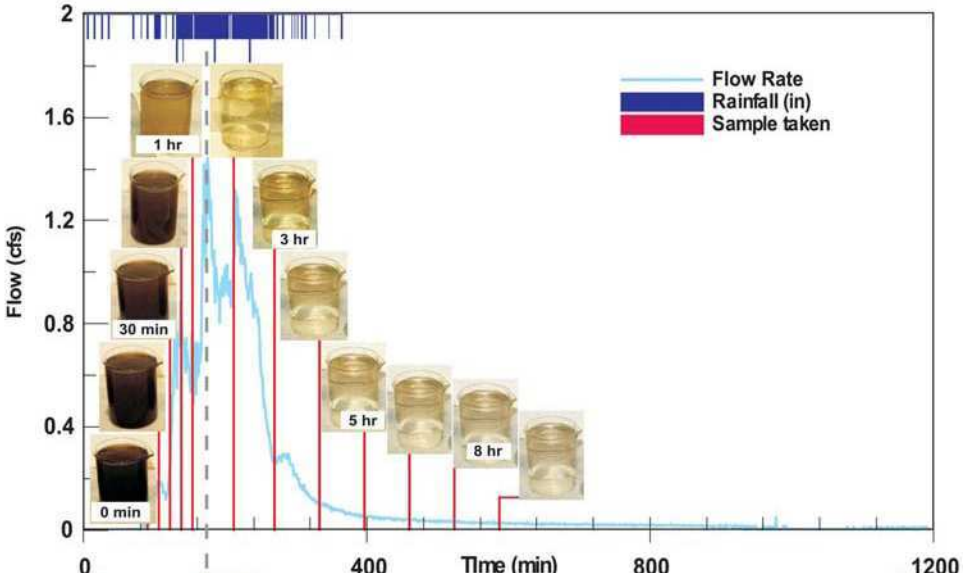

Figure 3.18: First Flush Phenomenon (CADOT 2005)

The EPA defines the first flush based on the event mean concentration (EMC) and the partial event mean concentration (PEMC). The EMC is defined as the storm's total pollutant mass divided by the storm's total runoff volume. The PEMC is any discrete point along the corresponding storm event pollutograph. The first flush is said to occur until the PEMC is less than the EMC (EPA 1993). Generally, the first flush is commonly defined as the first 0.5 inches of rainfall or the first 40-60% of the storm volume (Sansalone and Hird 2002).

In a study conducted on Villanova's Infiltration Trench, the first flush phenomenon for total suspended solids was found to occur up to 0.98 inches of rainfall (Batroney, et al. 2010). Based on the definitions of the first flush phenomenon, an inflow magnitude of

618 mL was chosen. This corresponds to the first 0.66 inches or first 31% by volume of a 10 year, 1 hour storm.

3.5.6 Temperature Calibration

Due to the revision in experimental procedures, the initial temperature response of the column was able to contain more detail and accuracy. As mentioned previously, the temperature readout from thermocouples can be monitored in real time via a USB connection to a computer. In this way, the surface and ambient temperature of the final column was tweaked during the experiment to produce a more realistic temperature profile as the first flush of the storm simulation enters the system.

The temperature response of a typical summer storm over Villanova's pervious parking lot was needed to determine general trends of the surface, first flush runoff, and aggregate bed temperatures. In total, 8 summer storms from 2008 to 2011 were evaluated, and it was determined that the storm occurring on June 10, 2008 displayed typical rainfall patterns and temperature responses (Figure 3.19).

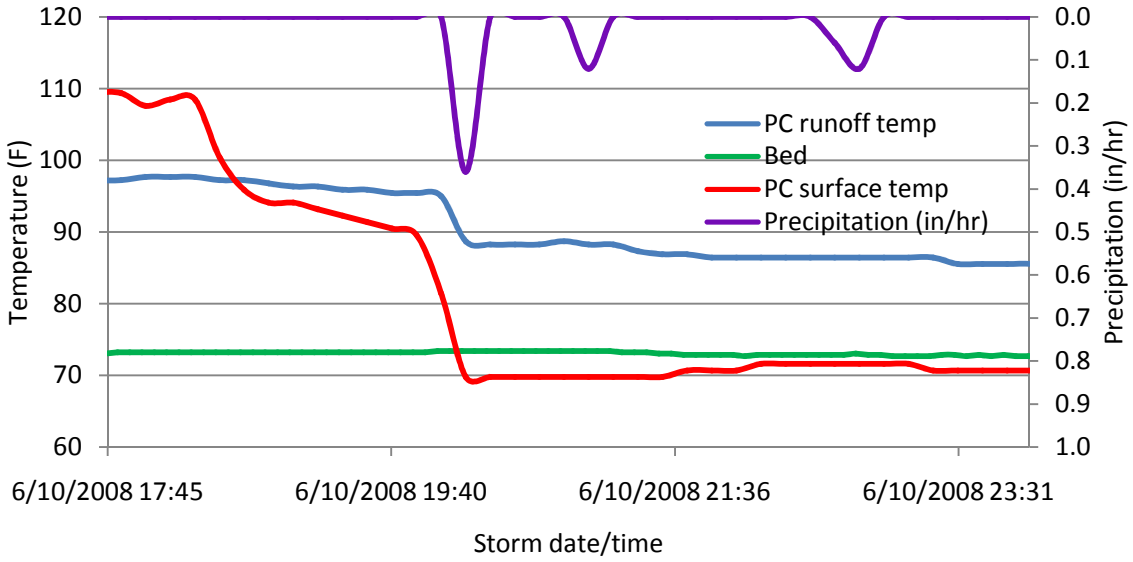

Figure 3.19: Storm for Temperature Response Calibration

The surface temperature of the pervious concrete parking lot (denoted in red) initially hovers around 110°F. As clouds appear in the sky and air becomes more turbulent prior to rainfall, the surface temperature steadily drops to 90°F. This temperature drop was not observed for dry evenings in June 2010 (Weather Underground 2010). At this point, the first flush of the storm hits the pavement (purple line), which results in another drop in surface temperature until it stabilizes at 70°F. The first flush or inflow temperature can be estimated from Figure 3.18 using the blue line. Once the storm hits the pervious concrete system, the average inflow temperature is estimated to be 86°F. Furthermore, the bed temperature of the system (denoted by the green line) remains between 73°F and 74°F for the duration of the storm.

To calibrate the experimental setup to mimic surface temperature conditions at the pervious concrete parking lot, the Workforce lamp was used at various distances away from the test column until a constant temperature of 110°F was achieved. Then, the lamp

was turned off to allow the surface to cool until it reached 90°F. The first flush was then poured into the test column heated via a Rival warming tray. Experimental temperature calibration can be seen in Figure 3.20 using the pervious concrete column.

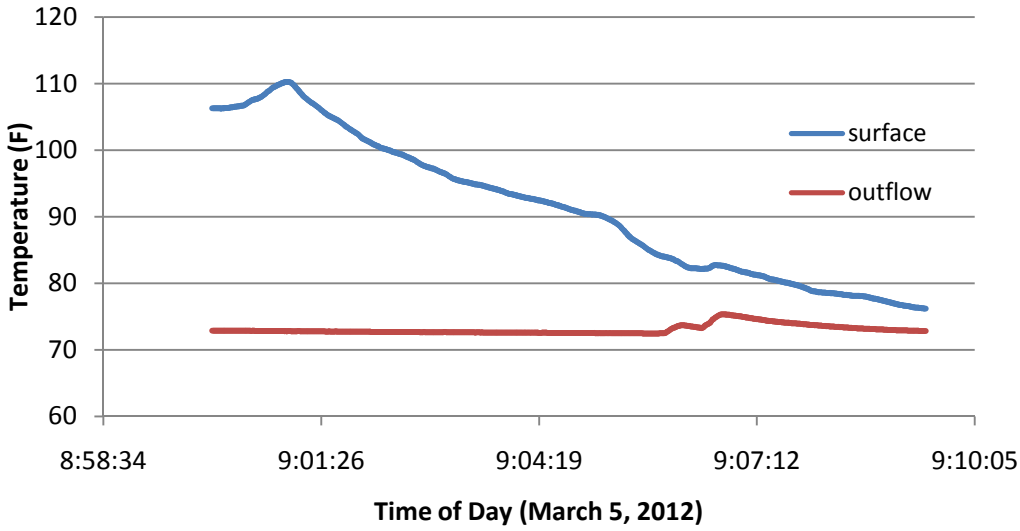

Figure 3.20: Temperature Calibration for Final Experimental Setup

The temperature responses for the pervious concrete and sand columns are provided in Chapter 4.2.

3.5.7 Mass Balance Calculations

To gain an understanding of the fate of the nutrients in the test column, it was decided that a mass balance should be used for final experimentation. By definition, the mass that enters the system must, by conservation of mass, either leave the system or accumulate within the system (Himmelblau 1967). Unlike the proof-of-concept testing, the retrieval of all outflow water was necessary to obtain a mass balance of the system. The original proof-of-concept nutrient concentrations were kept consistent with the final design experiments (0.81 mg/L as P, 25 mg/L as N). In addition, a tracer consisting of 593 mg/L as chloride was added to the inflow mixture. By remaining inert in water, chloride is

commonly used as a hydrological tracer to characterize chemical processes in an experimental system.

Through the proof-of-concept testing, it was realized that the fate of phosphorus and nitrogen was still fairly unknown. For example, the phosphorus in the spiked inflow could either be adsorbing, or simply being retained in the pore spaces of the aggregate bed. Nutrient retention could be possible in the proof-of-concept experiments because there was notable detention of the storm simulation volumes (especially the smaller magnitude "storms"). To separate retention processes from removal, the final experimental process involved the immediate flushing of the spike plug from the column through the addition of deionized water. The estimated pore volume in the sand column was found to be 1.4 liters, so 1.6 liters of deionized water was chosen after adding a small factor of safety. This magnitude was used for both test columns in the final experimental procedure for consistency. With the addition of the chloride tracer, flushing of the spiked inflow plug, and mass balance calculations, the fate of the nutrients in the test columns were clearly identified.

The general equation for the mass balance used in the final column experiments is shown below, where M_u is mass unaccounted for, M_r is mass retained, M_i is mass into the system, and M_o denotes mass leaving the system.

$$M_u = M_i - (M_r + M_o)$$

M_i and M_o are found by multiplying the concentration of the sample by the associated volume. The inflow and outflow concentrations are known parameters found from the

spectrophotometer analysis. The retained mass (M_r) is the mass of nutrients that are still present in solution trapped in the pore spaces of the test column. This mass was calculated by multiplying the inflow concentration by the volume of water remaining in the system, assuming total mixing of the first flush and deionized flush. Therefore, the mass difference or unaccounted for in the system (M_u) can give an indication of the removal processes of the nutrients. The experimental results for the mass balances are provided in Chapter 4.2.

3.6 Final Design Experimental Procedure

The 24 inch long pervious concrete column system and the 24 inch long sand bed were both tested three times for temperature and nutrient response when exposed to the first flush storm simulation. Similar the proof-of-concept testing, the first flush inflow was heated using the Rival electric griddle. The surface of the test column was heated by the Workforce portable lamp, and temperature was monitored in real time by the thermocouples. Figure 3.21 shows the general setup for the final design experiment.

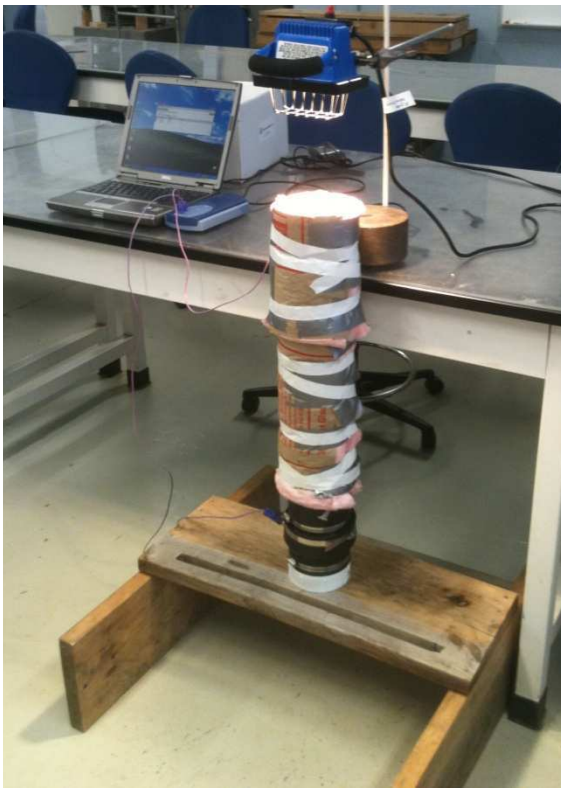

Figure 3.21: Final Experimental Apparatus

Once the surface of the test column was sufficiently heated, the Workforce lamp was turned off and the surface was allowed to cool to 90°F. At this point, the heated first flush inflow was poured through the test column, mimicking the surface temperature responses seen at Villanova's pervious concrete site. After the temperature effects were apparent in the test column, deionized water was flushed through the system to remove the first flush spike. As mentioned previously, the mass balance equation requires a known outflow i.e. a full capture of the outflow from the test column. Gilson stainless steel weighing bowls were placed underneath of the wooden base to capture discharge during experimentation (Figure 3.22).

Figure 3.22: Gilson Stainless Steel Weighing Bowls

Eleven outflow samples were collected in increments throughout the experimental process for both columns. Effluent collected from the Gilson bowls were transferred into Nalgene plastic containers and taken to Villanova's Water Resources Laboratory for chemical testing. Between each experiment, the test columns were flushed with five pore volumes of deionized water. Samples of this flush were preserved and tested in the laboratory for chlorides to ensure the columns did not retain residual loadings from previous experiments.

Chapter 4

Column Experimental Results and Discussion

4.1 Experimental Results of Proof-of-concept

This section presents the temperature responses of the proof-of-concept columns when exposed to summer storm simulations of the 1 year, 25 year, and 100 year one-hour storm magnitudes. Under the same temperature conditions, a nutrient response was observed from the 42 inch long column for the 5 year one hour storm spiked with nitrogen and phosphorus. These parameters are compared and used to estimate nutrient removal for a temperature decrease through the storm water control measure. In the following section, the 42 inch long column is commonly referred to as the "long" column, and the 14 inch long column is designated the "short" column.

4.1.1 Temperature Response

Both the 42 and 14 inch long pervious concrete column systems were tested for temperature responses using the 1, 25, and 100 year 1 hour storm simulations. During the experimental process, the surface of the test column was heated to 90°F and the ambient temperature of the room was measured to verify it was within a reasonable range of 70-74°F. Thermochron I-buttons were used to measure surface and outflow temperature fluctuations in 20 second intervals. Figure 4.1 shows the temperature results for the 42 inch column testing.

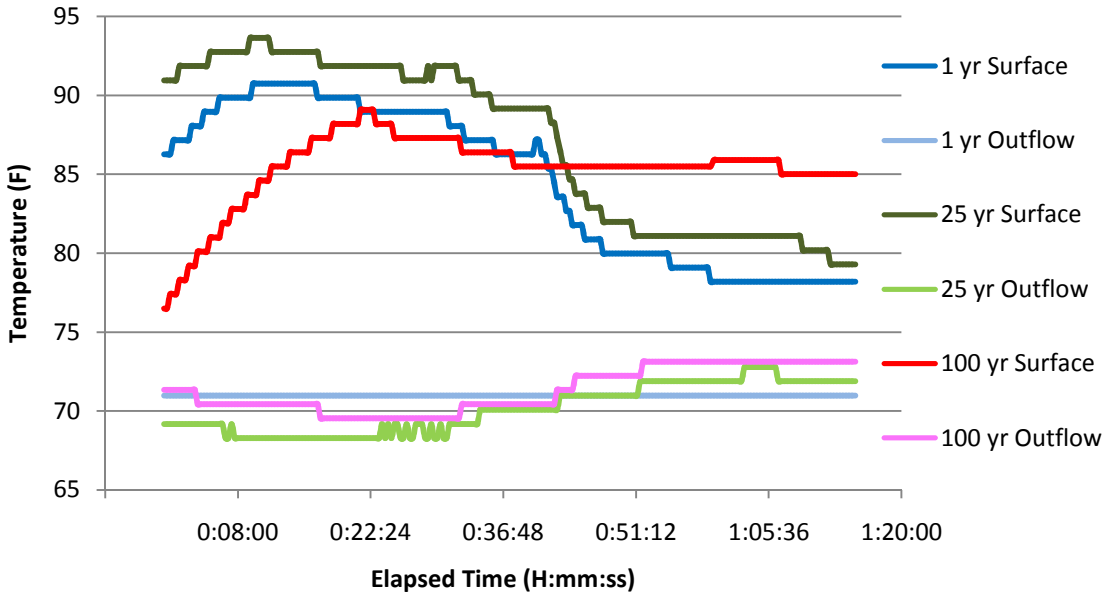

Figure 4.1: 42 Inch Column: Temperature Response

All three temperature responses produced similar trends, with variations directly related to the magnitude of the storm inflow. The surface temperature responses for the 1 year and 25 year closely resemble each other with the 25 year surface temperature test starting at a higher initial temperature. The surface temperature trend for the 100 year storm simulation maintains a relatively constant temperature of 85°F. This is due to the high magnitude of heated inflow entering the system throughout the experiment. The outflow temperature did not increase for the 1 year storm so it can be assumed that the full storm was cooled to the ambient bed temperature while travelling over the aggregate. As seen from the 25 and 100 year outflow, the storm simulations were cooled considerably from their inflow temperature of 85°F, but were not cooled to the initial bed temperatures, exceeding the temperature mitigation capacity of the system

Using the same experimental process, the 14 inch pervious concrete column's temperature response was also tested for the 1, 25, and 100 year 1 hour storm events.

Figure 4.2 shows the respective surface and outflow temperatures throughout the storm simulations.

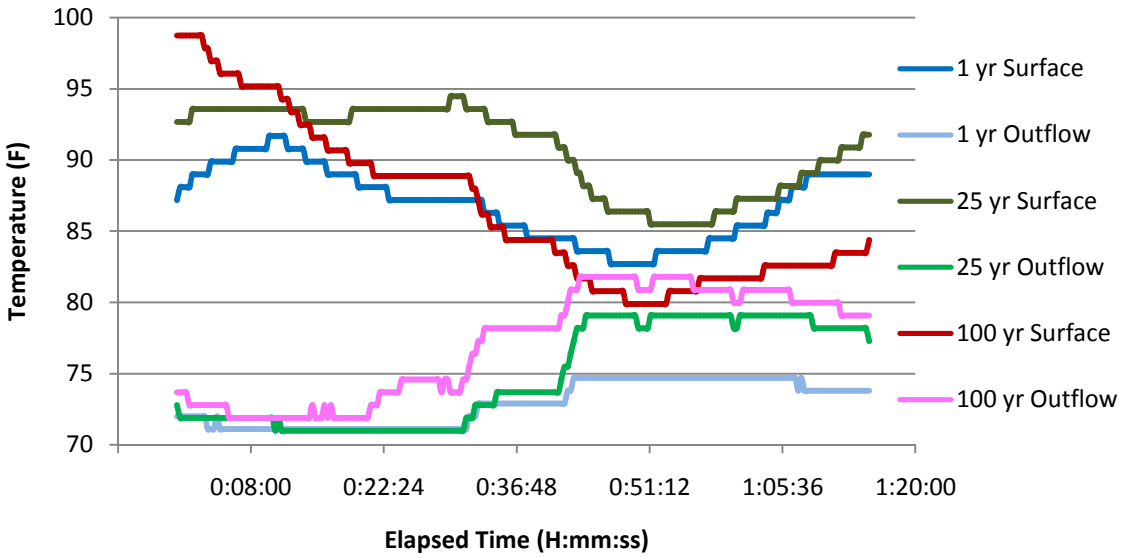

Figure 4.2: 14 Inch Column: Temperature Response

Similar to the long column, the observed temperature trends can be directly related to the storm magnitude/intensity. It became apparent that the short column was not able to effectively mitigate temperature for the 100 year storm, as the outflow temperature exceeds the surface temperature towards the end of the experimental simulation. Predictably, the 1 and 25 year storms are more effectively cooled as they travel through the system. Unlike the long column, the 11 inch aggregate bed of the short column does not completely cool the inflow to the 1 year storm. Interference from the Workforce lamp produced a temperature increase of the surface towards the end of each simulation. This error in testing methodology was altered in the final design experiment.

Based on the six proof-of-concept temperature experiments, a general relationship can be observed between storm magnitude/intensity and column length while holding initial temperature parameters and storm duration constant (Figure 4.3).

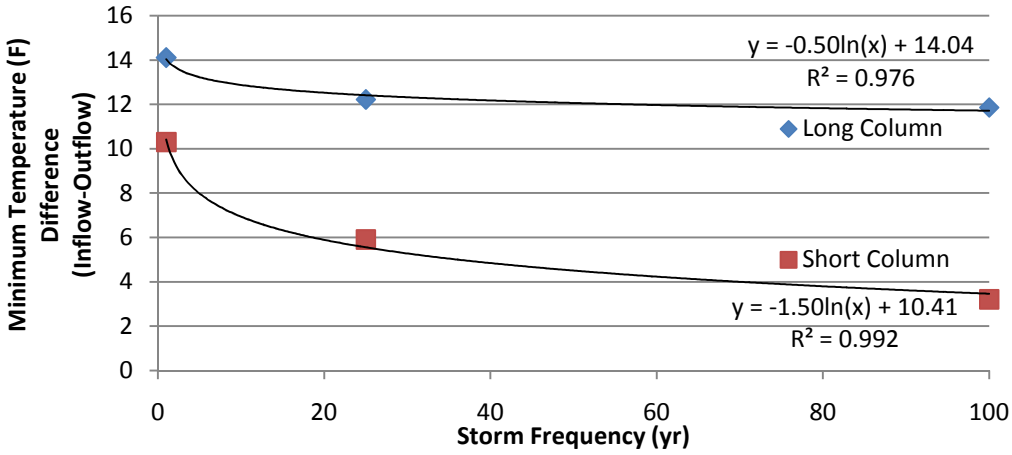

Figure 4.3: Minimum Temperature Difference as a Function of Storm Frequency

The minimum temperature difference is defined as the maximum bed temperature throughout the simulation subtracted from the initial inflow temperature (85°F). From the three data points obtained for each column, a logarithmic trend line was developed, with the equations displayed in Figure 4.3. The logarithmic trend lines generally fit the data as represented by the squared Pearson correlation coefficient (R^2). As seen from the trend lines, the ability to reduce inflow temperatures rapidly decreases between the 1 year and 25 year storm magnitude for both columns. The logarithmic trend indicates that the minimum temperature difference will approach a horizontal line as the storm frequency approaches infinity. The long column shows indicates a greater ability to mitigate inflow temperature as storm frequency increases due to the larger aggregate bed length.

In general, accuracy errors in achieving the initial surface temperature of 90°F can be attributed to the use of Thermochron I-buttons. By using the I-buttons, real time

temperature could not be directly monitored, and had to be estimated using an ASTM 5F thermometer. Given differences in thermal properties, it was found that the thermometer would heat faster than the I-button, and therefore was a relatively inaccurate method to monitor real time surface temperature. The temperature monitoring procedure was revised to include thermocouples in the final experimental design.

4.1.2 Nutrient Response

The proof-of-concept testing for nutrient response included an inflow spiked with nitrogen and phosphorus, which was simulated through the 42 inch long column. The 5 year 1 hour storm was used along with a spiked inflow concentration of 0.81 mg/L P and 25 mg/L N. The purpose of nutrient testing for proof-of-concept is to verify the reduction of pollutants as the design storm is simulated through the test column. During the one hour storm, three outflow samples were collected at the 30, 40, and 50 minute mark. Table 4.1 shows the average percent reduction in concentration obtained from the total phosphorus and total nitrogen testing.

Table 4.1: Proof-of-concept Nutrient Response (42" Column)

Sample ID	Time Elapsed into Storm (min)	Concentration (mg/L P)	Removal %	Avg. % Removal
Inflow	0	0.81	---	---
Outflow 1	30	0.48	40.1	36.2
Outflow 2	40	0.54	32.8	
Outflow 3	50	0.52	35.6	
Sample ID	**Time Elapsed into Storm (min)**	**Concentration (mg/L N)**	**Removal %**	**Avg. % Removal**
Inflow	0	24.9	---	---
Outflow 1	30	22.3	10.4	8.3
Outflow 2	40	22.5	9.6	
Outflow 3	50	23.7	4.8	

The 42 inch test column was able to remove approximately one third of the total phosphorus entering the system for the 5 year, 1 hour storm simulation. Removal of total phosphorus was expected to occur given the tendency of orthophosphate to adsorb onto soil surfaces. One can assume that a greater removal of dissolved phosphorus can be achieved by increasing the surface area of exposure. For example, a sand filtration layer underneath the aggregate bed of a pervious concrete system would, in theory, allow for more adsorption surfaces of the dissolved phosphorus contaminant.

The 8.3% removal of total nitrogen may be as a result of pore water retention within the test column, or slight variations with the spectrophotometer testing equipment. A relatively low nitrogen removal was expected from the test column, as nitrogen removal processes in SCMs are typically governed by long term microbial action, and also plant uptake. In the field, greater nitrogen removal may be achieved in pervious pavement systems by long-term storage/ slow infiltration of the runoff into the underlying native soils.

The removal rates of the 42 inch test column were compared with nutrient removal efficiencies of the Villanova pervious concrete parking lot, selected research sites, and expected standards set forth by the Department of Environmental Protection and the Portland Cement Association (Table 4.2).

Table 4.2: Typical Nutrient Removal Trends for Pervious Pavement Systems			
SCM Type	**Phosphorus Removal**	**Nitrogen Removal**	**Reference**
Pervious concrete, interlocking pervious concrete pavers, concrete grid pavers	[a]No significant removal	Minimal, leaching	Collins, et al. 2008
Various pervious concrete grid systems	75% removal or greater for 10 storm simulations	Partial ammonia adsorption, nitrate/nitrite leaching	Day 1981
Villanova's pervious concrete parking lot	[b]60.0%	[b]15.0%	Barbis 2009
Porous pavement material	65.0%	80.0-85.0%	Portland Cement Assoc. 2007
Pervious pavement with infiltration bed	85.0%	30.0% (as NO_3)	PADEP BMP manual 2006
Permeable pavement	[c]25.0%	[c]25.0%	VA Dept. of Conservation & Recreation 2011
Pervious concrete with infiltration bed	94.3%	95.3%	Horst, et al. 2011
42" Proof-of-concept Column	36.2%	8.3%	-

[a]No separation of pervious concrete systems from the in situ soil
[b]Samples taken at pore-water depths of 6, 12, and 18 inches in native soil under aggregate bed
[c]Removal explicitly defined as outflow mass reduction via runoff reduction

Upon reviewing industry standards and other research endeavors, it became apparent how uncertain nutrient removal behavior can be, with design and environmental influences proving to be influential variables. When compared to the proof-of-concept testing, the Villanova pervious concrete parking lot reflected higher nutrient removals for both total phosphorus and total nitrogen. This can be attributed to the secondary filtering of the native soil underneath the aggregate bed (where the pore-water samples were gathered for testing). Interestingly, PADEP and PCA recommend relatively high expected nutrient

removal capacitates for pervious concrete systems as compared to actual removal rates experienced by the research studies listed.

4.2 Experimental Results of Final Design

The final design experimental apparatus was revised to simulate the first flush of a 1 year, 24 hour storm which represented 0.66 inches of runoff or 618mL. Repeatability of the final experimental procedure was verified by running three first flush simulations through each test column. The first flush spike comprised of 0.81 mg/L P, 25 mg/L N and 593 mg/L Cl. Approximately 1.6 liters of deionized water was flushed through each column after the addition of the first flush samples to completely flush the spiked plug through the system. Eleven outflow samples were collected from each test and taken to Villanova's Water Resources Laboratory for concentration determination on the laboratory spectrophotometer units. After concentrations of the samples were found, mass balances were obtained for phosphorus, nitrogen, and the chloride tracer.

4.2.1 Temperature Response

The temperature profile of the system was amended to mimic a typical summer storm at Villanova's pervious concrete parking lot. As explained in Chapter 3, an afternoon storm during June 2011 was chosen. Experimental testing was carried out during summer of 2012 in Villanova's Soil Laboratory. Ambient temperature in the lab was measured prior to any testing to ensure it was within the temperature range experienced at the pervious concrete parking lot (72-74°F). Figure 4.4 displays the surface (S) and outflow (O)

temperatures for the three experiments involving the pervious concrete column. Each test is designated by month and day completed during the 2012 year.

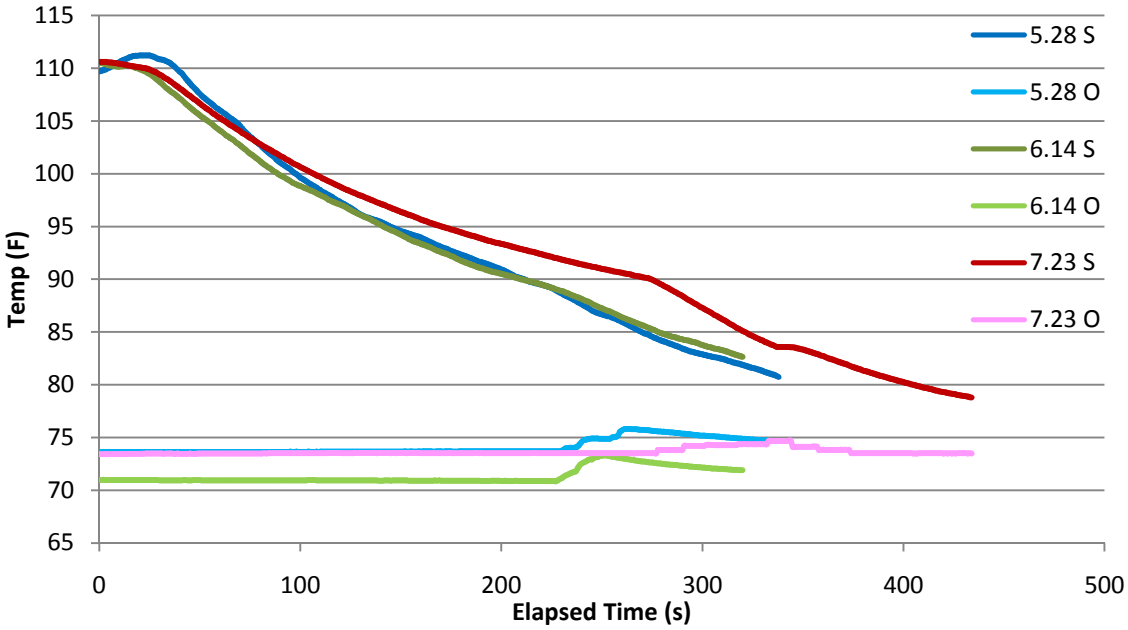

Figure 4.4: Final Design: Pervious Concrete Surface (S) and Outflow (O) Temperature Response

Slight variations in temperature can be seen between each test run which may be attributed to irregularities in testing procedure and atmosphere. The tests performed on 5/28 and 6/14 show very similar surface temperature trends and similarly shaped outflow temperature responses, with a 2.5°F difference in initial bed temperature. The test performed on 7/23 contains different surface and outflow temperature response trends. Even though the testing protocol remained consistent, the 7/23 surface temperature required more time to cool to 90°F prior to the introduction of the first flush volume. With this lag in surface cooling, the outflow temperature response is also inherently delayed, and does not follow the shape of the other outflow trends.

The surface and outflow temperature variation can possibly be explained if one looks at the relationship between relative humidity, dew point, and ambient temperature. An investigation of the dew points during the testing days using the Mendel rain gage station revealed that the dew point during the 7/23 test session was equal to the ambient air temperature, whereas the dew point during the other test sessions was lower than the ambient temperature (Weather Underground 2012a). Humidity will increase if the ambient temperature is equal to or lower than the dew point. This increase in humidity for the 7/23 test can explain the cooling lag observed in the temperature results, as radiated cooling power decreases with an increase in water vapor in the air (Eriksson and Granqvist 1982).

Three first flush storm simulation tests were also performed on the sand bed column to offer a comparison in bed materials in relation to temperature mitigation and nutrient removal capacity. Figure 4.5 displays the surface (S) and outflow (O) temperature responses for the sand test column along with their month and day of completion in 2012. In general, the surface temperatures for all sand tests exhibited similar temperature trends, but took approximately 1.3 times longer to cool to 90°F than the pervious concrete tests. The 6/5 and 7/30 storms displayed strikingly similar surface temperature responses, whereas the 8/7 test required a greater cooling time. The dew points during these test days were investigated using the Mendel rain gage station, which revealed no indication of a higher humidity based on dew point and temperature. However, a rain event took place the day prior to the 8/7 test (Weather Underground 2012b). Therefore, it

was assumed that the humidity was elevated, which increased cooling time during this test session.

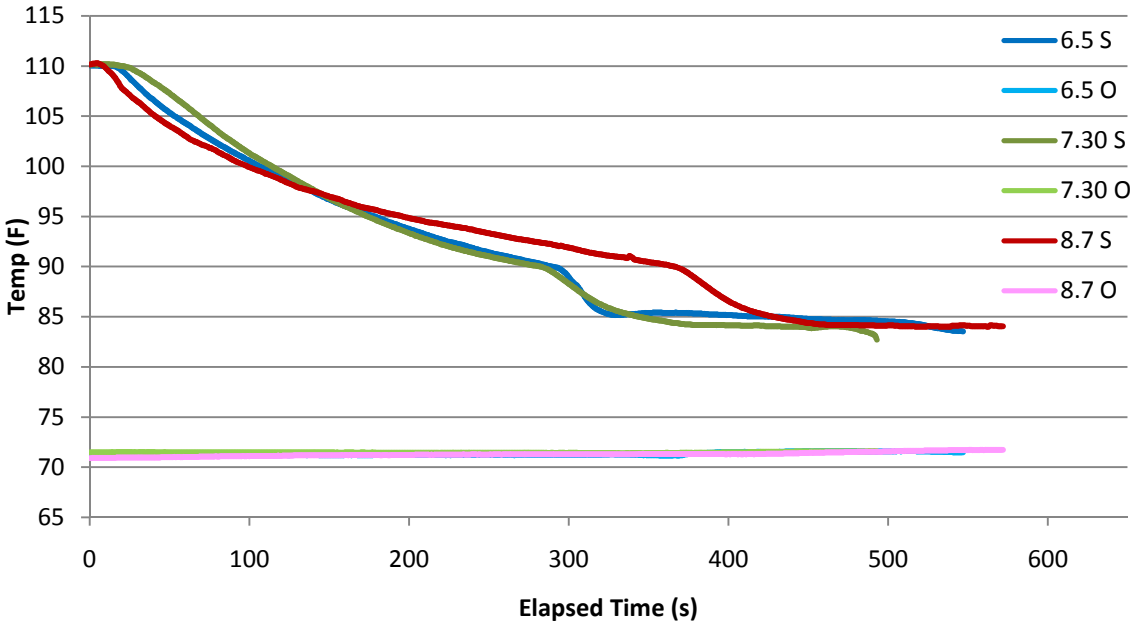

Figure 4.5: Final Design: Sand Surface (S) and Outflow (O) Temperature Response

The outflow temperature remained constant for all three sand tests which illustrated the sands capacity to mitigate heat from stormwater runoff. The total surface area of sand in the test column is much greater than that of the aggregate bed in the pervious concrete column, thus allowing for a greater temperature reduction.

4.2.2 Mass Balance of Phosphorus

Each experimental test produced eleven outflow samples that were transferred to Villanova's Water Resources Laboratory for chemical testing. As mentioned previously, total phosphorus testing was performed on the DR/4000 HACH Spectrophotometer. Table 4.3 displays a summary of the total phosphorus mass balances performed on the pervious concrete column. Detailed mass balances for each experiment can be found in

Appendix A. On average, the pervious concrete column showed 0.12 mg (24%) of unaccounted mass for total phosphorus, indicating that a pollutant removal mechanism was present during the experiment.

Table 4.3: Phosphorus Mass Balance – Pervious Concrete Column

Test date	Mass Inflow (mg)	Mass Outflow (mg)	Mass Retained (mg)	Mass Unaccounted (mg)
5/28/2012	0.50	0.33	0.08	0.08
6/14/2012	0.53	0.24	0.10	0.19
7/23/2012	0.46	0.29	0.08	0.09
AVG	0.50	0.29	0.12	0.12

Based on the chemical behavior of orthophosphate, one can assume that the removal mechanism is adsorption to the surfaces of the aggregate bed. It is important to note that the mass unaccounted for (i.e. mass removed from aqueous solution) has been underestimated in the mass balance equation. By assuming complete mixing of the spike plug and deionized flush, the retained mass value is overestimated, thus decreasing the unaccounted mass. Therefore, the mass removed can seen as a conservative lower limit of possible phosphorus removal via adsorption.

A similar trend can be seen in the total phosphorus mass balance for the sand column experiments (Table 4.4). In this batch of experiments, an average total phosphorus mass removal of 0.37 mg (60%) was observed. In general, sand should have an increased orthophosphate adsorption capacity when compared to the pervious concrete column due to differences in surface area. These results also verify that adsorption can be assumed the primary (possibly only) removal mechanism present in the system for total phosphorus.

Table 4.4: Phosphorus Mass Balance – Sand Bed Column				
Test date	**Mass Inflow (mg)**	**Mass Outflow (mg)**	**Mass Retained (mg)**	**Mass Unaccounted (mg)**
6/5/2012	0.61	0.12	0.12	0.37
7/30/2012	0.80	0.10	0.25	0.46
8/7/2012	0.44	0.07	0.10	0.28
AVG	0.62	0.10	0.16	0.37

4.2.3 Mass Balance of Nitrogen

Total nitrogen mass balances for both experimental columns were obtained through chemical data results from the DR/4000 HACH Spectrophotometer. Table 4.5 and 4.6 display the mass balances for the pervious concrete column and sand column respectively. As mentioned in Section 3.5.7, the retained mass was calculated assuming total mixing of the spiked inflow and deionized flush to determine the nutrients remaining in the column in solution. Based on the nitrogen mass balance results, it became clear that the retained mass was over estimated, producing a negative mass unaccounted for. A more realistic scenario would to perhaps assume no mixing of the spiked inflow and deionized flush, thereby setting the retained mass to zero. Appendix B displays this alternative and less conservative mass balance scenario.

Table 4.5: Nitrogen Mass Balance – Pervious Concrete Column				
Test date	**Mass Inflow (mg)**	**Mass Outflow (mg)**	**Mass Retained (mg)**	**Mass Unaccounted (mg)**
5/28/2012	13.51	12.93	2.30	-1.71
6/14/2012	13.95	14.18	2.65	-2.88
7/23/2012	16.75	17.07	2.86	-3.18
AVG	14.74	14.73	2.60	-2.59

Table 4.6: Nitrogen Mass Balance – Sand Bed Column				
Test date	**Mass Inflow (mg)**	**Mass Outflow (mg)**	**Mass Retained (mg)**	**Mass Unaccounted (mg)**
6/5/2012	15.14	14.29	2.92	-2.07
7/30/2012	13.47	13.56	4.11	-4.20
8/7/2012	13.18	13.43	2.88	-3.12
AVG	13.93	13.76	3.30	-3.13

It can be assumed that no removal mechanism was present for total nitrogen in either column during experimentation. This result was expected, as nitrogen removal processes are typically biological, and require a relatively longer time period than the adsorption removal mechanism of phosphorus. Long term removal of nitrogen in non-vegetative Stormwater Control Measures has been observed when conditions allowed for the growth of nitrogen processing microorganisms (Collins 2007). However, the pervious concrete and sand columns did not produce an environment favorable to nitrogen removal processes.

4.2.4 Mass Balance of Chloride

A mass balance of the chloride tracer was performed between experimentation to verify that no residual pollutants remained in the test columns. Chloride concentrations were obtained from the Systea EasyChem Spectrophotometer. Since chloride is an inert chemical, the complete mass balance was comprised of the inflow and outflow concentrations of chloride. In general, all tests showed under a 10% error in chloride concentrations, which verified complete flushing of the spiked first flush simulation (Table 4.7).

Table 4.7: Chloride Tracer Check					
Pervious Concrete Column			**Sand Bed Column**		
Test date	**Mass Inflow (mg)**	**Mass Outflow (mg)**	**Test date**	**Mass Inflow (mg)**	**Mass Outflow (mg)**
5/28/2012	133.78	136.25	6/5/2012	344.82	341.22
6/14/2012	344.86	315.31	7/30/2012	410.68	457.85
7/23/2012	337.96	303.06	8/7/2012	362.69	349.50
AVG % error	7.68		AVG % error	5.39	

In general, the tracer was kept to approximately 600 mg/L chloride, but incorrect dosing led to the disparity in chloride mass observed in the 5/28/2012 testing. Based on the mass balance however, this test was considered to produce valid results.

4.3 Retention Versus Removal in SCMs

Currently, it appears that non-vegetative SCMs do not have the capacity to remove nitrogen from stormwater as illustrated by the total nitrogen mass balances from the final column experimentation. In the field, reductions of total nitrogen in non-vegetative SCMs are most likely due to retention of stormwater runoff volume. This retention may lead to an overall reduction in outflow concentrations, but using the term "removal" is an incorrect way to describe this phenomenon.

It appears that much of the current design recommendations for SCMs do not make the clarification between nitrogen removal and nitrogen retention via volume storage. This ambiguity can cause misconceptions in the functionality of many stormwater control measures. To avoid confusion, design guidelines should be revised to create clear distinctions in how pollutants are handled when introduced to the SCM in question. The "removal mechanism" should refer to a chemical or biological process that disconnects a

pollutant from the hydrologic cycle. Whereas the "retention mechanism" should describe a pollutant that is hydraulically hindered through some physical process but can still technically be transported if the system is overloaded with stormwater inflow. For example, a pervious pavement system can offer short term nitrogen retention through volume storage and can also offer long term nitrogen removal when the stored water infiltrates the native soil and is converted to nitrogen gas by denitrifying bacteria. However, if not enough time is allowed for this retained nitrogen to be removed from the system, another storm may transport the retained nitrogen from the SCM (which is what was observed in the column experiments).

4.4 Temperature as a Proxy for Nutrient Reduction

Based on the results obtained from the column studies, a removal range was found for total phosphorus (as total nitrogen showed no removal process). This removal range was found by assuming two scenarios for the mass balances: complete and no mixing of the spiked plug with the deionized flush (see Appendix B). The two removal regimes in Figure 4.6 correlate to the bed materials used in the laboratory experiments, i.e. aggregate and sand beds. This figure displays the minimum temperature difference observed for each test with respect to the total phosphorus removal range. It can be noted that the sand bed column produced more precise temperature results, attributed to minimal bed temperature fluctuations. Conversely, the pervious concrete material appeared to have a greater range of temperature fluctuations.

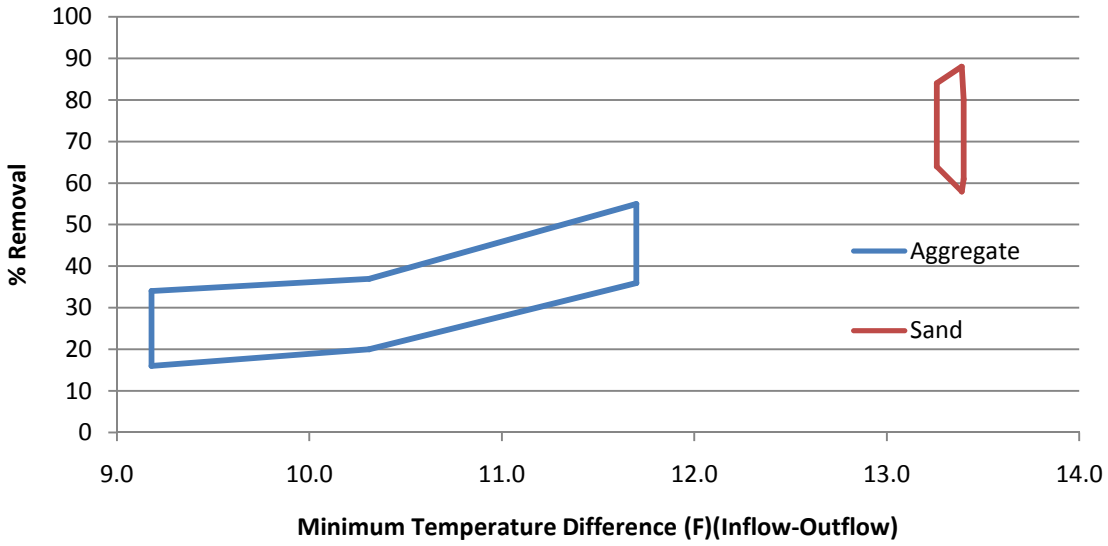

Figure 4.6: Expected TP Removal using Temperature Mitigation as a Proxy

A few limitations are present in the application of the aforementioned graph. First of all, these results are based on non-vegetative SCMs such as pervious pavements or infiltration beds. Due to the known removal mechanisms of phosphorus, higher removal efficiencies should be expected as grain size decreases, and also for vegetated systems such as rain gardens or constructed wetlands. Nevertheless, this monitoring system may be able to provide minimum phosphorus removal estimate for vegetated SCMs. In terms of temperature mitigation, it can be assumed that finer grained soil such as silt will be able to perform similarly to sand. Slower infiltration rates and a larger surface area would most likely provide for the complete cooling of inflow to bed temperatures in a fine grained soil.

Another limitation to note is the environmental conditions in which testing was performed. The experimental design was based off of temperatures typical for the months of June through September in Pennsylvania. Therefore, this monitoring protocol should

be used in areas that are similar in climate during the appropriate seasons. Furthermore, the experimental results are based on a 1 year storm's first flush; caution must be applied when dealing with atypical storm events. Lastly, using removal in terms of total percent does not by itself give a good indication of the efficiency of the SCM. Even though it is a commonly used measurement for these systems, it gives no sense of pollutant magnitude (Davis, et al. 2010).

4.5 Example of Application

From the column experimentation, a low cost monitoring system was devised to estimate nutrient removal for Stormwater Control Measures. First, a visual inspection checklist must be completed to identify the functionality of the site in question. This visual inspection addresses possible issues with the inlet, outlet, infiltration capabilities, and plant health of the various types of control measures (Greising 2011). Sample inspection checklists are provided in Appendix C, and should be used as a general guideline. If deficiencies are noted during visual inspection, appropriate maintenance or corrective actions should be taken. If no deficiencies are noted from the visual inspection, stormwater temperature mitigation through the site can be used as a proxy to estimate total phosphorus removal.

The SCM in question should be prepared for temperature data gathering prior to a storm event. Remote temperature recorders such as Thermochron I-buttons should be placed at the inflow and outflow locations. Preferably, the inflow location should be insulated from the sun, but must come into direct contact with stormwater runoff entering the control

measure. The "outflow" location should be within the system at a place where water will most likely collect once it has infiltrated into the control measure. A visual inspection may be required during the storm event to determine if the temperature sensors are positioned correctly. Once the storm event concludes, data from the temperature recorders should be retrieved and plotted over time. The temperature difference between the inflow and outflow stormwater should be estimated. Figure 4.7 shows an example of how to estimate this temperature difference, using Villanova's pervious concrete site.

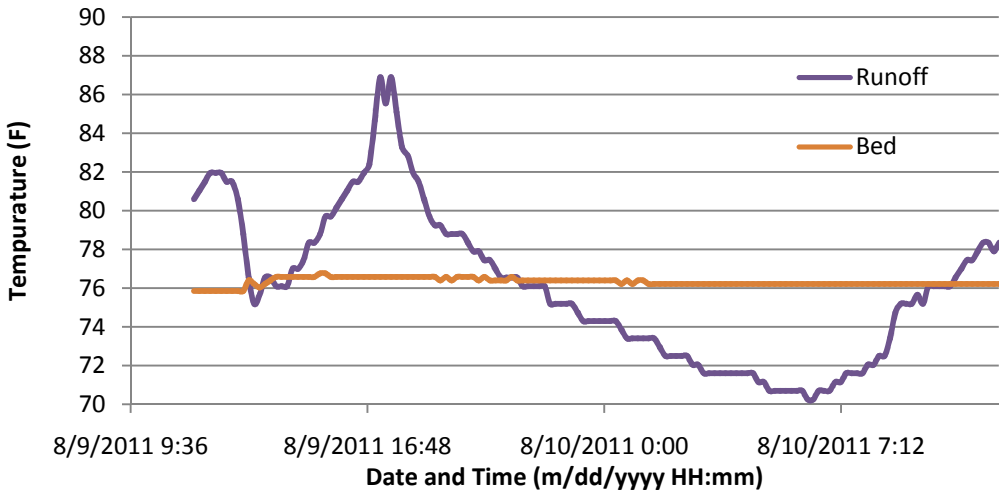

Figure 4.7: Example of Temperature Estimation using the Villanova PC Site

Prior to analyzing the temperature data collected from a control measure, precipitation rates and amounts should be verified. Weather Underground is a free website that offers rain gauge data in many areas of the United States. From this website, it was confirmed that rainfall of 0.89 inches occurred in the area of Villanova on the afternoon of August 9th, 2011 (WU 2011). From the example figure, the runoff temperature trend correlates to an influx of heated stormwater runoff, then cools as the storm progresses. It is clear that the storm's first flush inflow temperature is an average 87°F. The bed temperature does not appear to fluctuate with the rainfall, so it can be assumed that the heat from the

stormwater was completely mitigated as it travelled through the system. Therefore, the bed temperature is 76°F, and the temperature difference is approximately 11°F. Once this value is known, the total phosphorus removal can be estimated to be between 25 and 45% (see Figure 4.6).

Nitrogen retention and possible long term removal can be estimated based on existing low level monitoring practices. If the observed SCM appears to have successfully captured and retained a percentage of the inflow stormwater runoff, one can assume that nitrogen retention is taking place. If outflow is observed for a typical rain event, an investigation should be conducted, and corrective actions should be taken.

Part II: Watershed-Scale Effects of Rain Gardens Using EPA SWMM

Chapter 5

Introduction & Literature Review

5.1 Background

The capacity of stormwater control measures (SCMs) to reduce or eliminate stormwater runoff through volume reductions has been verified through various observations and research ventures (e.g.; Finnemore and Lynard, 1982; Debo and Reese, 2003; Davis, et al. 2012) Most recently, the focus has shifted to studying the volume reduction effects of multiple SCMs, often called "treatment trains." Storm volume reductions on a watershed scale are typically unknown as large scale implementation of SCMs and data collection is uncommon. In the following section, three scenarios were researched to determine the volume reduction capacities of various stormwater control measures, and their effects from the site to the watershed level. Furthermore, current studies of SCM implementation on a watershed scale within modeling systems were investigated.

5.2 On Site Volume Reductions of SCMs

Numerous studies have been performed to determine the effectiveness of storm volume reduction for various stormwater control measures. Studies conducted at Villanova University have shown effective volume reductions in both vegetative and non-vegetative control measures. For example, a two-year study of a pervious concrete infiltration basin revealed highly efficient runoff capture and infiltration capacity up to a 2 inch storm (Horst, et al. 2011). Furthermore, pressure transducer data gathered from a bioretention

rain garden in 2012 revealed a 99% volume capture from a 3.5 inch storm (unpublished data).

A comprehensive study conducted on the international stormwater BMP database revealed general trends in terms of volume reduction capacity and type of control measure. It was found that dry vegetated control measures appear to have the greatest potential for runoff volume reduction on a long term basis. Interestingly, retention ponds and wetlands did not offer a substantial volume reduction on average (Clary, et al. 2011).

5.3 Volume Reductions of SCMs in Series

Implementing SCMs in series is a fairly new practice designed with sequential components to effectively treat stormwater before it leaves the site. Typical components of a treatment train consist of swales, prairies, wetlands, and rain gardens (AES 2006). Usually stormwater runoff will enter the system and travel along a swale before entering some type of retention measure. Intuitively, these systems offer a greater capacity for volume capture as opposed to a singular control measure.

A study conducted in North Carolina of stormwater wetlands in series revealed greater volume reduction capacities than expected in the initial design. A greater storage volume was experienced due to higher than expected infiltration rates into the native soils (Hathaway and Hunt 2010). A treatment train constructed at Villanova University in 2011 consists of a vegetated swale connected to two rain gardens, and finally an infiltration trench. This system has a total estimated capture volume of 825 cubic feet and is expected to successfully retain the volume of typical storm events (Lyons, et al. 2012).

5.4 Watershed Volume Reductions due to SCMs

Flow impacts due to stormwater control measures on a watershed scale are difficult to quantify in the field due to time and budget constraints. It has been theorized that the role of stormwater control measures are diminished when viewing the entire watershed. In an attempt to quantify the role of stormwater control measures, computer models have been utilized by researchers.

Traver and Chadderton (1983) recognized that the effectiveness of detention basins will most likely decrease as basin density increases. In one study of the 24 square mile Valley Creek watershed in Pennsylvania, 82 detention basins were modeled in HEC-HMS to determine their influence on hydrology in the watershed (Emerson 2003). It was found that these detention basins had little attenuating effect on the overall storm flow. In two of the six measured storm events, the detention basins actually served to increase peak flow rates. Based on these results, it was concluded that the detention basin, which offers a set flow release rate, is not an effective means of limiting peak flow rates throughout a watershed (Emerson, et al. 2003).

Another study (Carter and Jackson 2006) modeled the volume reduction due to the implementation of vegetated roofs in the Tanyard Branch watershed located in Athens, Georgia. This urbanized watershed is comprised of approximately 54% impervious area with residential and commercial buildings. The total roof area makes up approximately 30% of the watershed's imperviousness. To model runoff, the StormNet Builder program was used, which utilizes the analysis engine from EPA's SWMM 5.0. After analysis, it

was found that changes in hydrology across the watershed will be minimal for events greater than the 2-year, 24-hour storm. Approximately 80% of the yearly events for this watershed are less than the 2-year, 24-hour storm, and therefore the implementation of green roofs can be said to have beneficial impacts on the watershed. However, it is recommended that green roofs alone cannot be solely relied upon to provide complete stormwater management (Carter and Jackson 2006).

The Milwakee Metropolitan Sewerage District assessed the combined effect of eleven different types of SCMs in a typical residential neighborhood and commercial watershed using the Hydrologic Simulation Program FORTRAN software (2005). Volume reductions from historic storm events were compared to an existing condition with a combined sewer system with no SCMs. Table 5.1 shows the storm volume reductions compared to the existing combined sewer outflow.

Table 5.1: Simulation Volume Reductions for a Residential Watershed

Stormwater Control	Combined Sewer Outflow (MG/yr)	% reduction
Residential Baseline	0.28	-
Downspout Disconnection	0.25	12
Rain Barrel	0.24	14
Rain Garden	0.18	36
Rain Garden & Rain Barrel	0.17	38
Commercial Baseline	1.17	-
Green Roof	0.91	22
Bioretention	0.35	70
Green Parking Lot	0.28	76

(MMSD 2005)

The volume reductions shown are based on the full implementation of the stormwater control measures. To achieve the results produced from the model, widespread implementation of the stormwater control measures would be necessary (MMSD 2005).

A study in Indiana evaluated the combined effect of rain barrels, cisterns, and porous pavement within two urbanized watersheds using the Long-Term Hydrologic Impact Assessment (L-THIA) model. An 8% reduction in runoff flow was experienced with the implementation of rain barrels to handle 1/4th of all the structures, and pervious pavement to handle 1/4th of "in-city non-busy" roads. Furthermore, this combination of stormwater controls also produced a 4% stream flow reduction (Ahiablame, et al. 2013).

5.5 Research Focus

The purpose of the second part of this research effort was to assess the volume reduction that occurs as a result of the implementation of rain gardens on a watershed scale. EPA's SWMM 5.0 software was used as it is a widely accepted program within the industry, and contains a robust method of modeling low impact development (LID) practices. Using the Mill Creek watershed located in Montgomery County, Pennsylvania, 45 models were developed that varied overall percent impervious area and level of rain garden addition. Furthermore, ecological impacts were assessed using the River Chub fish (a keystone species) as a health indicator.

Chapter 6

Methods

This section describes the development of the EPA SWMM 5.0 model used in the analysis of a typical urban watershed as well as the hydrologic/hydraulic equations employed. Input parameters were based on the Mill Creek Watershed which includes a portion of the Villanova University Campus. Once the base model was created, 45 scenarios were developed that varied imperviousness of the watershed (3, 5, 9, 10, 20, 25, 60, 70, and 80% impervious area) and percent rain gardens in each subwatershed associated with the number of existing structures (0, 0.25, 0.50, 0.75, and 1.00 rain garden to structure ratio). Known existing control measures were also included in each model in an attempt to accurately define stormwater runoff behavior before the implementation of theoretical rain gardens.

6.1 SWMM Runoff and Routing Equations

SWMM offers an array of fluid equations to solve for surface runoff/ infiltration, and flow routing iterations. The SWMM infiltration solver can utilize the Horton, Green-Ampt, or the SCS runoff curve number method. Only the soil type and distribution was known for the Mill Creek watershed so the curve number (CN) method was chosen. This method estimates runoff based on rainfall, and infiltration due to soil type using the SCS runoff equation (USDA 1986):

$$Q = \frac{(P - I_a)^2}{(P - I_a) + S}$$

Where Q is the runoff in inches, P is the total rainfall in inches, I_a is the initial abstraction in inches, and S is the potential maximum retention after runoff begins (in inches). The

initial abstraction defines all losses before runoff begins, and can be calculated using the following equation:

$$I_a = 0.2S$$

S is related to the nature of the soil and also cover conditions of the watershed which is defined by a CN value ranging from 0 to 100 where low numbers indicate a low runoff potential and vice versa. S is calculated using the following equation:

$$S = \frac{1000}{CN} - 10$$

The curve number is found by determining the distribution of hydrologic soil groups within a particular watershed. Soils are classified into four hydrologic groups: A through D. Group A soils have a low runoff potential and high infiltration rates whereas group D soils have a high runoff potential with very low infiltration rates when thoroughly wetted. Table 6.1 displays the general characteristics of each hydrologic group.

Table 6.1: Hydrologic Soil Groups

Soil Group	Soil Textures	Typical Characteristics
A	Sand, loamy sand, or sandy loam	Low runoff potential and high infiltration rates even when thoroughly wetted
B	Silt loam or loam	Moderate infiltration rates when thoroughly wetted
C	Sandy clay loam	Low infiltration rates when thoroughly wetted
D	Clay loam, silty clay loam, sandy clay, silty clay, or clay	High runoff potential and very low infiltration rates when thoroughly wetted

(USDA 1986)

The routing model in SWMM can be set to use steady flow, kinematic wave, or dynamic wave equations. The dynamic routing model was chosen in an effort to maximize resolution and accuracy. The dynamic wave method utilizes the one-dimensional Saint Venant flow equations, which operate under unsteady flow conditions. These equations consist of the continuity and momentum equations for conduits and a volume continuity

equation at nodes. The routing model then uses these equations in an iterative procedure to determine parameters of conduit and node flow. The Saint Venant continuity (left) and momentum (right) equations are as follows:

$$\frac{\partial Q}{\partial x} + \frac{\partial A}{\partial t} = 0 \qquad\qquad -\frac{1}{g}\frac{\partial V}{\partial t} - \frac{V}{g}\frac{\partial V}{\partial x} - \frac{\partial y}{\partial x} + S_o = S_f$$

Where Q is flow, A is cross sectional area of the channel, t is the time step, V is the velocity, g is the acceleration due to gravity, S_o is channel bed slope, S_f is the friction slope, and x is the iteration distance. The Saint Venant equations assume that flow is one-dimensional and incompressible and that the streamline curvature and bottom slope of the channel is small. Furthermore, Manning's equation is used to describe resistance or friction effects. Lastly, vertical acceleration is negligible with this solving method (Sturm 2001).

The dynamic flow routing method uses the Manning equation to relate flow rate to flow depth and friction slope (Gironas, et al. 2009). This equation applies to uniform flow in open channels and is a function of the channel velocity. The general form of Manning's equation for imperial units is:

$$Q = VA = \left(\frac{1.49}{n}\right) AR^{2/3}S^{1/2}$$

Where Q is flow rate, V is velocity, and A is cross sectional flow area of the channel. The parameter, n, is Manning's roughness coefficient (unitless) which is dependent on surface roughness, geometry, and sinuosity of the channel. R is the hydraulic radius of the channel which is defined by the cross sectional area divided by the wetted perimeter.

Lastly, S is the slope of the energy grade line which can be taken as the channel bed slope under uniform flow conditions.

In theory, the dynamic wave equation offers more accurate results in comparison to the steady flow and kinematic wave equations. To minimize numerical dispersion, a variable time step was used for iteration. The variable time step allows for an adjustment factor to be applied at each successful flow routing iteration to satisfy the Courant number. The following equation relates the courant number to model parameters during one time step of an iterative equation:

$$C_r = \frac{v\Delta t}{\Delta x}$$

Where C_r is the Courant number, v is the average linear velocity, t is the iterative time step, and x is the length interval. When advection dominates dispersion, a small Courant number (<1) will decrease oscillations, improve accuracy, and decrease numerical dispersion (Bakhvlov 2001).

6.2 Hydrology

6.2.1 Subwatershed Development

The United States Geological Survey (USGS) StreamStats program is a free online database that allows users to delineate watersheds, and gather data such as land use, percent impervious cover, and average basin slope. By utilizing this database, geometric characteristics of the Mill Creek watershed were found, and subwatersheds were delineated.

The Mill Creek Watershed was found to have a total area of 8.34 mi^2, approximately 9% impervious cover, and an average slope of 4.9 degrees towards the Schuylkill River to the East. Subwatersheds were delineated on StreamStats based on the confluence of first order streams to the Mill Creek. The remaining areas were then divided into manageable regions. Figure 6.1 displays the 32 subwatersheds of Mill Creek overlaid onto Google Earth.

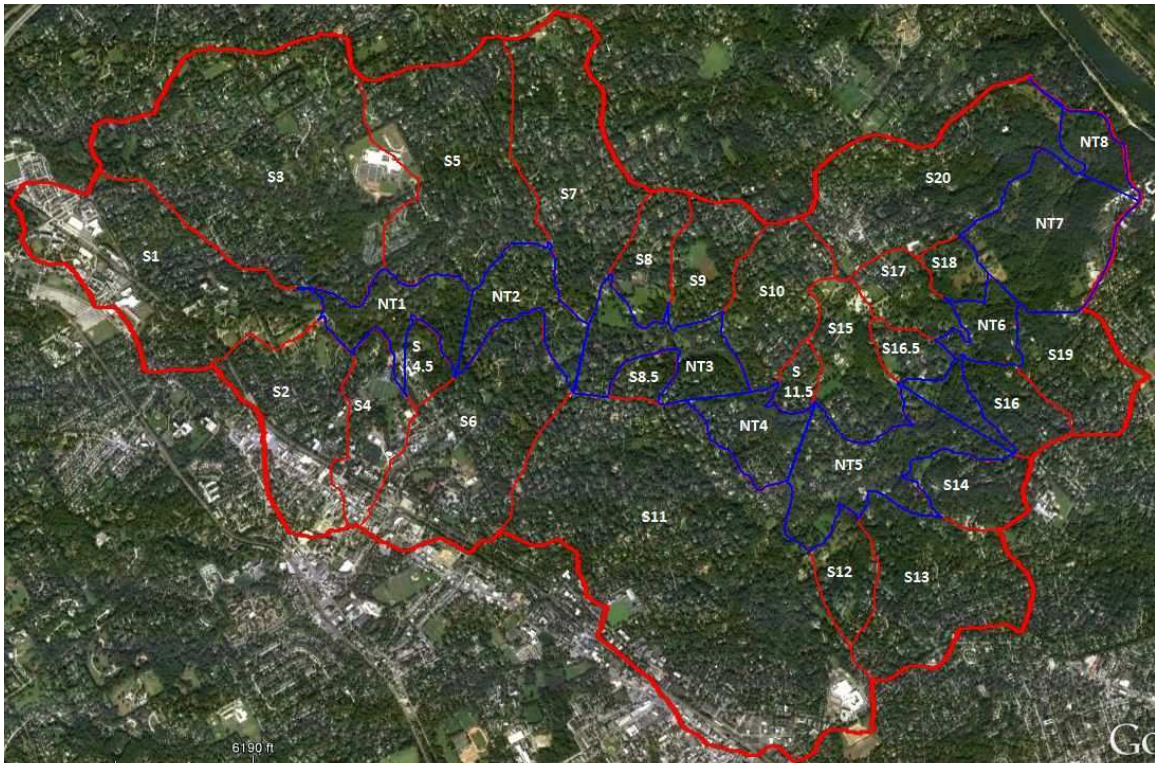

Figure 6.1: The Subwatersheds of Mill Creek

The subwatersheds denoted with an "S" were developed through StreamStats and contain a tributary of Mill Creek. The remaining area not associated with a stream confluence was broken up into 8 sections (outlined in blue) and labeled "NT" for non-tributary. Table 6.2 displays relevant information for each subwatershed that was used as the basis for the SWMM geometry inputs. Interestingly, the subwatersheds of Mill Creek are more

populated and urbanized in the upstream portions of the watershed, while the downstream portions become more forested as Mill Creek confluences with the Schuylkill River.

Table 6.2: Subwatershed Data From USGS StreamStats

ID	Area (mi^2)	% Imperv. area	ID	Area (mi^2)	% Imperv. area
S1	0.543	20.4	S14	0.130	2.9
S2	0.307	30.7	S15	0.202	4.3
S3	0.919	5.3	S16	0.100	1.4
S4	0.159	27.9	S16.5	0.057	2.4
S4.5	0.051	8.5	S17	0.110	4.8
S5	0.494	5.5	S18	0.064	0.6
S6	0.432	18.6	S19	0.192	6.8
S7	0.407	3.7	S20	0.440	6.2
S8	0.102	1.8	NT1	0.152	6.0
S8.5	0.072	2.8	NT2	0.170	5.0
S9	0.130	2.3	NT3	0.220	4.0
S10	0.189	4.0	NT4	0.189	4.0
S11	1.274	13.3	NT5	0.173	3.5
S11.5	0.041	2.0	NT6	0.160	4.0
S12	0.108	3.5	NT7	0.247	2.0
S13	0.340	6.3	NT8	0.165	1.5

Similar to a lag time, SWMM uses "overland flow width" to aid in runoff calculations. This parameter is defined by the subcatchment's area divided by the length of the longest overland flow path. Generally, true overland flow can only occur for distances of approximately 500 feet before consolidating into rivulet flow (Gironas, et al. 2009). Due to the large areas and inherently long flow paths of the subwatersheds in Mill Creek, the overland flow length for calculations was taken to be 500 feet. These parameters were altered during model calibration discussed in Section 6.4.

Manning's overland roughness coefficient (n) was estimated based on the land uses of each subwatershed. The Manning coefficient is used to describe the roughness of the material that a fluid is flowing across. The National Land Use Database (1992 and 2001) was utilized to determine the percent area covered by urban land, forest, and

miscellaneous uses. The roughness during overland flow on urban areas was estimated to be 0.06 (Arcement and Schneider 1990). Upon inspection of the aerial map of the watershed, "miscellaneous" land use was assumed to be light grass with a roughness of 0.15. Furthermore, forested land was determined to have an overland roughness of 0.4 (Engman 1986). Table 6.3 displays the weighted overland roughness coefficient of each subwatershed based on their respective land uses.

Table 6.3: Overland Manning's Roughness Estimation

ID	area (ac)	% urban	% forest	% misc	n overland	ID	area (ac)	% urban	% forest	% misc	n overland
S1	347.5	67.1	3.6	29.3	0.10	S14	83.2	23.0	0.7	76.3	0.13
S2	196.5	84.1	1.0	14.9	0.08	S15	129.3	38.7	6.6	54.8	0.13
S3	588.2	49.0	15.8	35.2	0.15	S16	64.0	19.0	0.0	81.0	0.13
S4	101.8	78.6	19.9	1.6	0.13	S16.5	36.5	33.7	0.0	66.3	0.12
S4.5	32.6	28.9	0.0	71.1	0.12	S17	70.4	40.4	0.0	59.6	0.11
S5	316.2	45.2	13.4	41.4	0.14	S18	41.0	12.3	11.6	76.1	0.17
S6	276.5	61.5	2.1	36.4	0.10	S19	122.9	51.5	14.6	33.9	0.14
S7	260.5	41.5	12.6	45.9	0.14	S20	281.6	34.3	45.5	20.2	0.23
S8	65.3	40.1	12.3	47.6	0.14	NT1	97.3	50.0	16.0	34.0	0.15
S8.5	46.1	38.0	0.0	62.0	0.12	NT2	108.8	45.0	15.0	40.0	0.15
S9	83.2	39.5	4.3	56.3	0.13	NT3	140.8	45.0	15.0	40.0	0.15
S10	121.0	47.7	2.3	50.0	0.11	NT4	121.0	45.0	20.0	35.0	0.16
S11	815.4	47.8	1.2	51.1	0.11	NT5	110.7	45.0	20.0	35.0	0.16
S11.5	26.2	29.5	0.0	70.5	0.12	NT6	102.4	45.0	20.0	35.0	0.16
S12	69.1	43.0	0.0	57.0	0.11	NT7	158.1	45.0	20.0	35.0	0.16
S13	217.6	44.3	0.0	55.7	0.11	NT8	105.6	45.0	45.0	10.0	0.22

The infiltration calculations in the SWMM model were set to solve via the runoff curve number (CN) method. The CN of the Mill Creek watershed was estimated using the Web Soil Survey software developed by the United States Department of Agriculture (USDA). The curve number is an empirical parameter used to predict direct runoff and infiltration of a storm event. Assuming this parameter would be altered during model calibration, finding the curve numbers of each subwatershed was deemed unnecessary. A map overlay of the Mill Creek Watershed was obtained from the PADEP and uploaded into

the Web Soil Survey interface. The soil map was then drawn by the program based on available soil data (Figure 6.2).

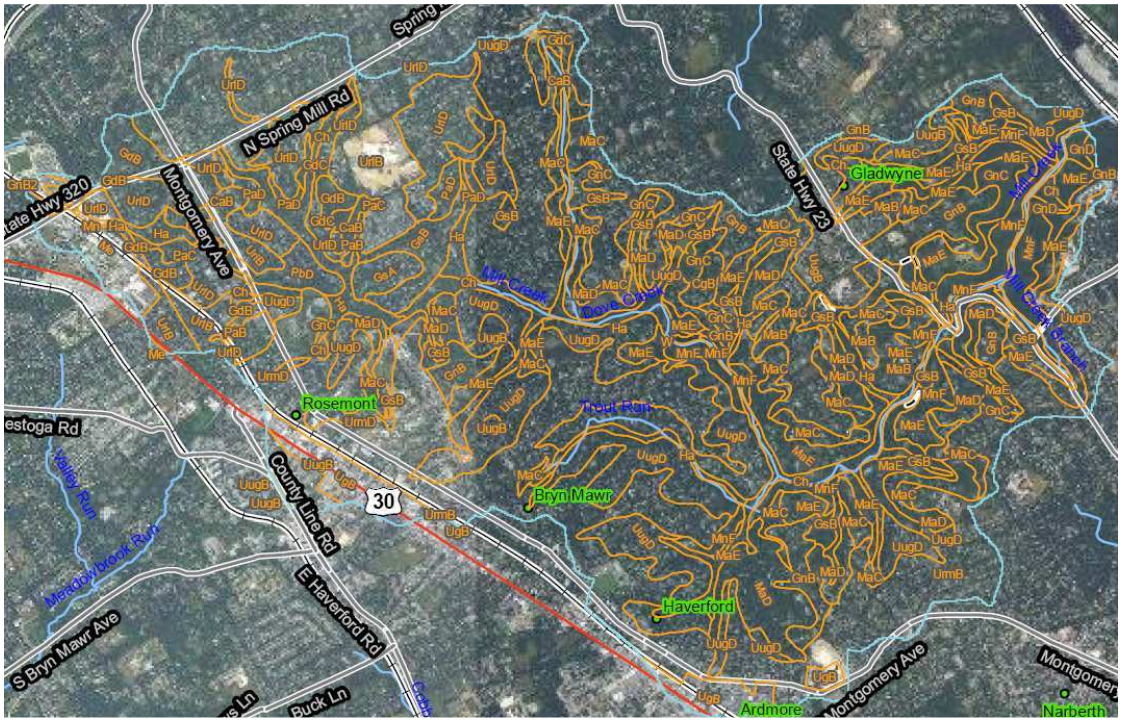

Figure 6.2: Soil Map of the Mill Creek Watershed

After the soil types were found for the Mill Creek watershed, they were correlated to the appropriate hydrologic soil group. Once the soil groups were assigned, a range of curve numbers associated with each group was determined (USDA 2009). A weighted CN of 77 was found based on the soil curve numbers and the amount of each type of soil within the area of interest.

In addition to providing soil distribution data, Web Soil Survey was used for assumptions in the development of the SWMM model. It was found that the probability of ponded water in surface depressions was minimal for the Mill Creek watershed. Ponding instances in SWMM were set to be insignificant by minimizing surface depression

storage areas. Furthermore, the Web Soil Survey indicated that the depth to the water table remained greater than or equal to 6.5 feet, therefore the SWMM model was set to run in unsaturated conditions.

6.2.2 Existing Low Impact Development Controls

Existing stormwater control measures located on Villanova's campus were input into SWMM as low impact development (LID) controls. The presence of these control measures should be accounted for in the model as they lessen stormwater runoff magnitudes. Emulating accurate runoff and infiltration amounts in SWMM is important for this study to assess the effects of widespread rain garden implementation.

The control measures present within the Mill Creek watershed consist of a porous asphalt/pervious concrete parking lot, infiltration trench, treatment train, rain garden, and a constructed stormwater wetland. These systems serve as research sites for the Civil Engineering department, and their design specifications are known. The control measures were input into SWMM using the "LID control editor". Within this editor, SWMM contains templates for five LID types: porous pavement, bio-retention cell, infiltration trench, rain barrel, and vegetative swale.

The porous asphalt/pervious concrete control system on Villanova's campus was input into SWMM as the "porous pavement" type. Required parameters for this type included the surface, pavement, and storage layers and under drain flow. Table 6.4 shows the parameters input for the pervious pavement system as per design specifications.

Table 6.4: Villanova's Porous Asphalt/Pervious Concrete SWMM Input							
Surface		**Pavement**		**Storage**		**Under drain**	
Storage Depth (inch)	0.0	Thickness (inch)	6	Height (inch)	42	Drain Coefficient	0.0
Vegetation Fraction	0.0	Void Ratio	0.2	Void Ratio	0.4		
Surface roughness (n)	0.01	Impervious Surface Fraction	0.0	Conductivity (in/hr)	300		
Surface Slope (%)	2.0	Permeability (in/hr)	700	Clogging Factor	0.0		
		Clogging Factor	0.0				

Because the porous asphalt/pervious concrete site is a continuous (non-modular) system, the impervious surface fraction was set to zero. Ideal conditions were assumed, so the clogging factor was set to zero for both the pavement and soil properties. Furthermore, no under drain was defined as there would be no expected outflow given the magnitude of the chosen storm simulation (see section 6.2.3).

Villanova's infiltration trench was input into SWMM using the "infiltration trench" LID editor. Required input parameters include the surface layer, storage layer, and under drain flow. Table 6.5 displays the data input for the infiltration trench.

Table 6.5: Villanova's Infiltration Trench SWMM Input					
Surface		**Storage**		**Under drain**	
Storage Depth (inch)	0.0	Height (inch)	72	Drain Coefficient (in/hr)	0.0
Vegetation Fraction	0.0	Void Ratio	0.25		
Surface roughness (n)	0.01	Conductivity (in/hr)	400		
Surface Slope (%)	1.0	Clogging Factor	0.0		

Again, no clogging was assumed to occur within the storage layer, and no under drain was defined as no overflow was expected to occur. The treatment train was input into SWMM as three separate controls: a vegetative swale, a bio-retention cell, and an infiltration trench. Table 6.6 shows the three segments of the treatment train, and their parameters input into SWMM.

Table 6.6: Villanova's Treatment Train SWMM Input

LID Control	Input Layer	Input Parameter					
Vegetative Swale	Surface	Storage Depth (in)	Vegetation Volume Fraction	Surface Roughness (n)	Surface Slope (%)	Swale Side Slope	
		21	0.0	0.09	5.4	2.0	
Bio-Retention Cell	Surface	Storage Depth (in)	Vegetation Volume Fraction	Surface Roughness (n)	Surface Slope (%)		
		18	0.0	0.1	2.2		
	Soil	Depth (in)	Porosity	Field Capacity	Wilting Point	Cond. (in/hr)	Suction Head (in)
		12	0.25	0.2	0.1	0.5	3.5
	Storage	Height (in)	Void Ratio	Cond. (in/hr)	Clog Factor		
		12	0.75	10	0.0		
Infiltration Trench	Surface	Storage Depth (in)	Vegetation Volume Fraction	Surface Roughness (n)	Surface Slope (%)		
		0.0	0.0	0.011	5.7		
	Storage	Height (in)	Void Ratio	Cond. (in/hr)	Clog Factor		
		51.6	0.49	10	0.0		

The SWMM users manual (2009) recommends a vegetation volume fraction of 0.1 to 0.2 for very dense growth. Even though the treatment train is a vegetated system, the vegetation volume fraction was chosen to be zero due to its sparse growth as a newly implemented system. Furthermore, an under drain was not defined for this control measure, and no clogging was assumed. A soil capillary suction head of 3.5 inches was assumed for the sandy-loam soil of the bio-retention cell (Rawls, et al. 1983).

Villanova's west campus rain garden was input into SWMM using the "bio-retention cell" LID editor. As seen in the treatment train input, this editor requires surface, soil, and storage information. Table 6.7 displays the relevant parameters for this control measure.

Table 6.7: Villanova's West Campus Rain Garden SWMM Input					
Surface		**Soil**		**Storage**	
Storage Depth (inch)	12	Thickness (in)	18	Height (inch)	12
Vegetation Fraction	0.0	Porosity	0.3	Void Ratio	0.45
Surface roughness (n)	0.25	Field Capacity	0.2	Conductivity (in/hr)	10
Surface Slope (%)	1.0	Wilting Point	0.1	Clogging Factor	0.0
		Conductivity (in/hr)	0.5		
		Suction Head (in)	3.5		

Lastly, Villanova's constructed stormwater wetland was input into SWMM. Unfortunately, no LID control was defined in the program for wetland systems, so the "Vegetative Swale" editor was used. This editor only requires the input of surface layer parameters. Table 6.8 displays the SWMM information for the constructed stormwater wetland.

Table 6.8: Villanova's Stormwater Wetland SWMM Input	
Surface	
Storage Depth (inch)	24
Vegetation Fraction	0.05
Surface roughness (n)	0.08
Surface Slope (%)	1.0
Swale Side Slope	2.0

In addition to the LID editor inputs, each control measure was assigned a percent of impervious area to treat within the Villanova subwatershed based on the surface area of the control measure. This percent impervious area treated correlates to the percent runoff

that is handled by each stormwater control measure. Furthermore, the LID controls were set to send any possible outflow to pervious areas (ex: a rain barrel irrigating a lawn). Table 6.9 displays the percent of impervious area treated associated with each Villanova LID control in SWMM.

Table 6.9: Summary of Existing LID Controls as Input into SWMM

Control Name	SWMM LID type	Surface Area (ft^2)	% Subwatershed Area	% Impervious Area Treated
Porous Asphalt/Pervious Concrete	Porous Pavement	3000	0.020	1.225
Infiltration Trench	Infiltration Trench	130	0.001	3.430
Treatment Train	Vegetative Swale	600	0.004	0.393
	Bio-Retention Cell	108	0.001	0.786
	Infiltration Trench	80	0.001	0.393
West Campus Rain Garden	Bio-Retention Cell	4225	0.084	1.960
Stormwater Wetland	Vegetative Swale	40768	0.269	5.995
Total			**0.362**	**14.182**

The existing stormwater control measures within the Villanova watershed (i.e. subwatershed "S1") treat approximately 14% of the stormwater runoff due impervious areas.

6.2.3 Storm Development

It was assumed that the SWMM model would undergo a typical summer rainfall event characterized by a high intensity storm of short duration. Upon reviewing summer storm events in the Villanova area during the 2011 and 2012 year, a typical event of a 6 hour, 0.5 inch storm was chosen. Based on the location of the Mill Creek watershed in Eastern

Pennsylvania, the SCS type II storm distribution was used. Figure 6.3 shows the cumulative rainfall over 6 hours using a time step of 6 minutes.

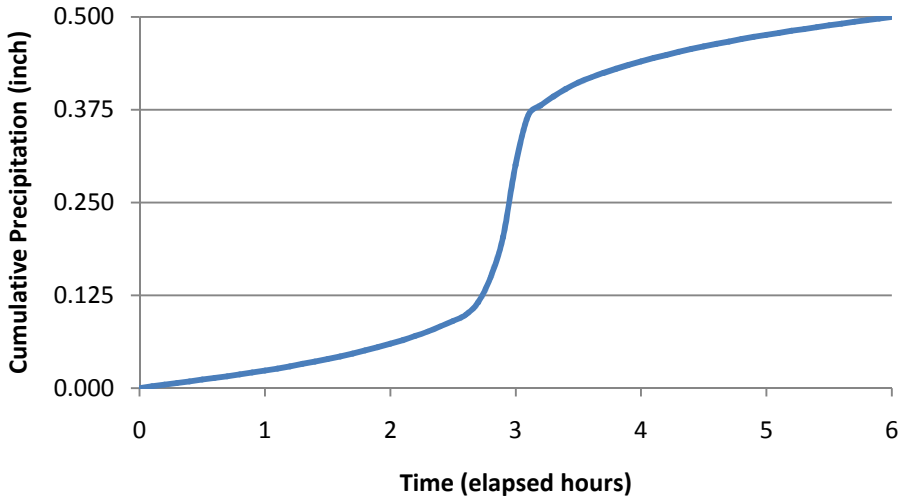

Figure 6.3: SCS Storm Distribution for SWMM

The rainfall event was input into SWMM as cumulative rain gauge data. During model simulation, the storm was assumed to occur over the entire Mill Creek watershed, and therefore was assigned to each subwatershed.

6.2.4 Climate Data

Temperature, evaporation, and wind speed data for the Mill Creek watershed was imported into SWMM to mimic typical summer conditions. Climate information for southeastern Pennsylvania was gathered from the National Climatic Data Center (NCDC) (NOAA 2011) for August of 2011. Conveniently, the files obtained from the NCDC database were compatible for direct upload into the SWMM program.

6.3 Hydraulics

6.3.1 Stream Flow Development

Mill Creek was input into SWMM as a series of nodes and conduits. Nodes are points of a conveyance system that connect conduits together. Conduits are pipes or channels that move water from one node to another. In the case of Mill Creek, each conduit section was defined as an open channel with an irregular geometry.

A FEMA Flood Insurance Study (FIS) (2010) was obtained for Mill Creek which defined the channel bed elevation, slope, and water surface elevations for chosen design storms. Node locations were chosen along Mill Creek that correlated to a change in channel bed slope. In total, 22 nodes were developed which represented the general morphology of Mill Creek. The invert elevation of each node was defined in SWMM using the data from the FIS.

Once the nodes were defined, 21 conduit sections were developed which connected each node. The reach lengths of each section were obtained by measuring the distance between nodes from the FIS. The slope of each conduit was automatically calculated by SWMM using the invert elevations of the two connecting nodes. Figure 6.4 shows the channel network and subwatershed arrangement in SWMM. The solid black circles represent nodes and the solid black lines represent the Mill Creek conduits. The dotted black lines represent the flow routing path from each watershed to a respective node. The black triangular node at the top right of the illustration denotes the outflow point, i.e. the confluence with the Schuylkill River.

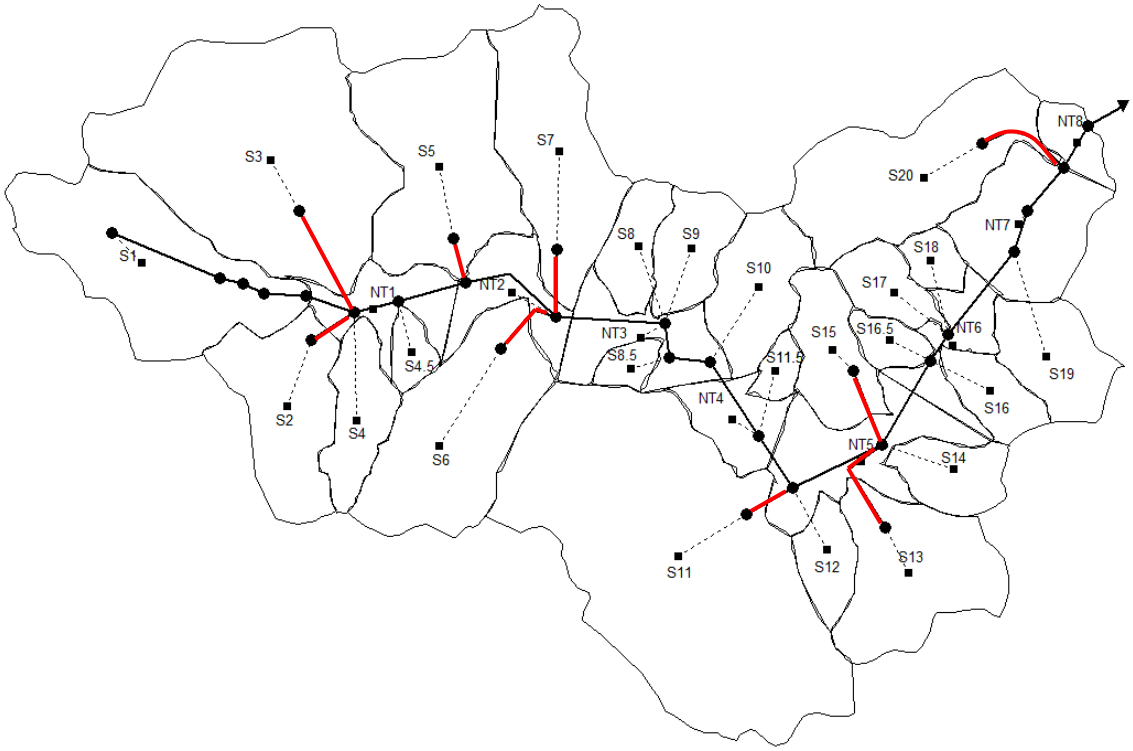

Figure 6.4: Mill Creek Stream Network in SWMM

In addition to the Mill Creek nodes and conduits, nine channels were defined which represented major tributaries to Mill Creek (marked with a solid red line). Invert elevations and reach lengths were estimated using Google Earth and Bing Maps. It is important to note that the visual representation displayed by SWMM has no effect on the surface runoff or flow routing calculations of the model.

6.3.2 Conduit Geometry

As mentioned previously, the conduits defined in SWMM were set to have an irregular geometry to mimic a natural channel. For simplicity, the channel was assumed to have a trapezoidal shape, with uniformly sloped channel banks and overbanks. With the invert elevations known for the Mill Creek sections, the channel depth and overbank elevations

were estimated using USGS topographic maps overlaid onto Google Earth. Furthermore, the channel top width was estimated and verified using Google Earth and Bing Maps respectively.

Once the Mill Creek conduits were developed, the geometry of the nine tributary conduits were estimated. Again, Google Earth and Bing Maps were used to approximate the overbank elevations and channel width. The channel bed depths were assumed based on the elevations of the Mill Creek nodes that the tributaries connected to. Figure 6.5 shows a representation of the channel geometry as defined in SWMM with uniformly sloped channel banks and flood plains.

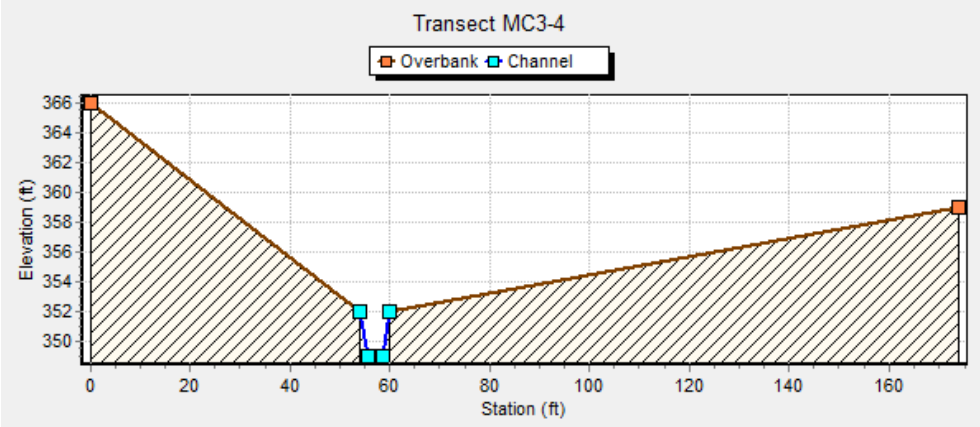

Figure 6.5: Typical Channel Geometry Displayed in SWMM

After constructing the cross sectional geometry for each conduit, it was found that a number of the channel side slopes were steeper than a 1 horizontal to 1 vertical ratio. A site visit was conducted in August 2012 to investigate the side slopes along Mill Creek as well as observe flow trends and vegetative cover (Figure 6.6a).

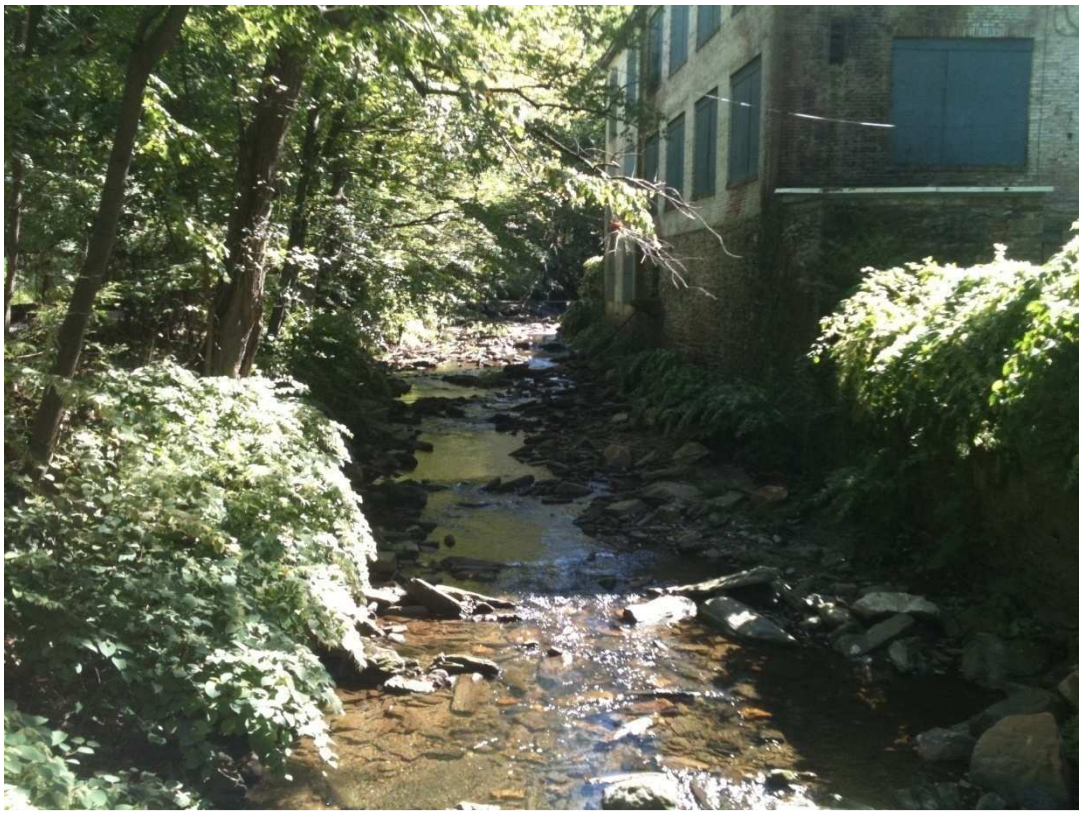

Figure 6.6a: Mill Creek Site Investigation

Interestingly, it was found that many sections of the reach contained rocky and steep side slopes. In some instances, old industrial buildings had become part of the channel geometry. Based on the site investigation, the relatively steep side slopes calculated for segments of the cross sectional geometry was deemed appropriate.

6.3.3 Conduit Manning's Coefficient

A roughness coefficient was determined for the channel and overbanks of each conduit section. The aforementioned site visit revealed that Mill Creek contained a fair amount of rocks within the channel. Figure 6.6b shows the typical vegetation density and channel shape of Mill Creek.

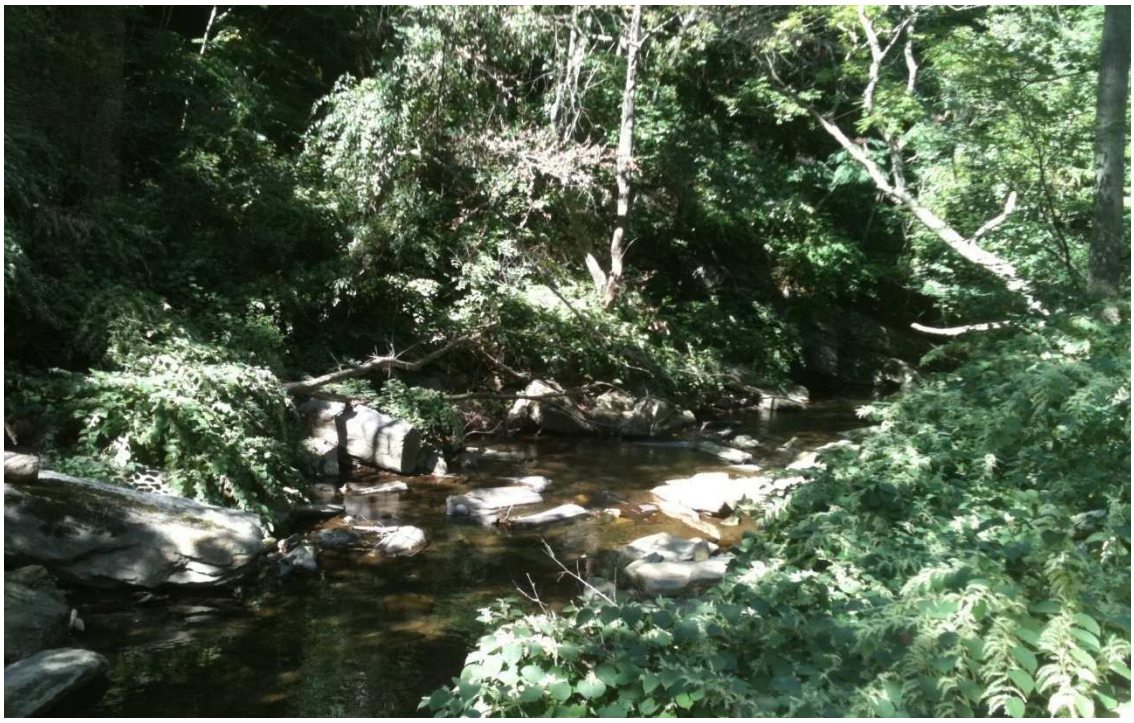

Figure 6.6b: Mill Creek Site Investigation

The overbanks appeared to be heavily vegetated at all observation points, with many broken limbs hanging into the channel itself. Furthermore, the channel contained many bends with turbulent areas due to flow obstructions. With this information, the roughness of the channel and overbanks were estimated to be 0.04 and 0.05 respectively (Engman 1986).

6.3.4 Base Flow Development

Base flow needed to be established in the model to parallel the behavior of Mill Creek. This can be developed in SWMM by establishing a ground water flow, defining an initial flow at a node, or defining a flow at certain conduits. With little information known about the ground water table and hydrologic soil parameters, base flow was defined at key

nodes along the channel in an attempt to mimic the influence of ground water as well as tributary stream confluences.

After observation of the stream depth along Mill Creek during the August 2012 site investigation, Manning's equation was utilized to obtain a base flow condition at each conduit section. Table 6.10 displays the base flow calculations where the conduit number increases from upstream to downstream.

Table 6.10: Base Flow Calculations Using Manning's Equation

SWMM Conduit #	Slope (%)	Side Slope	Depth (ft)	Base Width (ft)	Area (ft^2)	Wetted Perim. (ft)	Base Flow (cfs)
1	1.3	0.17	0.50	3.0	1.5	4.0	3.5
2	2.4	0.50	0.50	2.7	1.5	3.8	4.5
3	2.8	0.50	0.50	3.0	1.6	4.1	5.4
4	2.6	1.00	0.50	3.8	2.2	5.2	7.2
5	1.6	1.00	0.60	4.0	2.8	5.7	8.0
6	0.5	0.50	0.60	8.0	5.0	9.3	8.3
7	0.6	2.00	0.60	8.0	5.5	10.7	10.4
8	0.4	1.00	0.60	10.0	6.4	11.7	10.1
9	0.7	1.00	0.60	10.0	6.4	11.7	13.3
10	2.1	3.00	0.75	16.8	14.3	21.5	58.8
11	0.1	1.00	1.50	26.8	42.5	31.0	57.0
12	1.8	1.00	0.80	17.0	14.2	19.3	58.5
13	1.9	2.00	0.80	14.0	12.5	17.6	50.7
14	0.7	0.50	0.75	27.0	20.5	28.7	52.7
15	0.8	1.00	1.10	23.0	26.5	26.1	89.0
16	1.3	1.50	1.10	18.0	21.6	22.0	89.1
17	1.1	2.00	1.00	28.0	30.0	32.5	111.1
18	0.5	2.00	1.00	39.0	41.0	43.5	100.8
19	1.2	2.00	1.00	40.0	42.0	44.5	165.5
20	1.4	2.00	1.20	36.0	46.1	41.4	216.0
21	0.9	0.10	1.20	58.8	70.7	61.2	277.6

From the calculations, it was found that Mill Creek discharges approximately 278 cfs to the Schuylkill River during base flow conditions. The aforementioned table has been broken up into five distinct flow regimes denoted by color. Intuitively, the flow magnitude generally increases from upstream to downstream as tributaries converge with

Mill Creek. For simplicity, the five flow segments were modeled in SWMM by assigning an initial flow to key nodes along the Mill Creek conduit. Table 6.11 displays the average flow of each flow section input into SWMM compared to the Manning's calculations, with flow regime 1 being the farthest upstream, and flow regime 5 being Mill Creek's confluence with the Schuylkill River.

Table 6.11: SWMM Base Flow Versus Calculated

Flow Regime #	Avg SWMM Base Flow	Avg Calculated Base Flow
1	3	6
2	14	11
3	46	56
4	99	97
5	220	220

To determine if the SWMM base flow is within acceptable limits, data was gathered from two existing USGS stream gages along the Schuylkill River upstream and downstream of the Mill Creek confluence. The upstream gage is located in Norristown, P.A. and the downstream gage is located in Philadelphia, P.A. Three base flow time spans were evaluated from August 2011. Table 6.12 displays the average base flow of these time increments in comparison to the flow contributed by Mill Creek.

Table 6.12: Mill Creek Base flow Contribution to the Schuylkill River

Base Flow Time Span (2011)	Flow Difference (cfs)	Average (cfs)	Flow Contributed by Mill Creek (%)
8/9	453	343	81
8/10	349		
8/11	227		
8/16	717	523	53
8/17	451		
8/18	314		
8/19	612		
8/23	666	419	66
8/24	343		
8/25	150		
8/26	517		

From the data gathered, Mill Creek contributes to approximately 50-80% of the base flow between the gages. Upon investigation of topographic maps and Google Earth, there are three other 1st order streams aside from Mill Creek that contribute to the base flow of the Schuylkill River between Norristown and Philadelphia. Based on these observations, it seems that the base flow input into the SWMM model is acceptable for the purposes of this analysis.

The final step in the creation of base flow pertained to ensuring it's stability throughout the model computation. Base flow was observed by setting the rain gage to a dry condition (producing no precipitation). Figure 6.7 shows the base flow of the watershed observed at the outflow or confluence to the Schuylkill River during the first 10 hours of the simulation.

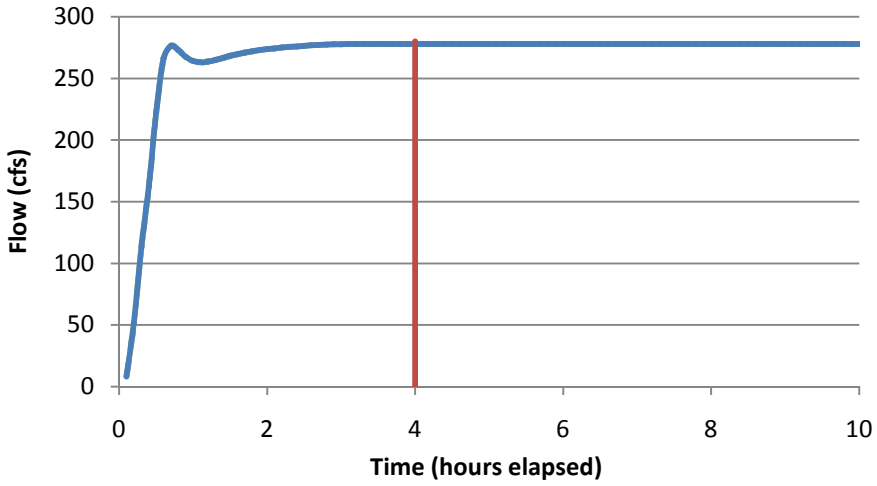

Figure 6.7: Base Flow Stabilization in SWMM

The base flow endures a stabilization period shortly after starting the model due to the introduction of flow at key nodes along the conduit. Base flow equalizes once

approximately 4 hours have passed (as denoted by the vertical red line). Therefore, the model was set to report data after 4 hours have elapsed during simulation. Similarly, the typical summer storm was set to occur 12 hours into the model simulation.

6.4 Model Calibration

Once the hydrologic and hydraulic parameters of the Mill Creek watershed were defined, the model was calibrated to verify the selected parameters. The previously obtained FEMA flood maps were used to determine the water surface elevation of the 10 year 24 hour storm (5 inches of precipitation) at each node along Mill Creek. Again, the SCS type II distribution in 6 minute intervals was used to develop the design storm, which is displayed in Figure 6.9.

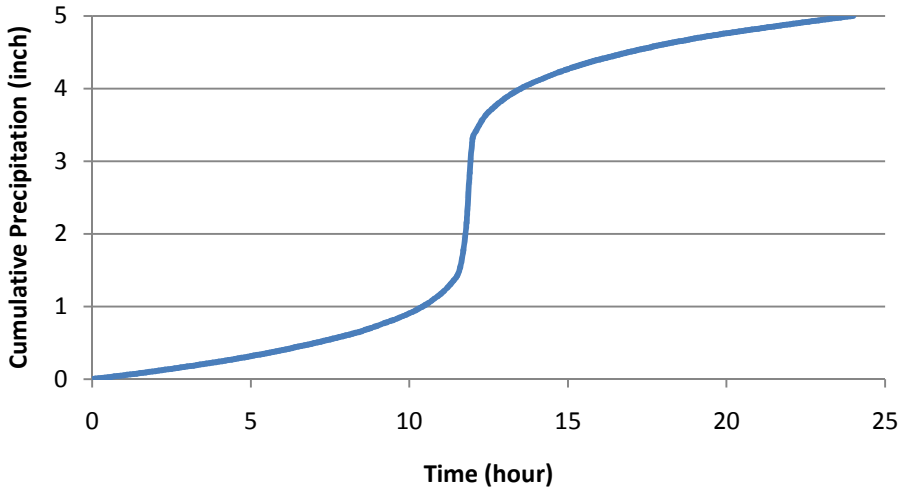

Figure 6.8: 10 Year 24 Hour Design Storm for Model Calibration

Once the design storm was input into SWMM, the model was run and the maximum water depth at each node was compared to the flood depth illustrated by the Mill Creek flood mapping. Initially, the uncalibrated model showed an average of 33% error at each node. Parameters of the model were then altered to obtain an error of under 20%.

To produce maximum flow depths parallel to the Mill Creek FEMA flood mapping, parameters were altered in both the subwatersheds and the conduits. Overland flow width and curve number were modified within the subwatershed editor of SWMM. In nodes that required a greater depth (higher peak flow), the curve numbers and overland flow widths were increased in the contributing subwatersheds (and vice versa).

Fine adjustments were made through the modification of the channel and overbank Manning's roughness coefficient of the conduit sections. Generally, as the roughness of the conduit increases (an increase of Manning's coefficient), flow will be impeded, and the depth of water in the conduit will increase. Table 6.13 displays the 10 year storm depth of the flood study compared to the node depth of the model pre and post calibration. Node values increase from upstream to downstream. Node #1 was not included in calibration as it was not present on the FEMA flood study.

After the parameter calibration was completed, an average error of 15% was achieved at each node. The upstream nodes were more difficult to calibrate, with nodes 2, 3, and 4 remaining above a 20% error. This difficulty in calibration was assumed to be caused by the boundary conditions of the model itself.

Table 6.13: Water Surface Elevation Calibration							
Node #	**channel bed elev. (ft)**	**10 yr elev. (ft)**	**Flood Depth (ft)**	**Uncalibrated Model Depth (ft)**	**% error**	**Calibrated Model Depth (ft)**	**% error**
2	354.7	361.5	6.8	4.09	40	3.81	44
3	349.0	355.5	6.5	3.50	46	5.12	21
4	337.4	341.5	4.1	3.49	15	2.99	27
5	311.0	315.0	4.0	2.72	32	3.35	16
6	292.0	297.0	5.0	4.22	16	4.73	5
7	286.0	291.5	5.5	4.19	24	5.33	3
8	275.5	284.5	9.0	4.17	54	6.94	23
9	266.0	271.5	5.5	4.14	25	5.00	9
10	247.8	253.0	5.2	3.87	26	4.92	5
11	230.9	238.5	7.6	6.15	19	7.72	2
12	230.0	236.5	6.5	6.13	6	6.64	2
13	190.0	198.0	8.0	3.72	54	8.50	6
14	160.0	170.0	10.0	4.24	58	7.30	27
15	141.5	145.5	4.0	4.44	-11	4.14	3
16	122.0	125.5	3.5	4.44	-27	5.62	61
17	112.0	117.0	5.0	4.41	12	4.91	2
18	78.5	85.0	6.5	3.74	42	7.24	11
19	74.5	82.0	7.5	3.74	50	6.66	11
20	60.0	65.5	5.5	3.22	41	5.49	0
21	36.0	49.0	13.0	7.07	46	13.24	2
22	35.3	48.5	13.2	7.07	46	8.09	39
Average Absolute % Error					**33**		**15**

The curve number was altered from the original 77 in each subwatershed to a range of 65 to 95. Overall, the average weighted curve number remained 77 for the entire watershed. Most of the subwatershed overland flow widths were altered for calibration purposes, all of which were decreased in width to produce a lower peak flow. The channel and overbanks Manning's coefficient was initially set to 0.04 and 0.05, respectively. After calibration, the roughness coefficients ranged from 0.1 to 0.01, generally decreasing in roughness from upstream to downstream. The specific calibrated parameters for each subwatershed and conduit section is presented in Appendix D.

6.5 Theoretical Rain Garden Implementation

To determine the number of rain gardens needed to produce a reduction in flow in an urbanized watershed, a typical rain garden design was developed and input into SWMM. Using Google Earth, the number of structures were counted in each subwatershed including residential and commercial buildings. Generally, residential buildings were the dominant structure type.

Schueler (1994) indicates that transportation related imperviousness (roads, parking lots, etc) comprises 63 to 70% of the total impervious cover in residential and commercial areas. Furthermore, a study of U.S. cities estimated that 30-50% of impervious cover was due to structures (Nowak and Greenfield 2012). Based on these findings, the percent impervious area due to structures in each subwatershed was estimated to be approximately 34% of the total impervious area.

An average roof imprint was estimated for each subwatershed by dividing the impervious area due to structures by the number of buildings counted. Assuming one rain garden is associated with each structure, the rain garden area was found by dividing the average roof area by 5 for each subwatershed. This is based on the PADEP recommendation of a 5:1 drainage to infiltration area for stormwater control measures (2006). Table 6.13 displays the development of the rain garden (RG) area for each subwatershed. As expected, buildings with a large average roof area will require a larger rain garden in order to handle the roof runoff during a storm event.

Table 6.14: Rain Garden Development									
ID	Structure IA (ac)	# of Structures	Roof Area (ft^2)	RG Area (ft^2)	ID	Struc. IA (ac)	Total Struc.	Roof Area (ft^2)	RG Area (ft^2)
S1	24.1	197	5330	1066	S14	0.8	27	1305	261
S2	20.5	475	1881	376	S15	1.9	45	1817	363
S3	10.6	404	1138	228	S16	0.3	20	682	136
S4	9.7	82	5128	1026	S16.5	0.3	9	1411	282
S4.5	0.9	12	3424	685	S17	1.2	67	752	150
S5	5.9	258	1004	201	S18	0.1	6	597	119
S6	17.5	230	3311	662	S19	2.8	99	1254	251
S7	3.3	144	997	199	S20	5.9	221	1166	233
S8	0.4	26	654	131	NT1	2.0	82	1054	211
S8.5	0.4	37	515	103	NT2	1.8	73	1104	221
S9	0.7	33	870	174	NT3	1.9	55	1517	303
S10	1.6	80	891	178	NT4	1.6	44	1629	326
S11	36.9	655	2452	490	NT5	1.3	45	1275	255
S11.5	0.2	15	523	105	NT6	1.4	38	1596	319
S12	0.8	38	954	191	NT7	1.1	35	1338	268
S13	4.7	269	758	152	NT8	0.5	19	1235	247

Next, the volume capacity of the rain garden associated with each subwatershed was checked against the 0.5 inch 6 hour design storm. It was found that the rain gardens would be able to successfully capture and infiltrate roof runoff from their respective structures. The design parameters of the proposed rain garden was implemented into SWMM using the "bio-retention cell" LID editor. Table 6.15 shows the values used to develop the typical rain garden, as recommended by the PADEP (2006). It was assumed that no clogging would occur, and there would be no under drain for these structures. It was also assumed that tall grasses, trees and shrubs were abundant, so a vegetation fraction of 0.1 was chosen.

Once the parameters were developed for the typical rain garden, four scenarios were created that varied the magnitude of rain gardens throughout the Mill Creek watershed. The scenarios included the implementation of 25%, 50%, 75%, and 100% of the rain

gardens possible within the watershed. For simplicity, an even distribution of the rain gardens was assumed.

Table 6.15: Typical Rain Garden SWMM Input					
Surface		**Soil**		**Storage**	
Storage Depth (inch)	12	Thickness (in)	18	Height (inch)	12
Vegetation Fraction	0.1	Porosity	0.5	Void Ratio	0.40
Surface roughness (n)	0.05	Field Capacity	0.2	Conductivity (in/hr)	10
Surface Slope (%)	1.0	Wilting Point	0.1	Clogging Factor	0.0
		Conductivity (in/hr)	0.5		
		Suction Head (in)	3.5		

The 25% scenario indicates that one of four structures within any given subwatershed will have a rain garden handling the roof runoff. The 100% scenario means that every structure throughout the entire watershed will have a rain garden associated with it, yielding a theoretical runoff reduction of 34% throughout the entire watershed.

6.6 Impervious Area Iterations

Once the SWMM model was calibrated and the typical rain garden was developed, eight more models were built to create a range of percent impervious areas for the Mill Creek watershed. By developing a spectrum of impervious areas, the models could be compared to the impervious cover model theory, and flow reduction efficiency of the proposed rain gardens could be determined. The impervious cover model theory suggests that the behavior of urban stream indicators can be predicted on the basis of percent impervious cover in their contributing watershed (Schueler, et al. 2009). Figure 6.9 displays the most recent findings for the impervious cover model, with the dashed regions indicating transitional stages.

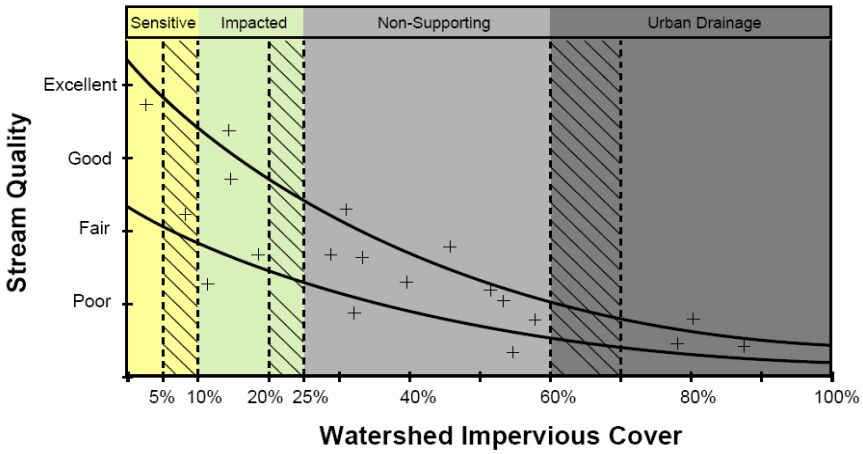

Figure 6.9: Impervious Cover Model (Schueler and Fraley-McNeal 2008)

Four classifications exist to define the quality of the stream: sensitive, impacted, non-supporting, and urban drainage. Impacted streams show clear signs of declining stream health, while non-supporting streams no longer fulfill their designated uses in terms of hydrology, channel stability, habitat, water quality, or biological diversity. Urban drainage is used to classify streams that have highly unstable channels, and poor to nonexistent habitats (CSN 2008).

After considering the impervious cover model, the impervious area of the Mill Creek watershed was scaled to reflect the stages of stream impairment. 3, 5, 10, 20, 25, 60, 70, and 80% weighted imperviousness was achieving by scaling the original model (recall the existing conditions of Mill Creek involved a 9% impervious area). The percent imperviousness of each subwatershed was proportionally altered as shown in the following equation:

$$IA_{s1} = IA_{s0} - IA_{s0}\left(\frac{IA_{w0} - IA_{w1}}{IA_{w0}}\right)$$

Where IA_{s0} and IA_{w0} denote the original impervious area of the subwatershed and entire watershed respectively. IA_{s1} and IA_{w1} describe the new impervious area of the model for

the subwatershed and entire watershed respectively. With the overall impervious areas defined as the stages of stream impairment from Schueler (2008), the only variable becomes IA_{s1}. This method forced areas that already had a high percent imperviousness to increase faster than that of a wooded subwatershed.

The number of structures in each subwatershed were also altered to reflect a large or small impervious area. The average roof areas found for the original model (of 9% impervious area) were held constant, and the total number of structures was back calculated. Table 6.16 shows the number of structures associated with each impervious area.

Table 6.16: Impervious Area Iterations and # of Structures

Weighted Impervious Area (%)	# Structures	±% From Existing
3	1,281	-67
5	2,135	-44
9	3,840	-
10	4,270	+11
20	8,539	+122
25	10,674	+178
60	29,101	+658
70	36,492	+850
80	43,908	+1,043

As the impervious area of the watershed increases, the number of structures dramatically increases from the existing conditions. In the models with the higher percent impervious areas, a handful of subwatersheds reach 100% imperviousness. This is not a realistic scenario, but will be useful when comparing SWMM results to Schueler's impervious cover model.

Nine SWMM models were built that varied the watershed's impervious cover. These models will be run in two scenarios: existing and proposed conditions. Existing conditions imply that there are no added rain gardens and will be referred to the "0% rain garden" condition throughout the text. Proposed conditions utilize the previously developed typical rain garden for catching roof runoff from the structures within each subwatershed. In addition, the proposed conditions will encompass the 25, 50, 75, and 100% rain garden distribution. In other words, the 50% rain garden models will have a rain garden associated with half of the existing structures. In total, 45 models will be run in SWMM during the typical summer storm event. After completion of the runs, the hydrologic impacts were assessed for the different levels of imperviousness coupled with the implementation of rain gardens in varied magnitudes.

Chapter 7

Results

The 45 SWMM models consisted of varied overall impervious areas (3, 5, 9, 10, 20, 25, 60, 70, and 80%) and percent rain gardens associated to the structures (0, 25, 50, 75, and 100%). Each model was run in SWMM for a typical summer storm event which consisted of 0.5 inches of precipitation over a 6 hour time period. The following sections provide a summary of the peak flow, velocity, and depth for the storm event analyzed, and shows the influence of the rain gardens. Furthermore, storm outflow volumes were compared for each SWMM model.

7.1 SWMM Calculation Errors

Prior to interpreting data results, the errors associated with each run were investigated to ensure accuracy of the models. Once completed, each of the 45 runs displayed percent error in the form of runoff continuity and flow routing. Table 7.1 shows the runoff continuity errors associated with each model analyzed.

Table 7.1: % Surface Runoff Continuity Error

	% RG				
%IA	**0 %(existing)**	**25**	**50**	**75**	**100**
3	-0.26	-0.26	-0.26	-0.27	-0.27
5	-0.23	-0.24	-0.24	-0.25	-0.25
9	-0.26	-0.27	-0.28	-0.29	-0.29
10	-0.27	-0.28	-0.29	-0.30	-0.31
20	-0.30	-0.32	-0.34	-0.36	-0.38
25	-0.33	-0.35	-0.38	-0.40	-0.42
60	-0.17	-0.23	-0.31	-0.37	-0.46
70	-0.21	-0.29	-0.37	-0.45	-0.55
80	-1.45	-0.33	-0.44	-0.52	-0.63

Runoff continuity errors occur when the initial volume storage is different than the final storage for the entire drainage system. As seen in the above figure, the surface runoff errors are typically below 1%, with the exception of the 80% impervious area model with no rain gardens. Generally, higher runoff continuity errors are associated with models of high impervious areas. Furthermore, the runoff error increased as the percent rain gardens associated with structures increased.

Table 7.2 below displays the flow routing continuity errors for each model analyzed. The flow routing errors remained minimal for all of the models, with a decrease in error as the impervious are increased. This may be caused by a higher magnitude of runoff being routed through the system as less infiltration occurs.

Table 7.2: % Flow Routing Continuity Error

	% RG				
%IA	**0% (existing)**	**25**	**50**	**75**	**100**
3	-0.03	-0.03	-0.03	-0.03	-0.03
5	-0.03	-0.03	-0.03	-0.03	-0.03
9	-0.03	-0.03	-0.03	-0.03	-0.03
10	-0.03	-0.03	-0.03	-0.03	-0.03
20	-0.02	-0.02	-0.02	-0.03	-0.03
25	-0.02	-0.02	-0.02	-0.02	-0.02
60	0.01	0.00	0.00	-0.01	-0.01
70	0.02	0.00	0.00	0.00	-0.01
80	0.02	0.01	0.01	0.00	0.00

The magnitude of continuity errors is a function of the size and complexity of the system being modeled in SWMM. The relatively small continuity errors experienced can be attributed to the simplification of many aspects of Mill Creek during development (short conduit lengths, intricate node systems, and small subwatersheds were typically avoided). EPA SWMM suggests an acceptable continuity error of less than 10% to ensure model

validity (Young, et al. 2009), which implies that the models developed are within an acceptable error range.

7.2 Peak Volumes and Volume Reductions

The effects of the percent impervious areas rain gardens were evaluated by looking at the total outflow volumes of the summer storm event. The total outflow volume includes the volume due to base flow conditions plus the stream flow volume from runoff during the storm event. Figure 7.1 displays the total outflow taken at the most downstream SWMM node (MC19) during the 0.5 inch, 6 hour storm for each model analyzed. As expected, the outflow volume increases with increasing impervious area and decreases with an increase in rain gardens.

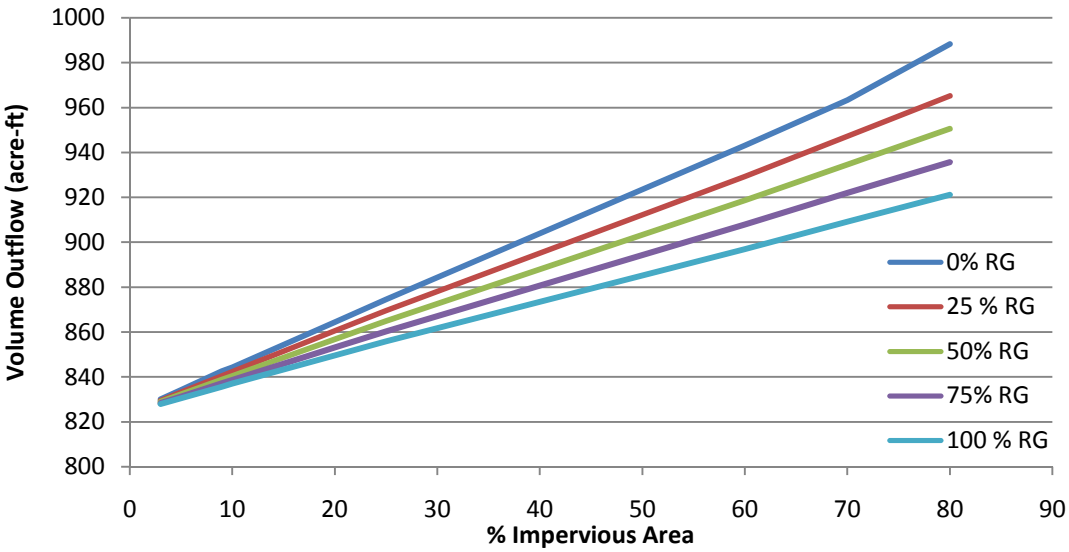

Figure 7.1: Total Volume Outflow (Base Flow & Storm Flow)

By looking at the outflow volumes, it was determined that the base flow of approximately 278 cfs (818 acre-ft) contributed to the bulk of the total outflow volume. To determine

the influence of the rain gardens on volume reduction, the volume attributed to the 0.5 inch 6 hour storm was separated from the base flow component for each SWMM run (Figure 7.2).

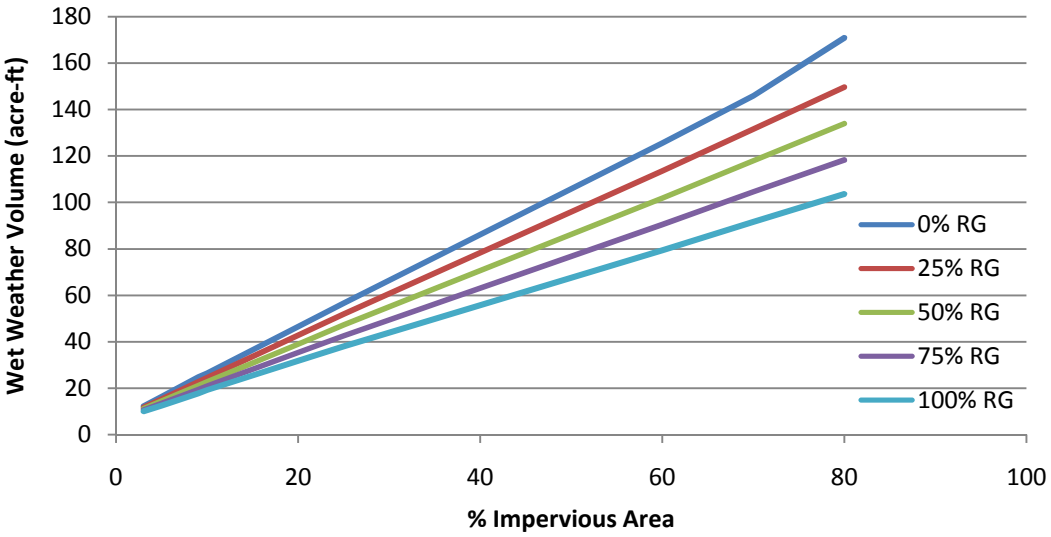

Figure 7.2: Storm Volume Outflow

As impervious area increases, more runoff occurs during the storm event which contributes to the increase in volume. The implementation of the rain gardens counteracts this by infiltrating the precipitation associated with roof runoff. Table 7.3 displays the percent volume reduction associated with each impervious area scenario as the total percentage of rain gardens increase.

Table 7.3: Outflow Volume Reductions (%) of the 0.5 Inch, 6 Hour Storm

	%IA								
% RG	**3**	**5**	**9**	**10**	**20**	**25**	**60**	**70**	**80**
0	0	0	0	0	0	0	0	0	0
25	4.5	6.8	8.6	6.9	8.1	8.4	9.5	9.8	12.4
50	8.7	12.3	15.1	13.8	16.2	16.7	18.9	19.2	21.6
75	13.1	17.7	21.7	20.6	23.9	24.9	28.0	28.4	30.8
100	17.4	23.1	28.2	27.4	31.6	32.9	36.9	37.3	39.4

Intuitively, as the fraction of rain garden to number of structures increases, the overall volume reduction will also increase. Furthermore, as the percent impervious area

increases from 3 to 80%, the volume reduction will also increase. This is due to the fact that the number of structures was set to grow based on the percent impervious area (see Chapter 6.5). The percent volume reduction per rain garden was found by dividing the overall volume reduction by the number of rain gardens for each SWMM model. These values were found to be very small, so Table 7.4 displays the 0.5 inch, 6 hour storm volume reduction per 1000 rain gardens.

Table 7.4: Storm Volume Reductions (%) per 1000 Rain Gardens

	%IA								
% RG	**3**	**5**	**9**	**10**	**20**	**25**	**60**	**70**	**80**
0	0	0	0	0	0	0	0	0	0
25	14.1	12.8	9.0	6.5	3.8	3.1	1.3	1.1	1.1
50	13.7	11.5	7.9	6.5	3.8	3.1	1.3	1.1	1.0
75	13.6	11.1	7.5	6.4	3.7	3.1	1.3	1.0	0.9
100	13.6	10.8	7.3	6.4	3.7	3.1	1.3	1.0	0.9
AVG	13.7	11.5	7.9	6.4	3.8	3.1	1.3	1.1	1.0

The influence of rain gardens on volume reduction is based on the percent impervious area of the watershed. As seen in the aforementioned table, the implementation of 1000 rain gardens in a watershed with 80% impervious area will produce a 1% volume reduction for the 0.5 inch, 6 hour storm event. Conversely, a watershed with 3% impervious area will produce an approximate 14% storm volume reduction.

7.3 Peak Outflow and Flow Reductions

The peak outflow of the storm refers to the greatest magnitude of stream flow during the storm event. Generally, as impervious area increases, peak flow will increase as more precipitation is contributing to overland runoff (Booth 1991). Figure 7.3 displays the outflow hydrograph trend of three impervious area scenarios for the 0 and 100%

theoretical rain garden implementation. These hydrographs were taken at node MC19 which is the most downstream point of the SWMM simulation.

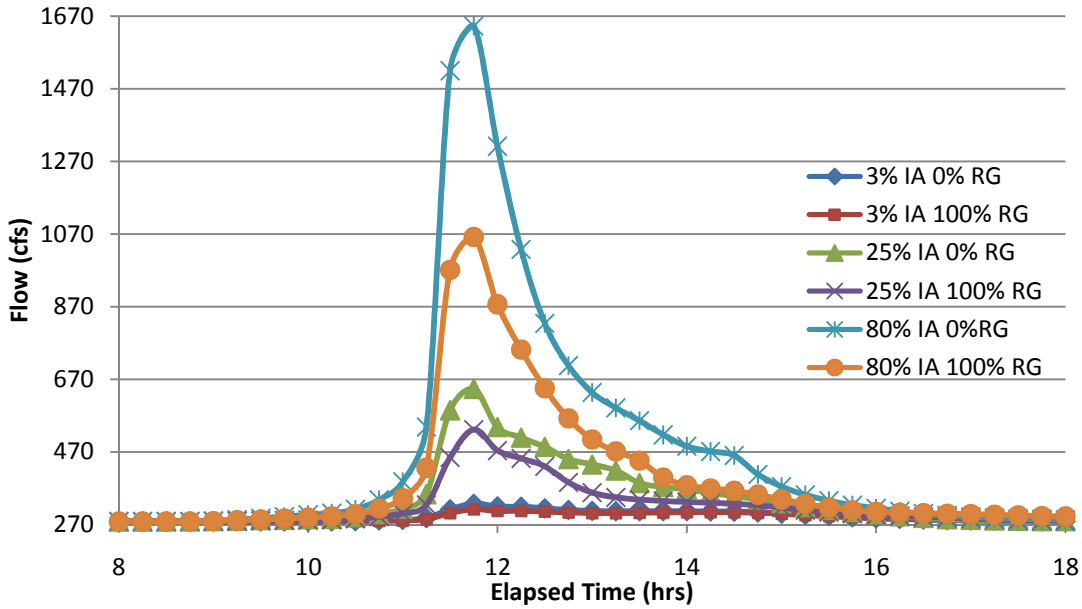

Figure 7.3: Storm Outflow Hydrograph Trend

One can see that the peak flow from the storm event dramatically increases as impervious area increases from 3% to 80%. Furthermore, the peak flow and overall area under the hydrograph is decreased as rain gardens are implemented, and a portion of stormwater is infiltrated rather than contributed to runoff. Appendix E displays the hydrographs for each SWMM scenario. After observing the outflow hydrographs for the 45 models, similar peak flows at node MC19 were noted for varying impervious areas and rain garden implementation. Table 7.5 lists the peak flow of each model during the storm event, and compares similar peak flows with a 4% tolerance. An arbitrary color scheme was used to denote models of comparable peak flows. Models with matching colors designate comparable peak flows shared by more than one scenario. Runs with dual colors indicate there is more than one model with comparable peak flows.

Table 7.5: Peak Outflow (cfs) and Model Equivalence

	%IA								
%RG	3	5	9	10	20	25	60	70	80
0	327.3	357.4	417.1	435.2	582.7	643.1	1228.8	1402.4	1643.2
25	323.2	350.9	406.2	421.0	560.6	616.5	1133.4	1282.9	1434.6
50	319.7	344.5	394.1	407.3	535.8	590.1	1043.1	1172.8	1303.9
75	315.9	338.1	382.1	393.8	510.2	562.5	957.0	1068.6	1176.8
100	312.1	331.7	370.4	380.5	482.5	531.5	876.2	969.5	1061.9

As seen, the 5% impervious area model with 100% rain garden implementation is comparable to the 3% impervious cover with no additional rain gardens. The 9, 10, 20, and 25% impervious area models showed similar peak flow reduction trends with the implementation of rain gardens. For example, the peak flow of the 10% impervious area model with 50% rain gardens is comparable to the 9% impervious cover model with no added stormwater control measures. The 60, 70, and 80% impervious area models seemed less efficient in reducing peak flow as the percentage of rain gardens increased.

The peak flow reductions were quantified by comparing the models with added rain gardens to the models with no additional storm water control measures (Table 7.6). Similar to the volume reduction trend, the peak flow due to the storm is further reduced as the number of rain gardens increase.

Table 7.6: Peak Flow Reductions (%) of the 0.5 Inch, 6 Hour Storm

	%IA								
%RG	3	5	9	10	20	25	60	70	80
0	0.0	0.0	0.0	0.0	0.0	0.0	0.0	0.0	0.0
25	1.2	1.8	2.6	3.3	3.8	4.1	7.8	8.5	12.7
50	2.3	3.6	5.5	6.4	8.1	8.2	15.1	16.4	20.7
75	3.5	5.4	8.4	9.5	12.4	12.5	22.1	23.8	28.4
100	4.6	7.2	11.2	12.6	17.2	17.3	28.7	30.9	35.4

The percent flow reductions were then divided by the number of rain gardens present in each run to determine the influence on peak flow reduction per rain garden. Table 7.7 displays the peak flow reduction of the 0.5 inch, 6 hour storm per 1000 rain gardens implemented for each SWMM model.

Table 7.7: Peak Flow Reductions (%) Per 1000 Rain Gardens

	%IA								
%RG	**3**	**5**	**9**	**10**	**20**	**25**	**60**	**70**	**80**
0	-	-	-	-	-	-	-	-	-
25	3.9	3.4	2.7	3.1	1.8	1.6	1.1	0.9	1.2
50	3.6	3.4	2.9	3.0	1.9	1.6	1.0	0.9	0.9
75	3.6	3.4	2.9	3.0	1.9	1.6	1.0	0.9	0.9
100	3.6	3.4	2.9	2.9	2.0	1.6	1.0	0.9	0.8
AVG	3.7	3.4	2.9	3.0	1.9	1.6	1.0	0.9	0.9

The influence of the rain gardens decreases with an increase in impervious area. Regardless of how many rain gardens implemented in the models, the influence per 1000 rain gardens stays roughly the same for each impervious area category. Overall, the addition of rain gardens does not seem to greatly influence the peak flow of the 0.5 inch, 6 hour storm.

7.4 Peak Velocities and Velocity Reductions

As the flow and volume are altered due to changes in impervious area and implementation of stormwater control measures, the velocity parameter is expected to be influenced as well. Velocity can be a contributor to stream impairment as increases in this parameter can lead to excessive erosion, pollutant transport, and/or aquatic habitat destruction (Leopold 1968; Barnes, et al. 2002). The maximum velocity during the 0.5 inch, 6 hour storm was evaluated at node MC19 for the 45 SWMM models. Figure 7.4

displays the maximum velocity trends as a function of impervious area and rain garden percentage.

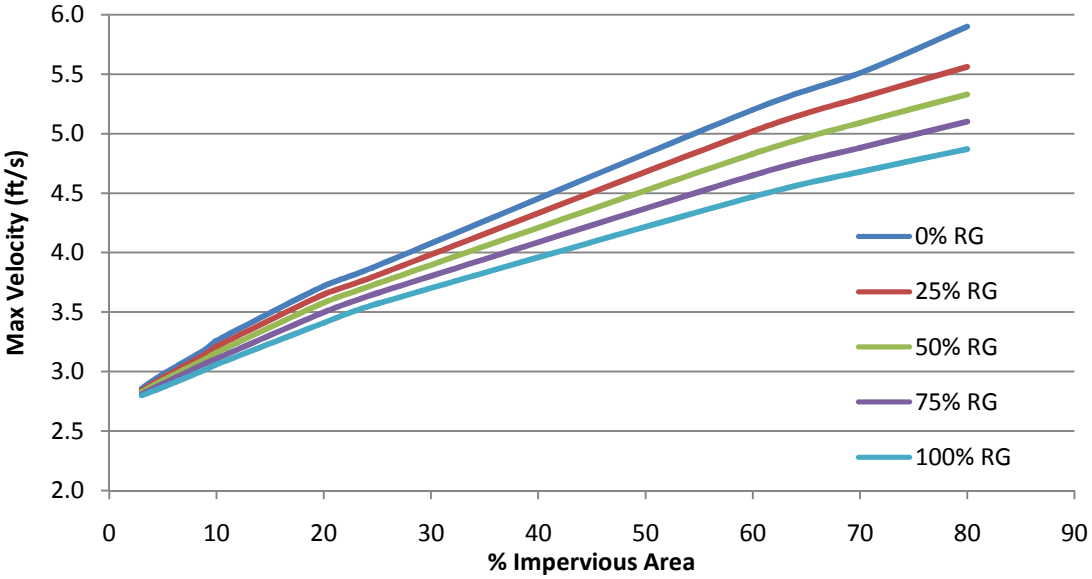

Figure 7.4: Maximum Storm Velocity

As expected, the results show an increase in velocity with greater watershed impervious area, but a decrease in velocity as more rain gardens are implemented. Equivalent SWMM models were assessed based on the peak velocity parameter with a 2% difference tolerance, as shown in Table 7.8.

Table 7.8: Peak Velocity (ft/s) and Model Equivalence

	%IA								
%RG	3	5	9	10	20	25	60	70	80
0	2.86	2.98	3.19	3.26	3.72	3.89	5.20	5.51	5.90
25	2.84	2.95	3.15	3.21	3.65	3.81	5.02	5.30	5.56
50	2.83	2.93	3.11	3.16	3.58	3.74	4.83	5.09	5.33
75	2.81	2.90	3.07	3.11	3.50	3.66	4.65	4.88	5.10
100	2.80	2.87	3.02	3.06	3.41	3.57	4.47	4.68	4.87

The model equivalence based on velocity aligns with the trend seen when comparing the model equivalence for peak outflow. The influence on velocity per rain garden was determined by dividing the percent velocity reduction for each SWMM scenario (as

compared to the 0% rain garden condition) by the number of rain gardens in the watershed. Table 7.9 shows the expected peak velocity reduction during the 0.5 inch, 6 hour storm per 1000 rain gardens.

Table 7.9: Velocity Reductions (%) per 1000 Rain Gardens

	%IA								
%RG	**3**	**5**	**9**	**10**	**20**	**25**	**60**	**70**	**80**
0	-	-	-	-	-	-	-	-	-
25	2.2	1.9	1.3	1.4	0.9	0.8	0.5	0.4	0.5
50	1.6	1.6	1.3	1.4	0.9	0.7	0.5	0.4	0.4
75	1.8	1.7	1.3	1.4	0.9	0.7	0.5	0.4	0.4
100	1.6	1.7	1.4	1.4	1.0	0.8	0.5	0.4	0.4
AVG	1.8	1.7	1.3	1.4	0.9	0.8	0.5	0.4	0.4

As impervious cover of the watershed increases, the influence from the rain gardens on peak velocity reduction is minimized. At 3% impervious area, the peak velocity during the 0.5, 6 hour storm event is only reduced by approximately 1.8% with the addition of 1000 rain gardens.

7.5 Peak Depth and Depth Reductions

Since peak flow and velocity during a storm event is influenced by the addition of rain gardens within the watershed, one can assume that the peak depth will change as well. Figure 7.5 shows the maximum depth experienced by the most downstream node in SWMM during the 0.5 inch, 6 hour storm event for each model analyzed. The maximum depth generally increases as impervious area of the watershed increases, but decreases with the introduction of rain gardens (as seen with both the peak flow and velocity as well).

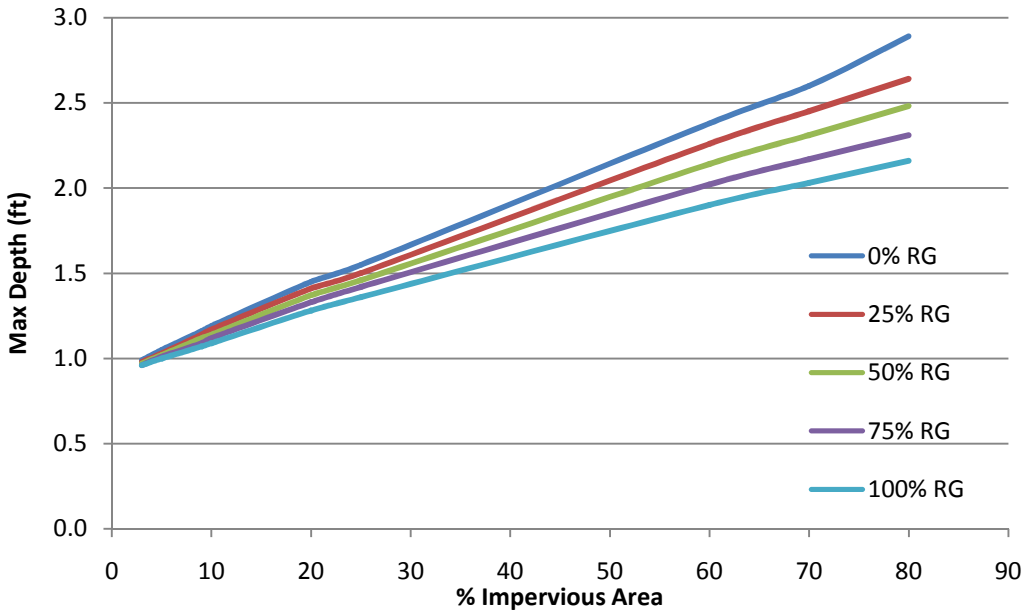

Figure 7.5: Maximum Storm Depth

From these results, model equivalence was again assessed using the peak storm depth parameter (Table 7.10). Using a 2% difference tolerance, comparable SWMM models were found which aligned with the results obtained from the peak flow and peak velocities (Table 7.5 and Table 7.8 respectively). This further substantiates the claim that certain models can be used to predict theoretical reduction in the watershed impervious area based on the percentage of rain gardens implemented.

Table 7.10: Peak Depth (ft) and Model Equivalence

	%IA								
%RG	3	5	9	10	20	25	60	70	80
0	0.99	1.05	1.16	1.19	1.45	1.55	2.38	2.60	2.89
25	0.98	1.03	1.14	1.17	1.41	1.50	2.26	2.45	2.64
50	0.97	1.02	1.12	1.14	1.37	1.46	2.14	2.31	2.48
75	0.96	1.01	1.09	1.12	1.33	1.42	2.02	2.17	2.31
100	0.96	1.00	1.07	1.09	1.28	1.36	1.90	2.03	2.16

The influence that a rain garden has on the peak depth component was determined by dividing the depth reduction for each scenario (compared to the 0% rain garden model)

by the number of rain gardens. Table 7.11 displays the reduction in peak storm depth per 1000 rain gardens for each SWMM model.

Table 7.11: Depth Reductions (%) per 1000 Rain Gardens									
	%IA								
%RG	**3**	**5**	**9**	**10**	**20**	**25**	**60**	**70**	**80**
0	-	-	-	-	-	-	-	-	-
25	3.2	3.6	1.8	1.6	1.3	1.2	0.7	0.6	0.8
50	3.2	2.7	1.8	2.0	1.3	1.1	0.7	0.6	0.7
75	3.2	2.4	2.1	1.8	1.3	1.1	0.7	0.6	0.6
100	2.4	2.2	2.0	2.0	1.4	1.1	0.7	0.6	0.6
AVG	3.0	2.7	1.9	1.8	1.3	1.1	0.7	0.6	0.7

The rain gardens' influence on peak depth reduction is minimized as the overall impervious cover of the watershed increases. The highest influence is witnessed with the 3% impervious area model, producing an average 3% peak depth reduction for the 0.5 inch, 6 hour storm event.

7.6 Results Summary

As designed, the "typical rain garden" developed to handle a 0.5 inch 6 hour summer storm did not overflow during any of the 45 model simulations. Table 7.12 provides a summary of the flow parameters evaluated during the simulated storm event, and their reductions based on the watershed being amended by 1000 rain garden units. Overall, relatively low reductions in these flow parameters were found, with the impacts due to rain gardens decreasing as the impervious area of the watershed increased.

Table 7.12: Average Storm Reductions (%) per 1000 Rain Garden									
	%IA								
Criteria	**3**	**5**	**9**	**10**	**20**	**25**	**60**	**70**	**80**
Storm Volume	13.7	11.5	7.9	6.4	3.8	3.1	1.3	1.1	1.0
Peak Flow	3.7	3.4	2.9	3.0	1.9	1.6	1.0	0.9	0.9
Depth	3.0	2.7	1.9	1.8	1.3	1.1	0.7	0.6	0.7
Velocity	1.8	1.7	1.3	1.3	0.9	0.8	0.5	0.4	0.4

To quantify the effects of stormwater control measures on entire watersheds, one must look to stream impacts on a case-by-case basis. From an ecological perspective, strained aquatic species may benefit from a decrease in overall storm volume entering their environment. If these general trends hold true to most urban watersheds, they can be used as a guide when attempting to reach specific water quality/ quantity goals.

Similarly, the SWMM model equivalence may be valuable as a guide when determining the benefit of establishing storm water controls to handle runoff from structures. Table 7.13 displays the overall model equivalency as verified from the peak flow, velocity, and depth parameters. Equivalent models are color coded and assigned arbitrary Greek letters for the color impaired.

Table 7.13: Model Equivalency Based on Depth, Velocity, and Outflow

	%IA								
%RG	**3**	**5**	**9**	**10**	**20**	**25**	**60**	**70**	**80**
0	α	β	γ		η		κ		
25			δ	γ	θ		λ	κ/ξ	
50			ε	δ	ι	η	μ	λ/ο	ξ
75			ζ	ε		θ	ν	μ/π	ο
100		α	β	ζ		ι		ν	π

This method could be used in conjunction with other ecological indicators to gain an understanding of stream impairment and possible effects to the ecology based on the integration of stormwater control measures.

Chapter 8

Utilizing the River Chub as an Ecological Indicator

8.1 Background

The River Chub (*Nocomis Micropogon*) is a large minnow that resides in clear, medium to large creeks and rivers. They can often be found hiding in pockets of deep water behind boulders (Froese and Pauly 2012). Chubs in general are considered rheophiles, meaning they thrive in fast moving currents in or near stream riffles (Lasne, et al. 2007). They inhabit many locations throughout North America including the Susquehanna River in New York, and the James River in Virginia. Figure 8.1 displays the current known extents of River Chub habitation in North America.

Figure 8.1: Known Habitats of the River Chub (USGS 2012)

The River Chub can live up to 5 years, and reach sexual maturity within the second year. Adult male River Chubs are typically 5 to 9 inches in length, with the females being 1/2 to 1/3 the size of the males. Their coloring is usually a dark olive tone on the topside and

a dusty yellow belly, with orange-red fins and relatively large scales (Figure 8.2). During mating season, the male will grow horn like projections called tubercles on its forehead.

Figure 8.2: Adult Male River Chub (ODNR 2012)

Common to many Chub species, the male will construct a nest from river bottom pebbles during the spring spawning season. This interesting reproductive process is a delicate balance as the velocity and depth conditions in the nest area need to remain within an acceptable tolerance. Decreases in stream health due to urbanization can disrupt River Chub nest building with increased channel erosion, velocity, and peak flows (McManamay, et al. 2010).

The River Chub nests can be as large as 10 to 12 inches high and 3 to 4 feet across. During construction, it is estimated that the male Chub will make 6,000 trips to transport about 88 pounds of river stones in total (Reighard 1943). Figure 8.3 displays the typical pebble sizes used in River Chub nest construction observed in the Cheoah River, North Carolina.

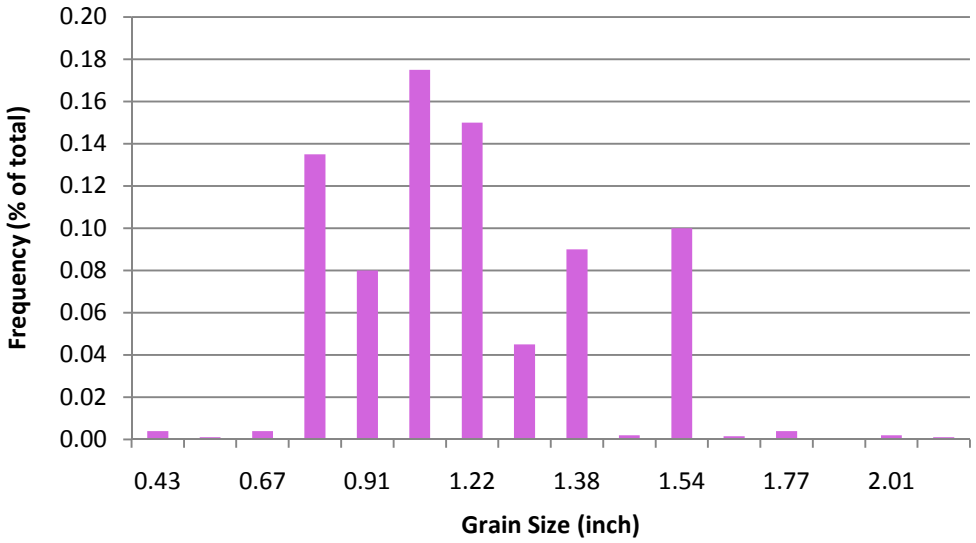

Figure 8.3: Grain Size Distribution of River Chub Nests (Orth, et al. 2011)

Based on the results, it seems River Chub prefer to use 0.7-1.4 inch stones as well as 1.5 inch stones. With the stone size and overall nest dimensions in mind, the River Chub have limited areas within a waterway in which they can successfully breed. The River Chub have been found to prefer a specific range of velocities and depths when choosing a nesting site. Figure 8.4 shows the occurrences of River Chub nests as a function of water depth found in Catatonk Creek, New York.

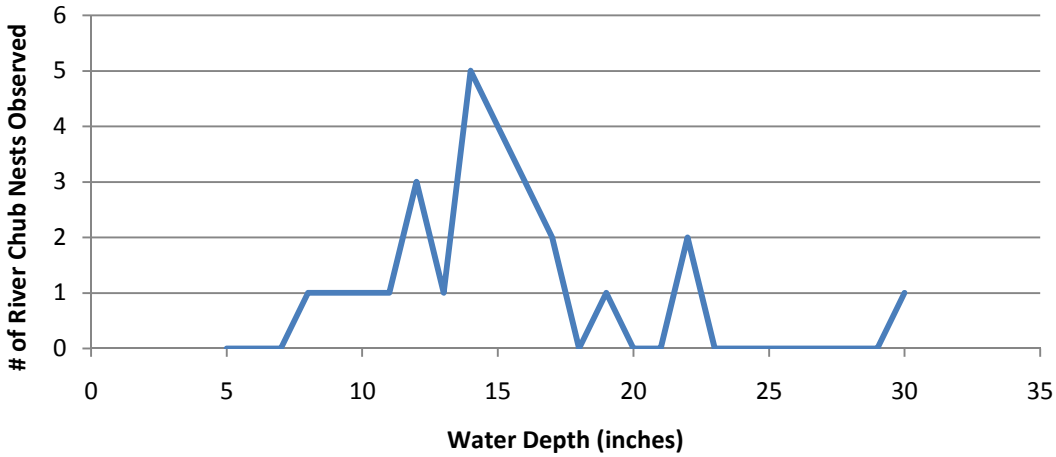

Figure 8.4: River Chub Nest Occurrence Versus Water Depth (Miller 1964)

Based on the study, the New York River Chubs seem to prefer building nests in water depths ranging from 8 to 17 inches, with the maximum nest occurrences at 14 inches. A Michigan study found that native Chub residing in the Huron River preferred to build nests in 18 to 24 inch pools, with the maximum observed depth at 36 inches (Reighard 1943). In a stream restoration project on the Cheoah River in North Carolina, it was observed that the River Chub nests were unaffected by water depths of 2.5 ft (Olsen 2009).

The velocity of the channel also impacts the location of the nest site as high velocities would carry away the nest material and also be dangerous to young River Chub. In a laboratory experiment, River Chub were subjected to varying flows in a flume and seemed to be able to function in a velocity range of 0.8-1.64 ft/s (Webb 1998). It has also been shown that River Chubs can easily adjust to velocities up to 3.6 ft/s from the aforementioned Cheoah River restoration project (Olson 2009). In a study of the closely related Hornyhead Chub (*Nocomis Biguttatus*), successful nest locations are typically in the velocity range of 1.18-1.31 ft/s (Wisenden et al 2009). Similarly, Creek Chubs (which grow to be approximately 7 inches) successfully breed in locations with velocities between 0.67 and 2.1 ft/s (McMahon 1982).

The River Chub species can be used effectively as a stream health indicator as they are considered a keystone species. In a study of the Allequash Creek in Wisconsin, 5 different fish species in the Cyprinid family rely on the River Chub nests as their eggs were consistently found within (Vives 1990). Another investigation showed that a drastic

decrease of Chub species in an area may greatly affect other species of fish that exhibit narrow geographic distributions (i.e an uncommon species) (Pendleton, et al. 2012). Furthermore, the larva of the endangered fine-rayed pigtoe mussel relies on fish such as the River Chub as a protective host until reaching maturity (Bruenderman and Neves 1993). By assessing the survival probability of the River Chub, assumptions can be made about the habitation of other species as well.

8.2 Chub Habitation in the SWMM Models

To test the theory of using River Chub as an indicator of stream health, the aforementioned velocity and depth criteria for successful nest builds was applied to the 45 SWMM models described in Chapters 6 and 7. Furthermore, a base flow condition was analyzed to determine the feasibility of nesting between storm events. A depth criterion of 0.67 to 2.5 ft was used along with a velocity criterion of 0.67 to 3.6 ft/s to define the largest possible nesting range based on the literature review. It is important to note that other key parameters for successful nesting sites were assumed to be favorable such as pebble size, temperature, and food sources.

The depth at each conduit was obtained by compiling results in SWMM. The minimum and maximum velocity component of each channel section was calculated based on the average velocity output by SWMM. Assuming a logarithmic velocity channel distribution (Figure 8.5), an average velocity can be assumed at a depth of 0.6 times the depth of the channel. Along the same lines, the minimum velocity lies on some point close to the

channel bottom (0.8 the total depth) and the maximum velocity lies just below the water/air interface (0.2 the total depth).

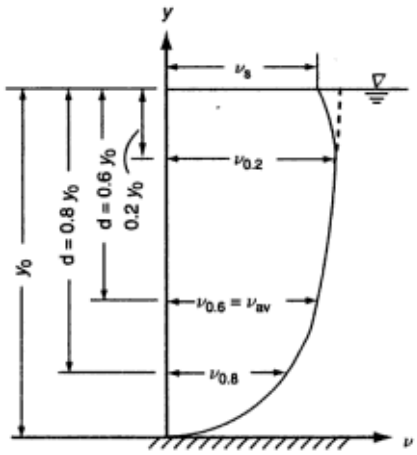

Figure 8.5: Typical Velocity Distribution in an Open Channel (Subramanya 2009)

The following series of equations were used to calculate the average maximum velocity for each channel reach based on a logarithmic velocity distribution:

$$\varepsilon = \frac{V_{max}}{V_{avg}} - 1$$

$$\alpha = 1 + 3\varepsilon^2 - 2\varepsilon^3 \qquad \beta = 1 + \varepsilon^2$$

Where V denotes velocity, α and β represent the geometry of the channel, and ε represents a factor based on channel geometry as well. The terms α and β were assumed to be 1.30 and 1.10 respectively to describe the non uniform alignment of natural streams (Thandaveswara 2009). Two values for ε were obtained and were used in conjunction with the average velocity obtained from SWMM to find an average maximum velocity. The minimum velocity was found by back calculating from the average equation:

$$V_{avg} = \frac{V_{max} + V_{min}}{2}$$

It can be assumed that the minimum velocity values will be experienced by the Chub fish on or near the bottom of the channel bed.

Nest destruction was assumed if a velocity greater than the criterion is reached during a storm event. Once the velocity increases to a certain point, the nest will experience soil grain transport and/or erosion. Figure 8.6 displays Hjulstrom's diagram for sediment transport with the River Chub pebble size and velocity range boxed in red.

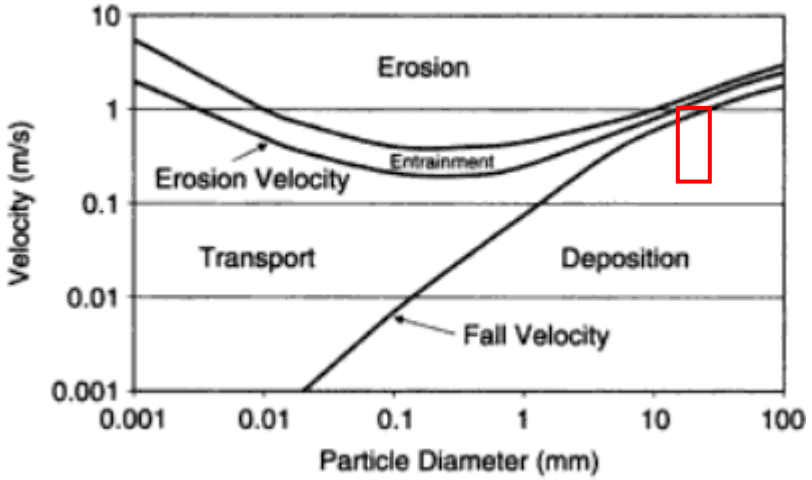

Figure 8.6: Hjulstrom's Diagram of Sediment Transport (Ward and Trimble 2004)

It appears that any velocity greater than 3.6 ft/s (~1.1 m/s) has the ability to entrain and carry away the pebble sizes associated with River Chub nests. A velocity that falls below the lower criterion limit was assumed to cause adverse conditions for the River Chub eggs, juveniles, or adults in the proximity of the nest. Along the same lines, a water depth that is too shallow or too deep during storm events may promote nest abandonment (Miller 1964).

8.3 Nest Build Locations During Base Flow Conditions

Base flow conditions were evaluated to determine feasible River Chub nesting sites prior to looking at the effects of a typical summer storm. Figure 8.7 displays the velocity and depth of the channel reach from upstream to downstream.

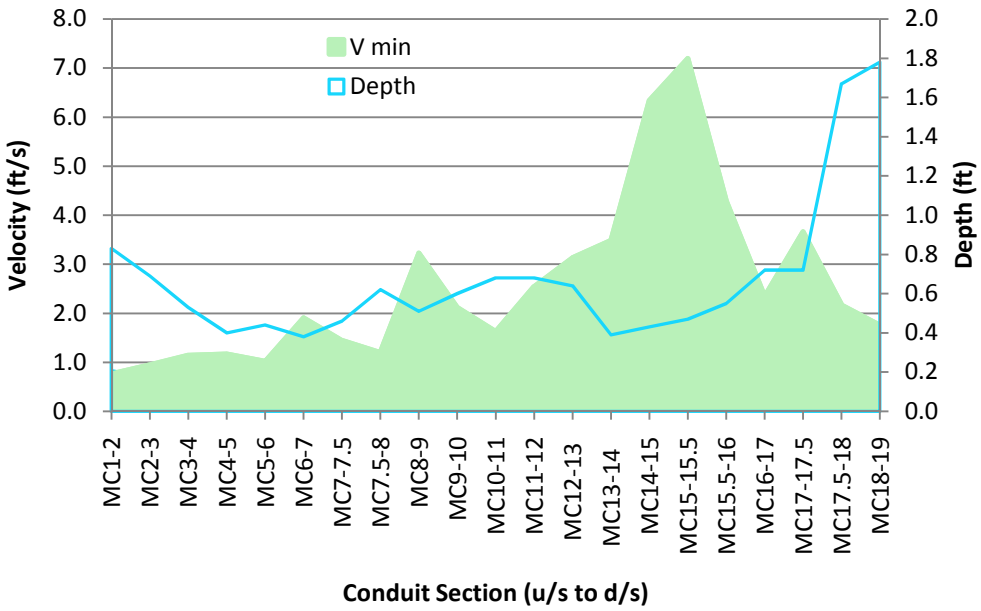

Figure 8.7: Base Flow Conditions for River Chub Nesting

When comparing the base flow conditions to the nesting criteria, seven conduit sections of the main reach are suitable: MC1-2, MC2-3, MC10-11, MC11-12, MC16-17, MC17.5-18, and MC18-19. In total, the River Chub have approximately 10,000 feet of stream in which they can construct their nests during base flow conditions. With the nesting site availability defined for the base flow conditions, nesting and nest survival during storm conditions can then be assessed.

8.4 Storm Flow Conditions

The 0.5 inch, 6 hour typical summer storm defined in Chapter 6 was evaluated for the 45 SWMM models to assess the relationship between River Chub nest sites, percent impervious area, and percent rain gardens. In each scenario, the velocities and depths were taken during the maximum flow of the storm hydrograph. The previously mentioned mathematical process was used to determine the minimum velocity at the channel bed during the peak flow of the storm event. Table 8.1 displays the number of SWMM conduit sections (and length) meeting the nest build criteria for each scenario analyzed.

Table 8.1: # of Conduits (and Length in ft) Suitable for River Chub Nesting

	% Impervious Area								
% RG	3	5	9	10	20	25	60	70	80
0	7 (10042)	6 (6790)	5 (4590)	5 (4590)	2 (2800)	1 (1050)	0 (0)	0 (0)	0 (0)
25	*6 (9802)	7 (10042)	*4 (4350)	*4 (4350)	2 (2800)	1 (1050)	0 (0)	0 (0)	0 (0)
50	*6 (9802)	7 (10042)	*5 (7602)	*4 (4350)	2 (2800)	2 (2800)	0 (0)	0 (0)	0 (0)
75	*6 (9802)	7 (10042)	*5 (7602)	*5 (7602)	3 (3500)	2 (2800)	0 (0)	0 (0)	0 (0)
100	*6 (9802)	7 (10042)	*6 (9802)	*5 (7602)	3 (3500)	2 (2800)	0 (0)	0 (0)	0 (0)

Because of the implementation of rain gardens which changed the hydrology of localized areas, one upstream conduit experienced a drop in velocity below the lower limit of the criterion. This special case is denoted with an asterisk (*), and should be kept in mind when viewing the results.

A percent impervious area ranging from 3-5% seems to be the ideal conditions for the River Chub, as a typical summer storm will not threaten the stability of the nests.

Interruption to nest builds in 2 to 3 of the 7 total habitable conduit sections is possible during the rain event for impervious areas of 9-10%. The River Chub species will most likely become strained in watersheds with 20-25% impervious areas, as half of all nests built will be destroyed during a 0.5 inch 6 hour storm. River Chub will not survive in watersheds with 60% or greater impervious area as all of their constructed nests will be destroyed during a typical summer storm. The survival trend of the River Chub based on percent impervious area closely resembles the revised Impervious Cover Model (Schueler, et al. 2009) where an impervious percentage between 10-25% is considered impacted and greater than 25% is considered ecologically non-supporting.

River Chub survival does not seem to be heavily influenced by the addition of the rain gardens. The River Chub nesting regions are not affected by the typical summer storm event for the 3% and 5% impervious scenarios, and therefore an ecological improvement with the addition of stormwater controls would not be seen. The 9, 10, 20, and 25% impervious cover scenarios show a decrease in nest habitat destruction by about one conduit as the rain garden percentage increases from 0 to 100%. With an impervious area of 60% and greater, no amount of rain gardens can produce favorable velocity and depth combinations to meet nest building criteria during a storm event.

Chapter 9

Conclusions

The work presented in this thesis evaluated stormwater control measures in a holistic micro and macro perspective. Part I proposed a low cost alternative to measuring nitrogen and phosphorus reductions in non-vegetated control measures. Phosphorus removal caused by adsorption was observed for both the pervious concrete and sand columns. Due to a greater surface area and longer travel time, phosphorus adsorption was greater within the sand column as opposed to the pervious concrete column. No short term removal mechanism was present for nitrogen in the pervious concrete column or the sand bed column. In design, it is important to make the distinction between temporary nitrogen retention through volume control and long-term nitrogen removal through chemical and biological processes.

Temperature reductions of the heated first flush inflow were correlated to a range of percent phosphorus removals, which could prove to be a handy monitoring tool in the field. The use of temperature recorders at a storm water control measure may prove to be much less costly than ordering water quality tests from a laboratory. Inherent limitations are present with this method, and results are dependent on geographic location and storm magnitude. Future research can be conducted by varying these parameters to obtain a range of location specific results.

This method to determine nutrient reduction through an SCM assumes that the control is properly functioning. In areas with high pollutant loadings in stormwater runoff, the

capacity for the SCM to reduce such loadings may decrease over time. In the case of phosphorus, the surface soil layers of the control measure may reach maximum adsorptive capacity at some point after construction. With this in mind, it may be imperative to check for inflow and outflow pollutant concentrations every couple of years.

Phase II of this research investigated storm volume and flow reductions in a typical urban watershed based on the implementation of rain gardens to handle roof runoff. In total, 45 SWMM models were created which varied impervious area (3, 5, 9, 10, 20, 25, 60, 70, 80%) and ratio of rain gardens to total number of structures (0, 0.25, 0.50, 0.75, and 1.00). After looking at a typical summer storm event (0.5 inch, 6 hour), it became clear that the rain gardens influence on peak flow, volume, depth, and velocity diminishes as impervious area increases. This indicates that a combination of stormwater control measures such as rain gardens and pervious pavement may produce more favorable results. In general, reductions to storm flow, volume, velocity, and depth were all minimal with the implementation of 100% rain gardens. Model equivalence was found when comparing the hydraulic parameters of each scenario. Typically, the implementation of rain gardens to handle 25% of all the structures in the watershed would correlate to models with no rain gardens and less impervious area. This model equivalence can be used as a tool to predict the impacts of widespread stormwater controls.

Possible ecological effects due to rain garden implementation were assessed by analyzing the depth and velocity criteria specific to River Chub nesting behavior. The River Chub nest-building criteria were applied to the 45 SWMM models to assess habitat availability during base flow and the typical summer storm. In the 3 and 5% impervious area models, nesting sites were not affected by the addition of rain gardens, as the depth and velocities experienced during the typical summer storm were low enough to remain within acceptable criteria. Adverse effects to the nesting sites during storm conditions typically decreased as rain garden implementation reached 100% for the 9, 10, 20, and 25% impervious area models. No amount of rain gardens were able to provide proper nesting conditions for the 60, 70, and 80% impervious area models, as all nests would be washed away during the storm event. Generally, the implementation of 100% rain gardens did not effectively counterbalance the stress placed on the ecology due to the effects of increasing urbanization. This trend closely follows Schueler's reformulated impervious cover model.

Future work should be conducted to merge ecological impacts with the results of these models for a variety of keystone species. In this way, the benefits of implementing control measures from a hydraulic and ecological perspective can be known prior to widespread implementation of stormwater control measures.

References

Abustan, I, Hamzah, M. O., Rashid, M. A. (2012). "Review of Permeable Pavement Systems in Malaysia Conditions". *J. of Sus. Dev.*, 4(2), 27-26.

Ahiablame, L. M., Engel, B. A., and Chaubey, I. (2013). "Effectiveness of Low Impact Development Practices in Two Urbanized Watersheds: Retrofitting with Rain Barrel/Cistern and Porous Pavement." *Journal of Environmental Management*, 119, 151-161.

Applied Ecological Services, Inc. (AES). (2006). "Alternative Stormwater Best Management Practices Guidelines; Chapter 3.15: Stormwater Treatment Train." Public Works and Utilities Department, Watershed Management Division, City of Lincoln, Nebraska.

Arcement, G. J., and Scheider, V. R. (1990). "Guide for Selecting Manning's Roughness Coefficients for Natural Channels and Flood Plains". *USGS Water Supply Paper 2339*.

ASTM Standard C1701/C1701M, 2009, "Standard Test Method for Infiltration Rate of In Place Pervious Concrete," ASTM International, West Conshohocken, PA.

ASTM Standard C136, 2006, "Standard Method for Sieve Analysis of Fine and Coarse Aggregates," ASTM International, West Conshohocken, PA.

ASTM Standard D7623, 2010, "Standard Test Methods for Laboratory Determination of Density (Unit Weight) of Soil Specimens," ASTM International, West Conshohocken, PA.

ASTM Standard D448, 2012, "Standard Classification for Sizes of Aggregate for Road and Bridge Construction," ASTM International, West Conshohocken, PA.

Bakhvalov, N. S. (2001). "Courant-Friedrichs-Lewy Condition". *Encyclopedia of Mathematics*, Springer,

Balades, J. D., Legret, M; and Madiec, H. (1995). "Permeable pavements: pollution management tools." *J. of Water Science and Technology,* 32(1), 49-56.

Barbis, J. (2009). *A Side-by-Side Water Quality Comparison of Pervious Concrete and Porous Asphalt, and an Investigation into the Effects of Underground Infiltration Basins on Stormwater Temperature, master degree thesis, Villanova University*. Villanova, PA.

Barnes, K. B., Morgan, John. M. III, and Roberge, M. C. (2002). "Impervious Surfaces and the Quality of Natural and Built Environments". *Department of Geography and Environmental Planning*, Towson University, MD.

Batroney, T., Wadzuk, B. M., Traver, R. G. (2010). "Parking Deck's First Flush." *J. of Hydrol. Eng.*, 15(2), 123-128.

Bernot, M. J., and Dodds, W. K. (2005). "Nitrogen Retention, Removal, and Saturation in Lotic Ecosystems." *J. of Ecosystems*, 8(4), 442-453.

Booth, D. B. (1991). "Urbanization and the Natural Drainage System- Impacts, Solutions, and Prognosis." *The Northwest Environmental Journal*, 7(1), 93-118.

Bruenderman, S. A., and Neves, R. J. (1993). "Lifer History of the Endangered Fine-Rayed Pigtoe, Fusconaia Cuneolus (Bivalva: Unionidae) in the Clinch River, Virginia." *American Malacological Bulletin*, 10(1), 83-91.

Burton, A. G., and Pitt, R. E. (2002). "Stormwater Effects Handbook: a Toolbox for Watershed Managers, Scientists, and Engineers". Chapter 2. Lewis Publishers, CRC Press, Washington D.C.

California Department of Transportation (CADOT). (2005). *First flush Phenomenon Characterization*. Division of Environmental Analysis, Sacramento, CA.

Carter, T., and Jackson, C. R. (2007). "Vegetated Roofs for Stormwater Management at Multiple Spatial Scales." *Landscape and Urban Planning*, 80(1-2), 84-94.

Chang, N. (2010). *Effects of Urbanization on Groundwater: An Engineering Case-Based Approach for Sustainable Development*, ASCE:EWRI, VA. 352-357.

Chesapeake Stormwater Network. (2008). "Technical Bulletin No. 3: Implications of the Impervious Cover Model". Version 1.

Clary, J., Leisenring, M., Porensky, A., Earles, A., and Jones, J. (2011)/ "BMP Performance Analysis Results for the International Stormwater BMP Database." *Proc., 8th Urban Watersheds Management Symposium*, 441-449.

Collins, K. A. (2007). *A Field Evaluation of Four Types of Permeable Pavement with Respect to Water Quality Improvement and Flood Control, masters degree thesis, North Carolina State University*, Raleigh, NC.

Collins, K. A.; Hunt, W. F.; Hathaway, J. M. (2010). “Side-by-Side Comparison of Nitrogen Species Removal for Four Types of Permeable Pavement and Standard Asphalt in Eastern North Carolina.” *J. of Hydrol. Eng.*, 15(special), 512-521.

Collins, K. A.; Hunt, W. F.; and Hathaway, J. M. (2008). “Hydrologic and Water Quality Evaluation of Four Permeable Pavements in North Carolina, USA.” Proc. *Int. LID Conference,* ASCE, WA., 1-10.

Commonwealth of Pennsylvania. (2009). *Specific Water Quality Criteria.* 93.7.

Davis, P. A.; Traver. R. G.; Hunt, W. F. (2010) “Improving Urban Stormwater Quality: Applying Fundamental Principles”. *J. of Contemporary Water Research & Edu.,* 146(1) 3-10.

Davis, Allen, P., Traver, R. G., Hunt, W. F., Lee, R., Brown, R. A., and Olszewski, J. M. “Hydrologic Performance of Bioretention Storm-Water Control Measures.” *J. of Hydrologic Engineering*, 17(5), 604-614.

Day, G. E. (1981). *Runoff and Pollution Abatement Characteristics of Concrete Grid Pavements*. Virginia Water Resources Center, Blacksburg, VA.

Debo, T. N., Reese, A. J. (2003). *Municipal Stormwater Management*, 2nd. Ed., CRC Press, Boca Raton, Florida.

Dukart, M. E. (2008a). "Standard operating procedure- VUSP-b-total p-total orthophosphate-total n, hach dr/400 spectrophotometer procedures." Quality Assurance Project Plans, Villanova Urban Stormwater Partnership, Villanova University, Villanova PA.

Dukart, M. E. (2008b). "Standard operating procedure-VUSP-P-Chloride USEPA by Discrete Analysis Method Easy Chloride 325.2-01." Quality Assurance Project Plans, Villanova Urban Stormwater Partnership, Villanova University, Villanova PA.

Emerson, C. H. (2003). *Evaluation of the Additive Effects of Stormwater Detention Basins at the Watershed Scale*, *masters degree thesis, Drexel University,* Philadelphia, PA.

Emerson, C. H., Welty, C., and Traver, R. G. (2003). "Application of HEC-HMS to Model the Additive Effects of Multiple Detention Basins over a Range of Measured Storm Volumes." *Proc., World Water & Environmental Resources Congress*, ASCE, 1-8.

Engman, E. T. (1986). "Roughness Coefficients for Routing Surface Runoff" *J. of Irr. And Drain. Eng.,* 112(1), 39-53.

Environmental Protection Agency (EPA). (1993). *Manual for Combined sewer overflow control*. EPA Rep. No. EPA/625/R093/007, US EPA, Washington D.C.

Eriksson, T. S.; Granqvist, C. G. (1982). "Radiative Cooling Computed for Model Atmospheres". *J. of Applied Optics,* 21(23), 4381-4388.

Federal Emergency Management Agency: Flood Insurance Study (FEMA:FIS). (2010). "Montgomery County, Pennsylvania: Mill Creek" Volume 1.

Field, R., and Sullivan, D. (2003). "Wet-Weather Flow in the Urban Watershed". Chapter 6: Treatment of Stormwater Runoff from the Urban Pavement and Roadways. CRC Press.

Finnemore, E. J., and Lynard, W. G. (1982). "Management and Control Technology for Urban Stormwater Pollution." *Journal of Water Pollution Control Federation*, 54(7), 1099-1111.

Froese, R., and Pauly, D. (2012). "Nocomis Micropogon: River Chub" *Fishbase Database*.<http://www.fishbase.org/Summary/SpeciesSummary.php?ID=2810&AT=river+chub>. (February 12, 2013).

Gironas, J., Roesner, L. A., and Davis, J. (2009). "Storm Water Management Model Applications Manual". *United States Environmental Protection Agency*. Cincinnati, OH.

Google Incorporated. (2012). "Google Earth Ver. 6.2.2".

Greising, K. L. (2011). *The Application of an Integrated Monitoring Plan of Stormwater Control Measures, masters degree thesis, Villanova University,* Villanova, PA.

Hagar., A. S. (2009). *Sustainable Design of Pervious Concrete Pavements*, *Dissertation, University of Colorado Denver.* Denver, Colorado.

Hathaway, J. M., Hunt, W. F. (2010). "Evaluation of Stom-Water Wetlands in Series in Piedmont North Carolina." *J. of Environmental Engineering,* 136(1), 140-146.

Hatt, B. E., Fletcher, T. D., Delectic, A. (2007). "Treatment Performance of Gravel Filter Media: Implications for Design and Application of Stormwater Infiltration Systems" *J. of Water Research*, 41(12), 2513-2524.

Healy, M.G.; Rodgers, M.; Mulqueen, J. (2007). "Treatment of Dairy Wastewater Using Constructed Wetlands and Intermittent Sand Filters." *J. of Bioresource Tech.*, 98(12), 2268-2281.

Hershfield, D. M. (1963). *Technical Paper No. 40: Rainfall Frequency Atlas for the United States for Durations from 30 minutes to 24 hours and Return Periods from 1 to 100 Years.* Washington, DC: U.S Department of Commerce: Hydrologic Services Division.

Himmelblau, D. M. (1967). *Basic Principles and Calculations in Chemical Engineering*. Upper Saddle River, NJ. Prentice- Hall.

Horst, M., Welker, A. L., and Traver, R. G. (2011). "Multiyear Performance of a Pervious Concrete Infiltration Basin BMP." *J. of Irrigation and Drainage Engineering*, 137(6), 352-358.

Indiana Design Manual (IDM). (2007). *Indiana Storm Water Quality Manual; Chapter 8: Storm Water Quality Measures: Post-Construction*.

Jeffers, P.A. (2009). *Water Quantity Comparison of Pervious Concrete and Porous Asphalt Products for Infiltration Best Management Practices, master degree thesis, Villanova University.* Villanova, PA.

Kadlec, R. H., and Wallace, S. D. (2009). *Treatment Wetlands*, 2nd Ed., CRC Press, FL. 267-281.

Lasne, E., Bergerot, B., Lek, S. and Laffaille, P. (2007) "Fish Zonation and Indicator Species for the Evaluation of the Ecological Status of Rivers: Example of the Loire Basin (France)". *River Research and Applications*, 23(8), 877-890.

Leopold, L. B. (1968). "Hydrology for Urban Land Planning- a Guidebook on the Hydrologic Effects of Urban Land Use". *U.S. Geological Survey Circular 554*, Washington DC.

Lower Merion Conservancy. (2009). *A Stream of New Data: The 2009 Mill Creek Report*.

Lyons, C., Traver, R., and Wadzuk, B. (2012). "Applying Stormwater Control Measures in Series: The Villanova Treatment Train." *The Journal for the Surface Water Quality Professionals*, 13(8), 36.

Massman, J. W., and Butchart, C. D. (2001). "Infiltration Characteristics, Performance, and Design of Storm Water Facilities." *Interim Report, Research Project No. T1803, Task 12,* University of Washington, Washington.

McMahon, T. E. (1982). "Habitat Suitability Index Models: Creek Chub" *USDI Fish and Wildlife Services*, Washington, DC.

McManamay, R. A., Orth, D. J., Dolloff, C. A., and Cantrell, M. A. (2010) "Gravel Addition as a Habitat Restoration Technique for Tailwaters". *N. A. J. of Fisheries Management*, 30(5), 1238-1257.

Microsoft Incorporated. (2012). "Microsoft Corporation: Bing Interactive Maps" <http://www.bing.com/maps/?FORM=MLOMAP&PUBL=GOOGLE&CREA=userid1743gobroadfphumem2khvlw7ml8dkb3h3kcgsoxz1369>. (Nov. 7 2012).

Miller, R. (1964). "Behavior and Ecology of Some N. American Cyprinids Fishes". *The American Midland Naturalist*, 72(2), 313-357.

Milwakee Metropolitan Sewerage District (MMSD). (2005). "The Application of Stormwater Runoff Reduction Best Management Practices in Metropolitan Milwakee". Stormwater Runoff Reduction Program Interim Report.

National Research Council (NRC). (2008). *Urban Stormwater Management in the United States*. The National Academic Press, Washington, DC.

Nemirovksy, E. (2011). *Evaporation from a Pervious Concrete Stormwater SCM: Estimating the Quantity and its Role in the Yearly Water Budget, master degree thesis, Villanova University*. Villanova, PA.

Nemirovsky, E., Welker, A., and Lee, R. (2013). "Quantifying Evaporation from Pervious Concrete Systems: Methodology and Hydrologic Perspective" *J. of Irrig. and Drain Eng.,* 139(4), 271-277.

New Jersey Department of Environmental Protection (NJDEP). (2004). *New Jersey Best Management Practices Manual*: *Standard for Pervious Paving Systems*. Chapter 9.7.
NOAA. (2011). "National Climatic Data Center". Meteorological record.

North Carolina Department of Environment and Natural Resources (NCDENR). (2007). *Best Management Practices Manual*. Chapter 7: BMP Inspection and Maintenance. Raleigh, NC.

Nowak, D. J., and Greenfield, E. J. (2012). "Tree and Impervious Cover Change in U.S. Cities". *Urban Forestry and Urban Greening*. 11(1), 21-30.

Olson, M. (2009). "Monitoring Plan for the Cheoah River Bypass Reach Minimum Flow and Ramping Rates". *Santeetlah Development*, Alcoa Power Generation Inc., FERC Project No. 2169, Baden, NC.

Orth, D.J., McManamay, R., Dollof, A. C., Cantrell, M. A., Fraley, S., Goudreau, C., and Reed, S. E. (2011). "Assessing Effects of Flow and Habitat Changes after Re-licensing at the Tapoco Hydroelectric Project on Cheoah River, North Carolina". *In Collaboration with the Dept. of Fisheries & Wildlife Sciences, U.S. Fish and Wildlife Service, NC Wildlife Resources Comission, Division of Water Resources-DENR.*, NC.

Pendleton, R. M., Pritt, J. J., Peoples, B. K., and Frimpong, E., A. (2012). "The Strength of Nocomis Nest Association Contributes to Patterns of Rarity and Commonness among New River, Virginia Cyprinids." *The American Midland Naturalist*, 168(1), 202-217.

Perry, S., Garbon, J., and Lee, B. (2009). "Urban Stormwater Runoff Phosphorus Loading and BMP Treatment Capabilities". *Proc., Mississippi Water Resources Conference*, MDEQ, MS, 132-141.

Pennsylvania Department of Environmental Protection (PADEP). (2006). *Pennsylvania Stormwater Best Management Practices Manual; Chapter 6: Structural BMPs*. Bureau of Watershed Management.

Pennsylvania Department of Environmental Protection (PADEP). (1997). *Implementation Guidance for Section 95.9 Phosphorus discharges to Free Flowing Streams*. Volume 29.

Rawls, W. J., Brakensiek, K. L., and Miller, N. (1983). "Green-Ampt Infiltration Parameters from Soils Data". *J. of Hydraulic Eng.,* 109(1), 62-70.

Reighard, J. “The Breeding Habits of the River Chub, Nocomis Micropogon” *Papers of the Michigan Academy of Science, Arts, and Letters,* Volume 28, 397-423.

Roseen, R. M., Ballestero, T. P., Houle, J. J., Briggs, J. F., and Houle, K. M. (2012). “Water Quality and Hydrologic Performance of a Porous Asphalt Pavement as a Storm-Water Treatment Strategy in a Cold Climate” *J. of Env. Eng.* 137(1), 81-89.

Sansalone, J. J.; and Hird, J. (2002). *Wet Weather Flow in the Urban Watershed: Technology and Management. Chapter 6: Treatment of Stormwater Runoff from Urban Pavement*. CRC Press, Boca Raton, FL.

Santa Clara Valley Urban Runoff Pollution Prevention Program (SCVURPPP). (2012) “Public Inspection and Maintenance Checklists” <http://www.scvurppp-w2k.com/bmp_om_forms/PublicInspectChklstAll.pdf> (February 4, 2013).

Schueler, T. (1987). *Controlling Urban Runoff; a Practical Manual for Planning and Designing Urban BMPs*. Washington, DC: Metropolitan Washington Council of Governments.

Schueler, T. R. (1994). “The Importance of Imperviousness”. *Watershed Protection Techniques*, 1(3), 100-111.

Schueler, T. R., and Fraley-McNeal, L. (2008). “The Impervious Cover Model Revisited: Review of Recent ICM Research”. *Proc., Symposium on Urbanization and Stream Ecology*, EPA, Utah.

Schueler, T. R., Fraley-McNeal, L., and Cappiella, K. (2009). “Is Impervious Cover Still Important? Review of Recent Research”. *J. of Hydrologic Eng*., 14(4), 309-315.

Slejko, F.L. (1985). *Adsorption Technology: A Step-by-Step Approach to Process Evaluation and Application*. Marcel Dekker, New York, 13.

Southeast Michigan Council of Governments (SMCG). (2008). *Low Impact Development Manual for Michigan*. Appendix F: Maintenance Inspection Checklists. Detroit, Michigan.

Sturm, T. W. (2001). *Open Channel Hydraulics*, 1st Ed., McGraw-Hill Higher Education, PA.

Subramanya, K. (2009). "Chapter 1: Introduction" Flow in Open Channels, 3rd Edition. New Delhi, Tata McGraw-Hill.

Thandaveswara, B. S. (2009). "Hydraulics: Energy and Momentum Coefficients" *Indian Institute of Technology Madras,* Chennai, India.

Traver, R., and Chadderton, R. (1983). "The Downstream Effects of Storm Water Detention Basins" *International Symposium on Urban Hydrology, Hydraulics, and Sediment Control,* University of Kentucky, Lexington, KY, 455-460.

United States Environmental Protection Agency (USEPA). (2013). "Watershed Assessment, Tracking and Environmental Results: National Summary of Impaired Waters and TMDL Information". <http://iaspub.epa.gov/waters10/attains_nation_cy.control?p_report_type=T> (January 28, 2013).

United States Department of Agriculture (USDA). (2009). "National Engineering Handbook, Chapter 7: Hydrologic Soil Groups". Washington DC.

United States Department of Agriculture, National Resources Conservation Service (USDA NRCS). (2012). "Web Soil Survey: Soil Map and Relevant Properties"<http://websoilsurvey.nrcs.usda.gov/app/HomePage.htm> (Aug. 2. 2012).

United States Department of Agriculture: Natural Resources Conservation Service (USDA NRCS). (1986). "Urban Hydrology for Small Watersheds". *Technical Release 55*. 2nd Edition.

United States Department of Environmental Protection (USDEP). (1995). "Water Quality Inventory". *Report to Congress*. Office of Water, Washington D.C.

United States Environmental Protection Agency (USEPA). (2005). *National Management Measures to Control Nonpoint Source Pollution from Forestry*. Office of Water, Washington D.C.

United States Environmental Protection Agency (USEPA). (2012). "BMP Inspection and Maintenance". National Pollutant Discharge Elimination System. <http://cfpub.epa.gov/npdes/stormwater/menuofbmps/index.cfm?action=factsheet_results&view=specific&bmp=91> (February 5, 2013).

United States Environmental Protection Agency. (2012). "CADDIS Volume 2: Sources, Stresses, and Responses of Ammonia". <http://www.epa.gov/caddis/ssr_amm_int.html> (Oct. 24, 2012).

United States Department of the Interior (USDI). (2006). *Erosion and Sedementation Manual: Chapter 3: Noncohesive Sediment Transport*, Sedimentation and River Hydraulics Group, Colorado. 3.2-3.8.

United States Geological Survey (USGS) Stream Statistics for Pennsylvania. (2010). "The Streamstats Program: PA Interactive Map" <http://water.usgs.gov/osw/streamstats/pennsylvania.html> (July 1, 2012).

United States Geological Survey (USGS). (2012). "Nocomis Micropogon: River Chub" Nonindigenous Aquatic Species Fact Sheet. <http://nas.er.usgs.gov/queries/factsheet.aspx?SpeciesID=577>. (February 12, 2013).

Virginia Department of Conservation and Recreation. (2011). "Stormwater Design Specification No.7: Permeable Pavement" <http://vwrrc.vt.edu/swc/NonPBMPSpecsMarch11/VASWMBMPSpec7PERMEABLEPAVEMENT.html> (July 11, 2012).

Vives, S. (1990). "Nesting Ecology and Behavior of Hornyhead Chub Nocomis Biguttatus, a Keystone Species in Allequash Creek, Wisconsin". *American Midland Naturalist*, 124(1), 46-56.

Wang, J., Zhang, Y., Feng, C., Li, J., and Li, G. (2009). "Adsorption Capacity for Phosphorus Comparison among Activated Alumina, Silica Sand, and Anthracite Coal" *J. Water Resource and Protection*, 1(4), 260-264.

Ward, A. D. and Trimble, S. W. (2004). "Chapter 6.6: Stream Stability and Sediment Transport" *Environmental Hydrology*. Second Edition. CRC Press, Boca Raton, Florida.

Weather Underground. (2012a). "Mendel Science Center Rain Gage Station History" < http://www.wunderground.com/weatherstation/WXDailyHistory.asp?ID=KPAVILLA1&month=7&day=23&year=2012> (May 1, 2013).

Weather Underground. (2012a). "Mendel Science Center Rain Gage Station History" < http://www.wunderground.com/weatherstation/WXDailyHistory.asp?ID=KPAVILLA1&month=8&day=5&year=2012> (May 2, 2013).

Weather Underground. (2011). "St. Davids Golf Club Rain Gage History" <http://www.wunderground.com/weatherstation/WXDailyHistory.asp?ID=KPAWAYNE5&month=8&day=9&year=2011> (Nov. 20, 2012).

Weather Underground. (2010). "Mendel Science Center Rain Gage Station History" < http://www.wunderground.com/weatherstation/WXDailyHistory.asp?ID=KPAVILLA1&month=6&day=10&year=2010> (March. 13, 2013).

Webb, P.W. (1998). "Entrainment by River Chub Nocomis Micropogon and Smallmouth Bass Micropterus Dolomieu on Cylinders" *J. of Experimental Biology*, 201(16), 2403-2412.

Welker, A.L., Barbis, J. D., and Jeffers, P. A. (2012a) "A Side-by-Side Comparison of Pervious Concrete and Porous Asphalt." *J. of the American WR Assoc*., 48(4), 804-819.

Welker, A. L., Jenkens, J. K. G., McCarthy, L., and Nemirovsky, E. (2012b). "Examination of the Material Found in the Pore Spaces of Two Permeable Pavements." *J. Irrig. Drain Eng.*, in press.

Welker, A. L., Mandarano, L., Greising, K., and Mastrocola, K. (2013). "Application of a Monitoring Plan for Stormwater Control Measures in the Philadelphia Region." *J. of Environmental Engineering*, posted ahead of print.

Williams, J. (1988). *Thermocouple Measurement: Application Note 28.* Linear Technology Corporation, Milpitas, CA.

Wisenden, B. D., Unruh, A., Morantes, S., Bury, B., Curry, Driscoll, R., Hussein, M., and Markegard, S. (2009). "Functional Constraints on Nest Characteristics of Pebble Mounds of Breeding Male Hornyhead Chub Nocomis Biguttatus" *J. of Fish Biology*, 75(7), 1577-1585.

Young, K. D., Younos, T., Dymond, R. L., and Kibler, D. F. (2009) "Virginia's Stormwater Impact Evaluation: Developing an Optimization Tool for Improved Site Development, Selection and Placement of Stormwater Runoff BMPs". *VWRRC Special Report No. SR44-2009*. Virginia Polytechnic Institute and State University, Blacksburg, VA.

Zehringer, J. (2012). “Division of Wildlife: River Chub” *Ohio Department of Natural Resources*.<http://www.dnr.state.oh.us/Home/species_a_to_z/SpeciesGuideIndex/riverchub/tabid/22148/Default.aspx>. (February 12, 2013)

Appendix A: Mass Balances for Column Experiments

Pervious Concrete column-5/28/2012

Sample	TP (mg/l as P)	TN (mg/l as N)	Cl (mg/l as Cl)	Volume (l)	Mass P (mg)	Mass N (mg)	Mass Cl (mg)
Inflow 1							
Inflow 2							
Inflow 3							
Avg Inflow	0.81	21.9	216.5	0.618	0.499	13.514	133.778
PC1	0.66	21.1	165.5	0.096	0.063	2.015	15.804
PC2	0.63	21.8	191.1	0.123	0.077	2.671	23.415
PC3	0.64	21.8	166.9	0.104	0.066	2.256	17.278
PC4	0.48	20.3	108.2	0.121	0.058	2.456	13.095
PC5	0.15	8.0	185.8	0.248	0.037	1.980	45.987
PC6	0.11	2.7	61.4	0.141	0.016	0.381	8.658
PC7	0.03	2.0	31.8	0.199	0.006	0.397	6.304
PC8	0.01	1.6	11.6	0.242	0.002	0.386	2.801
PC9	0.01	0.8	6.9	0.185	0.002	0.148	1.269
PC10	0.01	0.7	3.8	0.230	0.002	0.161	0.868
PC11	0.01	0.5	4.9	0.156	0.002	0.078	0.765

	Mass in	Mass out	Mass retained	Mass unaccounted	% unaccounted	mechanism
Phosphorus	0.50	0.33	0.08	0.08	16.56	sorb
Nitrogen	13.51	12.93	2.30	-1.71	-12.67	none
			% diff			

Chloride	133.78	136.25	1.81

Pervious Concrete column-6/14/2012

Sample	TP (mg/l as P)	TN (mg/l as N)	Cl (mg/L as Cl)	Volume (l)	Mass P (mg)	Mass N (mg)	Mass Cl (mg)
Avg Inflow	0.86	22.6	558.0	0.618	0.531	13.946	344.863
PC1	0.12	22.0	550.9	0.140	0.017	3.080	77.129
PC2	0.40	21.3	552.9	0.123	0.049	2.609	67.734
PC3	0.87	20.6	582.2	0.104	0.090	2.142	60.553
PC4	0.33	16.3	300.1	0.132	0.043	2.143	39.467
PC5	0.03	9.8	179.2	0.229	0.007	2.239	40.939
PC6	0.05	4.4	78.0	0.175	0.009	0.770	13.655
PC7	0.03	2.1	32.3	0.232	0.007	0.487	7.483
PC8	0.02	1.5	14.9	0.186	0.004	0.278	2.767
PC9	0.02	1.1	10.5	0.233	0.005	0.256	2.447
PC10	0.02	0.8	7.9	0.164	0.003	0.131	1.301
PC11	0.03	0.5	10.3	0.082	0.002	0.041	0.838

	Mass in	Mass out	Mass retained	Mass unaccounted	% unaccounted	mechanism
Phosphorus	0.53	0.24	0.10	0.19	36.55	sorb
Nitrogen	13.95	14.18	2.65	-2.88	-20.64	none
			% diff			
Chloride	344.86	314.31	-9.72			

Pervious Concrete column-7/23/2012

Sample	TP (mg/l as P)	TN (mg/l as N)	Cl (mg/L as Cl)	Volume (l)	Mass P (mg)	Mass N (mg)	Mass Cl (mg)
Avg Inflow	0.74	27.1	546.9	0.618	0.459	16.748	337.956
PC1	0.59	24.4	537.5	0.079	0.047	1.928	42.466
PC2	0.54	23.9	536.8	0.119	0.064	2.844	63.883
PC3	0.58	24.6	540.6	0.061	0.035	1.501	32.974
PC4	0.58	25.0	546.5	0.116	0.067	2.900	63.395
PC5	0.28	18.3	335.5	0.191	0.053	3.495	64.075
PC6	0.07	6.0	92.0	0.234	0.016	1.404	21.527
PC7	0.02	2.6	33.9	0.207	0.004	0.538	7.019
PC8	0.01	1.7	15.3	0.165	0.002	0.281	2.525
PC9	0.00	1.8	10.5	0.249	0.000	0.448	2.618
PC10	0.01	1.6	6.7	0.235	0.002	0.376	1.586
PC11	0.01	7.4	5.4	0.183	0.002	1.354	0.993

	Mass in	Mass out	Mass retained	Mass unaccounted	% unaccounted	mechanism
Phosphorus	0.46	0.29	0.08	0.09	19.05	sorb
Nitrogen	16.75	17.07	2.86	-3.18	-19.00	none
			% diff			
Chloride	337.96	303.06	-11.51			

Sand column-6/5/2012

Sample	TP (mg/l as P)	TN (mg/l as N)	Cl (mg/l as Cl)	Volume (l)	Mass P (mg)	Mass N (mg)	Mass Cl (mg)
Avg Inflow	0.99	24.5	557.957	0.618	0.6	15.1	344.817
Sand1	0.05	0.2	0.990	0.052	0.00	0.01	0.051
Sand2	0.07	0.2	3.484	0.066	0.00	0.01	0.230
Sand3	0.05	0.2	7.915	0.136	0.01	0.03	1.072
Sand4	0.06	0.1	0.897	0.098	0.01	0.01	0.088
Sand5	0.07	2.4	11.226	0.132	0.01	0.32	1.482
Sand6	0.03	4.5	80.313	0.159	0.00	0.71	12.730
Sand7	0.00	17.0	409.727	0.239	0.00	4.05	97.720
Sand8	0.00	18.9	455.814	0.185	0.00	3.50	84.326
Sand9	0.01	13.7	354.860	0.204	0.00	2.79	72.214
Sand10	0.09	8.0	249.513	0.218	0.02	1.74	54.269
Sand11	0.21	3.7	56.032	0.304	0.06	1.12	17.034

	Mass in	Mass out	Mass retained	Mass unaccounted	% unaccounted	mechanism
Phosphorus	0.61	0.12	0.12	0.37	61.14	sorb
Nitrogen	15.14	14.29	2.92	-2.07	-13.70	none
			% diff			
Chloride	344.82	341.22	1.04			

Sand column- 7/30/12

Sample	TP (mg/l as P)	TN (mg/l as N)	Cl (mg/l as Cl)	Volume (l)	Mass P (mg)	Mass N (mg)	Mass Cl (mg)
Avg Inflow	1.30	21.8	664.536	0.618	0.8	13.5	410.683
Sand1	0.09	1.6	25.184	0.038	0.00	0.06	0.957
Sand2	0.08	0.0	28.185	0.112	0.01	0.00	3.157
Sand3	0.06	0.7	36.549	0.073	0.00	0.05	2.668
Sand4	0.05	0.0	37.549	0.043	0.00	0.00	1.615
Sand5	0.03	1.0	44.440	0.137	0.00	0.14	6.088
Sand6	0.03	5.9	182.987	0.138	0.00	0.81	25.252
Sand7	0.02	18.2	469.412	0.154	0.00	2.80	72.289
Sand8	0.01	18.4	700.156	0.181	0.00	3.33	126.728
Sand9	0.03	14.8	565.519	0.251	0.01	3.71	141.945
Sand10	0.11	6.8	226.852	0.233	0.03	1.58	52.856
Sand11	0.17	5.9	134.230	0.181	0.03	1.07	24.296

	Mass in	Mass out	Mass retained	Mass unaccounted	% unaccounted	mechanism
Phosphorus	0.80	0.10	0.25	0.46	57.53	sorb
Nitrogen	13.47	13.56	4.11	-4.20	-31.20	none
			% diff			
Chloride	410.68	457.85	-11.49			

Sand column-8/7/12

Sample	TP (mg/l as P)	TN (mg/l as N)	Cl (mg/l as Cl)	Volume (l)	Mass P (mg)	Mass N (mg)	Mass Cl (mg)
Avg Inflow	0.72	21.3	586.877	0.618	0.4	13.2	362.690
Sand1	0.06	0.0	1.381	0.135	0.01	0.00	0.186
Sand2	0.09	0.0	0.660	0.094	0.01	0.00	0.062
Sand3	0.06	0.0	0.771	0.085	0.01	0.00	0.066
Sand4	0.04	0.8	0.644	0.087	0.00	0.07	0.056
Sand5	0.02	3.1	78.471	0.156	0.00	0.48	12.241
Sand6	0.02	11.2	317.155	0.151	0.00	1.69	47.890
Sand7	0.00	18.1	480.240	0.143	0.00	2.59	68.674
Sand8	0.01	17.5	482.530	0.172	0.00	3.01	82.995
Sand9	0.01	13.6	354.402	0.204	0.00	2.77	72.298
Sand10	0.06	8.3	179.579	0.248	0.01	2.06	44.536
Sand11	0.06	2.9	79.149	0.259	0.02	0.75	20.500

	Mass in	Mass out	Mass retained*	Mass unaccounted	% unaccounted	mechanism
Phosphorus	0.44	0.07	0.10	0.28	63.40	sorb
Nitrogen	13.18	13.43	2.88	-3.12	-23.66	none
			% diff			
Chloride	362.69	349.50	3.64			

Appendix B: Total and No Mixing of Spiked First Flush and Deionized Flush

Phosphorus Mass Balance – Pervious Concrete Column- Complete Mixing				
Test date	**Mass Inflow (mg)**	**Mass Outflow (mg)**	**Mass Retained (mg)**	**Mass Unaccounted (mg)**
5/28/2012	0.50	0.33	0.08	0.08
6/14/2012	0.53	0.24	0.10	0.19
7/23/2012	0.46	0.29	0.08	0.09
AVG	0.50	0.29	0.09	0.12

Phosphorus Mass Balance – Sand Bed Column- Complete Mixing				
Test date	**Mass Inflow (mg)**	**Mass Outflow (mg)**	**Mass Retained (mg)**	**Mass Unaccounted (mg)**
6/5/2012	0.61	0.12	0.12	0.37
7/30/2012	0.80	0.10	0.25	0.46
8/7/2012	0.44	0.07	0.10	0.28
AVG	0.62	0.10	0.16	0.37

Phosphorus Mass Balance – Pervious Concrete Column- No Mixing				
Test date	**Mass Inflow (mg)**	**Mass Outflow (mg)**	**Mass Retained (mg)**	**Mass Unaccounted (mg)**
5/28/2012	0.50	0.33	0	0.17
6/14/2012	0.53	0.24	0	0.29
7/23/2012	0.46	0.29	0	0.17
AVG	0.50	0.29	0	0.21

Phosphorus Mass Balance – Sand Bed Column- No Mixing				
Test date	**Mass Inflow (mg)**	**Mass Outflow (mg)**	**Mass Retained (mg)**	**Mass Unaccounted (mg)**
6/5/2012	0.61	0.12	0	0.49
7/30/2012	0.80	0.10	0	0.7
8/7/2012	0.44	0.07	0	0.37
AVG	0.62	0.10	0	0.52

Nitrogen Mass Balance – Pervious Concrete Column- Complete Mixing				
Test date	**Mass Inflow (mg)**	**Mass Outflow (mg)**	**Mass Retained (mg)**	**Mass Unaccounted (mg)**
5/28/2012	13.51	12.93	2.30	-1.71
6/14/2012	13.95	14.18	2.65	-2.88
7/23/2012	16.75	17.07	2.86	-3.18
AVG	14.74	14.73	2.60	-2.59

Nitrogen Mass Balance – Sand Bed Column- Complete Mixing				
Test date	**Mass Inflow (mg)**	**Mass Outflow (mg)**	**Mass Retained (mg)**	**Mass Unaccounted (mg)**
6/5/2012	15.14	14.29	2.92	-2.07
7/30/2012	13.47	13.56	4.11	-4.2
8/7/2012	13.18	13.43	2.88	-3.12
AVG	13.93	13.76	3.30	-3.13

Nitrogen Mass Balance – Pervious Concrete Column- No Mixing				
Test date	**Mass Inflow (mg)**	**Mass Outflow (mg)**	**Mass Retained (mg)**	**Mass Unaccounted (mg)**
5/28/2012	13.51	12.93	0	0.58
6/14/2012	13.95	14.18	0	-0.23
7/23/2012	16.75	17.07	0	-0.32
AVG	14.74	14.73	0	0.01

Nitrogen Mass Balance – Sand Bed Column- No Mixing				
Test date	**Mass Inflow (mg)**	**Mass Outflow (mg)**	**Mass Retained (mg)**	**Mass Unaccounted (mg)**
6/5/2012	15.14	14.29	0	0.85
7/30/2012	13.47	13.56	0	-0.09
8/7/2012	13.18	13.43	0	-0.25
AVG	13.93	13.76	0	0.17

Appendix C: Visual Inspection Checklists (Greising 2012)

Checklist for Evapotranspiration SCMs

Name of site	Typical Green Roof
Vegetation	
Color, quality and size of leaves	
Color, quality and size of stems	
Color, quality and size of flowers	
Correct Species	
Percent vegetative cover	

Checklist for Infiltration SCMs

Name of site	Typical Pervious Pavement
Drainage Problems	
Ponded water present for more than 48 hours after rainfall event	
Sediment accumulation in basin area	
Clogged inlet structures	
Clogged outlet structures	
Excessive Erosion	

Checklist for Bio-infiltration and Wetland SCMs

Name of site	Typical Bioinfiltration	Typical Wetlands
Drainage Problems		
Ponded water present for more than 48 hours after rainfall event		
Sediment accumulation in basin area		
Clogged inlet structures		
Clogged outlet structures		
Excessive Erosion		

Vegetation		
Color, quality and size of leaves		
Color, quality and size of stems		
Color, quality and size of flowers		
Correct Species		
Percent Vegetative Cover		
Wetland Plants		
Cattails		
Arrowheads		
Marsh Smartweeds		
Soil Core – for grain size analysis		

Appendix D: SWMM calibration parameters

subwatershed #	Tributary ID	subwatershed area (ac)	subwatershed area (ft2)	Overland flow Length (ft)	SWMM Subcatchment Width (A/L)	Calibrated flow Width	Curve Number
1	villanova	347.5	15137971	500	30276	30276	85.0
2	rosemont	196.5	8558669	500	17117	10117	75.0
3	gulf	588.2	25620250	500	51240	30240	70.0
4	bryn mawr college	101.8	4432666	500	8865	6865	75.0
4.5	cem	32.6	1421798	450	3160	3160	70.0
5	morris	316.2	13771930	500	27544	30544	85.0
6	harcum jr college	276.5	12043469	500	24087	24087	80.0
7	mountain	260.5	11346509	500	22693	22693	70.0
8	williamson	65.3	2843597	500	5687	5687	75.0
8.5	dove	46.1	2007245	400	5018	5018	70.0
9	williamson 2	83.2	3624192	500	7248	7248	75.0
10	merion square	121.0	5269018	500	10538	10538	65.0
11	trout run	815.4	35517082	500	71034	30034	85.0
11.5	mountain 2	26.2	1143014	400	2858	2858	75.0
12	cherry	69.1	3010867	500	6022	8022	75.0
13	moreno	217.6	9478656	500	18957	2957	75.0
14	righters	83.2	3624192	500	7248	1248	70.0
15	circle	129.3	5631437	500	11263	863	70.0
16	fairview	64.0	2787840	500	5576	576	70.0
16.5	mountain 3	36.5	1589069	350	4540	540	70.0
17	christopher	70.4	3066624	450	6815	6815	70.0
18	john	41.0	1784218	450	3965	3965	70.0
19	belmont	122.9	5352653	500	10705	5705	70.0
20	gladwyne	281.6	12266496	500	24533	3533	65.0
21	non trib 1	97.3	4237517	500	8475	8475	65.0
22	non trib 2	108.8	4739328	450	10532	10532	80.0
23	non trib 3	140.8	6133248	500	12266	12266	75.0
24	non trib 4	121.0	5269018	450	11709	11709	75.0
25	non trib 5	110.7	4822963	450	10718	3718	70.0
26	non trib 6	102.4	4460544	450	9912	4912	70.0
27	non trib 7	158.1	6885965	500	13772	7772	75.0
28	non trib 8	105.6	4599936	400	11500	11500	95.0

	Conduit #	Left Bank roughness coefficient	Right Bank roughness coefficient	Channel roughness coefficient
	1	0.1	0.1	0.1
	2	0.1	0.1	0.1
	3	0.08	0.08	0.08
	4	0.06	0.06	0.06
	5	0.06	0.06	0.06
	6	0.02	0.02	0.02
	7	0.015	0.015	0.015
	8	0.035	0.035	0.035
	9	0.02	0.02	0.02
	10	0.02	0.02	0.02
	11	0.015	0.015	0.015
	12	0.025	0.025	0.025
	13	0.04	0.04	0.04
	14	0.015	0.015	0.015
	15	0.005	0.005	0.005
	16	0.01	0.01	0.01
	17	0.01	0.01	0.01
	18	0.02	0.02	0.02
	19	0.025	0.025	0.025
	20	0.015	0.015	0.015
	21	0.045	0.045	0.045
Tributary Conduits	1	0.05	0.05	0.05
	2	0.03	0.03	0.03
	3	0.02	0.02	0.02
	4	0.02	0.02	0.02
	5	0.015	0.015	0.015
	6	0.025	0.025	0.025
	7	0.02	0.02	0.02
	8	0.01	0.01	0.01
	9	0.01	0.01	0.01

Appendix E: SWMM Outflow Hydrographs for the 0.5 inch, 6 hour storm

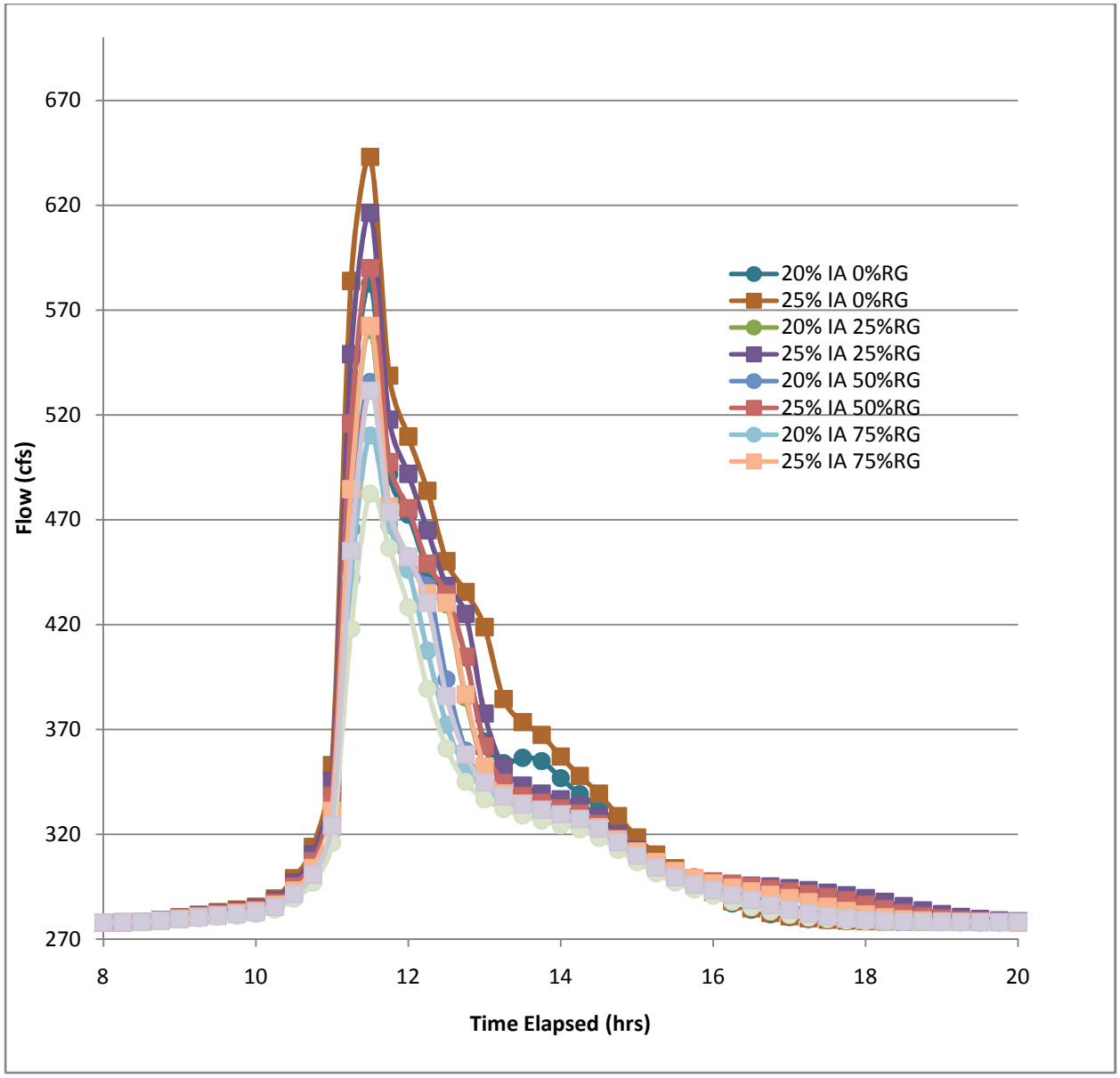

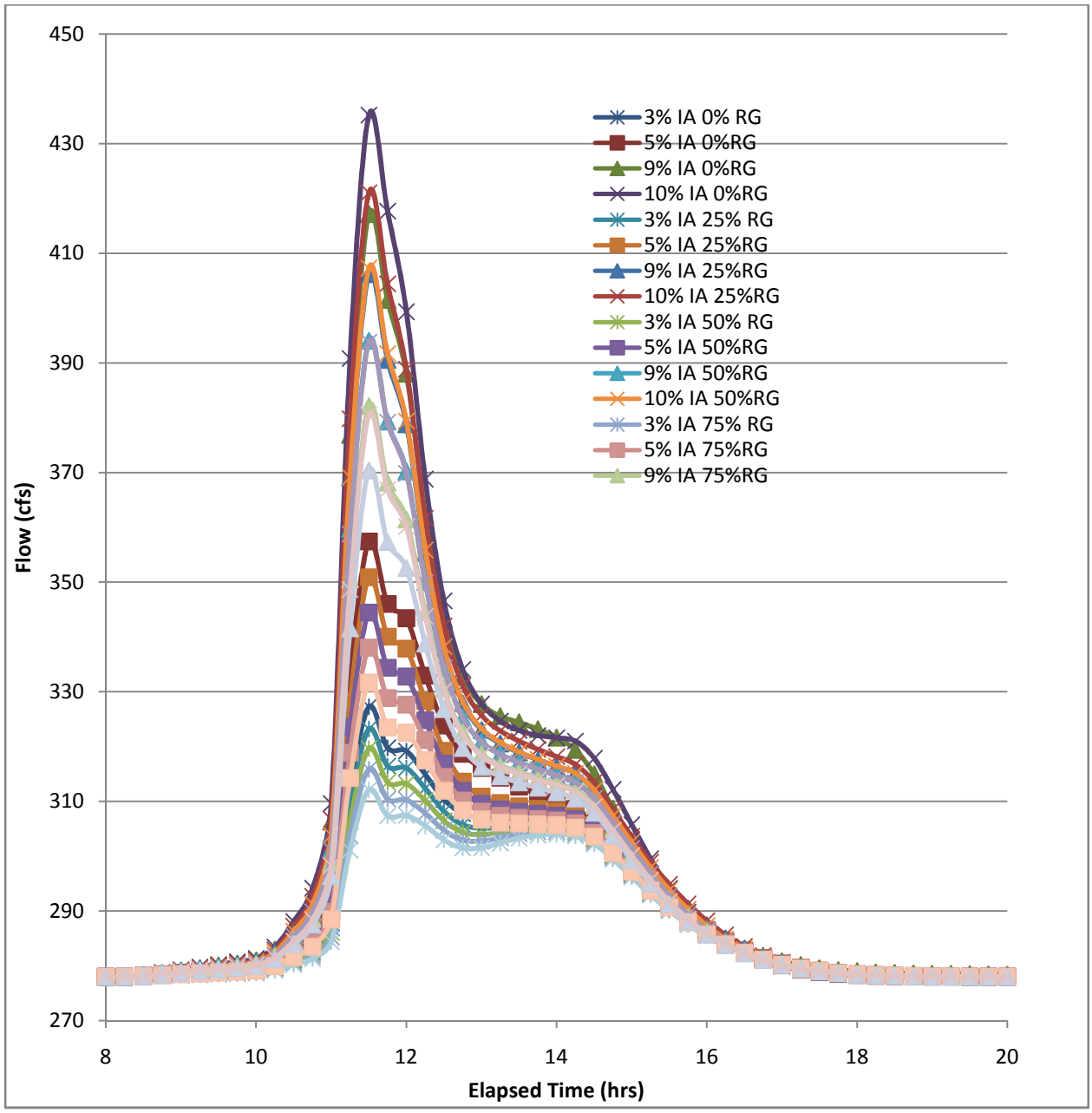
450
430
410
390
370
350
330
310
290
270
Flow (cfs)
8
10
12
14
16
18
20
Elapsed Time (hrs)
3% IA 0% RG
5% IA 0%RG
9% IA 0%RG
10% IA 0%RG
3% IA 25% RG
5% IA 25%RG
9% IA 25%RG
10% IA 25%RG
3% IA 50% RG
5% IA 50%RG
9% IA 50%RG
10% IA 50%RG
3% IA 75% RG
5% IA 75%RG
9% IA 75%RG

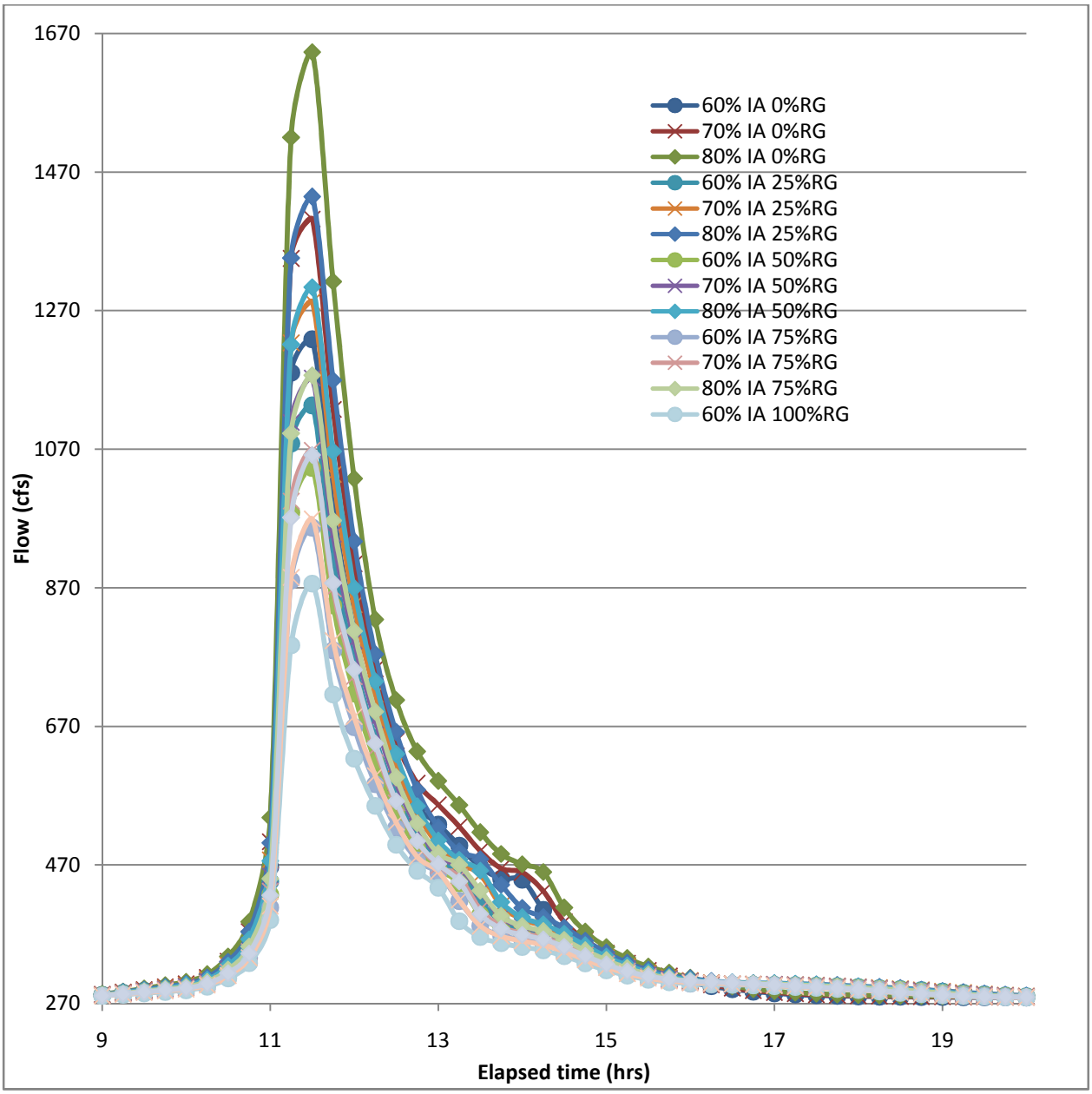
1670
1470
1270
1070
870
670
470
270
Flow (cfs)
9
11
13
15
17
19
Elapsed time (hrs)
60% IA 0%RG
70% IA 0%RG
80% IA 0%RG
60% IA 25%RG
70% IA 25%RG
80% IA 25%RG
60% IA 50%RG
70% IA 50%RG
80% IA 50%RG
60% IA 75%RG
70% IA 75%RG
80% IA 75%RG
60% IA 100%RG